



**Organic Micropollutants  
degradation from reverse osmosis concentrate water**

**Water Management  
MSc Thesis**

**October 2024**

**Jesús David Medina Hernández  
5625629**



**Organic Micropollutants  
degradation from Reverse Osmosis concentrate water:**

**Anodic oxidation with a Magnéli ( $\text{Ti}_4\text{O}_7$ ) reactive electrochemical membrane flow-through reactor towards drinking water production processes**

MSc Thesis Report

By

Jesús David Medina Hernández

Water Management  
Faculty of Civil Engineering and Geosciences  
Delft University of Technology

Supervisors

Prof.dr.ir. Doris van Halem  
Dr.ir. Sanne Smith  
Ir. Silvy Rijdsdijk, EngD.

TU Delft  
TU Delft  
TU Delft

# Preface and acknowledgements

This work on “Organic micropollutants degradation from Reverse Osmosis concentrate water”, is the graduation project in fulfilment of the Master programme in Civil Engineering, with a specialization in **Water Management**, section of Sanitary Engineering, at Delft University of Technology.

My journey started at Aguascalientes University in Mexico, where I studied civil engineering. The diverse environmental problems in my region, especially the lack of safe drinking water, sparked my interest in pursuing education in environmental sciences. Also an academic exchange at Rio Grande do Sul University in Brazil provided many valuable lessons that shaped my pathway. I worked in my hometown in construction management for urban development, where I gained valuable knowledge of civil engineering. Then, a summer school in Delft paved the way for my future. With the goal of contributing to solutions for the environmental challenges that threaten drinking water safety in Mexico, I found a shelter in TU Delft, studying for an MSc in Civil Engineering in Water Management.

I extend my gratitude to my friends, classmates, professors, and the Dispuut student association at TU Delft for their immense support. A special thanks to my thesis supervisors, Prof. Dr. Ir. Doris van Halem, Dr. Ir. Sanne Smith, and Ir. Silvy Rijdsdijk, EngD, for their guidance, as well as the Water Lab technicians for their assistance with the measurement equipment.

Additionally, I want to thank my family for their unconditional support from afar. To my parents Lupita and Luis, for encouraging me to pursue higher education and supporting me throughout my academic journey. To my brothers, sisters, nieces, and nephews, for motivating me. Special thanks to my uncle David, as well as to my other uncles, aunts, and cousins in Mexico and the USA. And last but not least, to my fiancée Laura, for her patience, support, and companionship throughout this journey.

## Key words

Magnéli, Anodic oxidation, Organic micropollutants (OMPS), Poly- Perfluoroalkyl substances (PFAS), Pharmaceuticals, Corrosion inhibitors, Synthetic dyes, Drinking water production, Reverse osmosis concentrate (ROC), Flow-through Reactor, Reactive electrochemical membrane (REM), water treatment, surface water remediation. Byproducts, Hardness influence, and energy consumption.

## Highlights

- The Magnéli REM is capable of simultaneously degrading a variety of OMPs.
- The reactor improves its degradation rates when mass transfer limitations are minimized.
- Benzotriazole degradation can be used to assess the overall degradation of a set of OMPs.
- PFAS degradation from ROC was lower compared to artificially spiked water, as reported in other research.
- By-product formation and scaling are important limitations when applying anodic oxidation technologies to remediate ROC.

# Abstract

Manmade emergent contaminants are posing a big treat to the environment and human health. Their accumulation in water resources threat the ecosystem equilibrium and challenges the current technologies to produce safe drinking water. This research explores anodic oxidation (AO) using a Magnéli phase reactive electrochemical membrane (REM) flowthrough reactor as an alternative to treat reverse osmosis concentrate (ROC) water containing a broad list of organic micropollutants (OMPs). ROC water produced in two drinking water treatment utilities in the Netherlands was used to test the technology. This study searches for insights to manage ROC waste containing recalcitrant OMPs and safely discharge effluent to surface water.

Throughout laboratory experimentation, the effectivity of degrading OMPs (per-polyfluoro-alkyl substances, pharmaceuticals, corrosion inhibitors, and synthetic dyes) was investigated. Main findings suggest that 100 mg/L Methylene blue (MB) spiked in an artificial water matrix is completely mineralized after an applied charge dosage (CD) of 22.56 kC/L.

In addition, pharmaceuticals and corrosion inhibitors spiked in an artificial water matrix and ROC at different initial concentrations (ranging from 5 mg/L to 5 µg/L) were degraded by over 80% after applying a charge dosage of 5.64 kC/L. Finally, the degradation of PFOA (50 to 15 ng/L) and PFOS (12 ng/L) in ROC from drinking water utilities 1 and 2 resulted in average reductions of 49.5% and 76.9%, respectively, after applying 120 kC/L.

Moreover, it was found that hardness in water inhibits the degradation capacity reducing the effective area of the anode with scaling deposition. Besides, the calcium and magnesium content slightly increase the energy consumption and the frequency of chemical cleaning required to maintain the reactor.

Furthermore, the Magnéli REM reactor demonstrated the capability to degrade a variety of OMPs when treating ROC. Operational parameters such as flow rate and current density (CD) can be adjusted to achieve better efficiencies. However, it is important to note that the treated water may contain byproducts with recalcitrant properties and potential toxicity, such as ultra-short and short-chain PFAS, bromate, chlorates, and perchlorates. For this reason, monitoring and further treatment are recommended before safely discharging the water back into surface water

# Table of contents

Preface and acknowledgements	i
Highlights	ii
Abstract	iii
Chapter 1	
Introduction	1
1.1 Organic Micropollutants	2
1.1.1 Poly- Perfluoroalkyl substances “PFAS”	3
1.1.2 Pharmaceuticals , Corrosion inhibitors, and Synthetic dyes	3
1.2 OMPs water remediation technologies	4
1.2.1 Reverse Osmosis	4
1.2.2 Electrochemical advanced oxidation processes, and Anodic oxidation	5
1.3 Literature review	8
1.3.1 Knowledge gap	8
1.4 Study approach	9
1.4.1 Research questions	9
Chapter 2	
Methodology	10
2.0.1 Experimental Set-up configuration	10
2.1 Degradation of Methylene blue	12
2.2 Pharmaceuticals and corrosion inhibitor degradation	13
2.3 RO concentrate treatment	15
Chapter 3	
Results	19
3.1 Degradation of Methylene blue	19
3.2 Degradation of Pharmaceuticals and corrosion inhibitors	21
3.3 RO Concentrate treatment	23
Chapter 4	
Discussion	27
4.1 MB degradation	27
4.2 Pharmaceuticals and corrosion inhibitors degradation	29
4.3 RO Concentrate treatment (PFAS)	33
4.4 Reactor operation	42
4.5 ROC remediation and disposal	44
Chapter 5	
5.1 Conclusion	45
5.2 Recommendation	46
References	47
Appendix	60

# List of Figures

Figure 1: Membranes removal mechanism	4
Figure 2: Magnéli REM anode degradation mechanisms	5
Figure 3: Magnéli REM system functionality	7
Figure 4: Magnéli REM reactor set up	10
Figure 5: Company 2 pilot treatment scheme	16
Figure 6: MB degradation rates comparison	20
Figure 7: Experiment OMP-1	21
Figure 8: OMP-2 & 3 experiments	22
Figure 9: PFAS degradation and charge dosage	23
Figure 10: Perfluoro carboxylic Acids degradation	24
Figure 11: Perfluoro Sulfonic Acids group degradation	25
Figure 12: Medium and long chain PFAS degradation	26
Figure 13: MB kinetic rates	28
Figure 14: Role of supporting electrolyte	30
Figure 15: PFAS degradation efficiency	35
Figure 16: COD and TOC degradation	36
Figure 17: Short chain PFAS	38
Figure 18: Blanco	40
Figure 19: Influence of hardness	41
Figure 20: Energy consumption Magnéli REM	42
Figure 21: Reactor potential efficiency inhibitors	43
Figure 22: Treatment scheme	44
Figure A1: OMPs pathways to water resources	60
Figure A2: PFAS family classification	60
Figure A3: MB Degradation	63
Figure A4: MB Degradation 2	64
Figure A5: MB degradation 3	65
Figure A6: PFAS Degradation DWU 1	66
Figure A7: PFOA and PFOS, PFHxA , PFPeA, PFHxS and PFHpA	67
Figure A8: PFBA,PFNA, 6:2 FTS, HFPO-DA (GEN-X) and PFPeS and FBSA	68
Figure A9: PFOA branched and PFOS branched normalized degradation	69
Figure A10: PFOA , PFOS , PFHxA and PFPeA normalized degradation	69
Figure A11: PFHxS and PFHpA, B-PFOA, B-PFOS, PFNA, PFPeS, HFPO and PFBS	70
Figure A12: Chloride & Total organic carbon C1	72
Figure A13: Chloride & active chlorine DWU1 & DWU2	72
Figure A14: Degradation kinetics of corrosion inhibitors OMP-3	73
Figure A15: Degradation of pharmaceuticals OMP-3	74
Figure A16: MB in ROC degradation	74
Figure A17: Magneli REM reactor experimental set-up	74

# List of Tables

Table 1: Series 1, MB and artificial water	12
Table 2: Pharmaceuticals degradation	13
Table 3: OMPs spiked mixture	14
Table 4: DWU 1 ROC water quality	15
Table 5: DWU 2 Concentrate water quality	16
Table 6: RO concentrate experiments	17
Table 7: BTA degradation comparison	32
Table A1: Literature review	61
Table A2: Charge Dosage Literature review	61
Table A3: Still botom water containing PFAS	62
Table A4: Spiked PFAS to artificial water	62
Table A5: Measured PFAS under detection limits	71
Table A6: Measured PFAS Blanco DWU 2	72



# List of abbreviations

OMPS - Organic micropollutants  
PFAS - Poly- Perfluoroalkyl substances  
REM- Reactive electrochemical membrane  
AO - Anodic oxidation  
WWTPs – Wastewater treatment plants  
RO - Reverse osmosis  
ROC – RO concentrate  
CD – Charge dosage  
i – Current density  
COD- Chemical oxygen demand  
TOC - Total organic carbon  
MB – Methylene blue  
BTA – Benzotriazole  
PFNA - Perfluorononanoic acid  
PFOS - Perfluorooctanesulfonic Acid  
PFOA - Perfluorooctanoic acid  
PFHxS - Perfluorohexanesulfonic acid  
PFHxA - Perfluorohexanoic acid  
PFHpA – Perfluoroheptanoic acid  
PFPeA - Perfluoropentanoic acid  
PFPeS - Perfluoropentanesulfonic acid  
PFBS - Perfluorobutane sulfonate  
PFBA - Perfluorobutanoic acid  
PFDA - Perfluorodecanoic acid  
TFA - Trifluoroacetic acid  
6:2 FTS - 6:2-fluorotelomersulfonic acid  
DWU 1 - Drinking water utility 1  
DWU 2 - Drinking water utility 2

# Chapter 1

---

## Introduction

---

Safe drinking water production has become a challenging duty due to the presence of anthropogenic substances in water resources. In many regions of the world, drinking water standards are barely reached, and water quality guidelines need to be redesigned to face recalcitrant contaminants. Emerging contaminants such as organic micropollutants (OMPs) are a risk to the environment and humans, thereby the application of water treatment technologies are essential to minimize the impact and side effects of such pollution (East 2021 ;Hoffman al. 2011). This research explores anodic oxidation as an alternative to degrade recalcitrant contaminants from reverse osmosis concentrate water, by using a Magnéli phase ( $\text{Ti}_4\text{O}_7$ ) reactive electrochemical membrane (REM) as anode in a flowthrough reactor.



Organic micropollutants (OMPs) are a group of anthropogenic, microscopic and hazardous compounds. These substances are widely used in industrial and daily life activities (Bhadouria et al. 2024). Their presence in water resources is a worldwide problem and a significant environmental concern, which challenges the production of safe drinking water (Chow et al. 2021). Examples of OMPs are per-polyfluoroalkyl substances (PFAS), pharmaceuticals, corrosion inhibitors, pesticides, and synthetic dyes among others (Hartmann 2022).

OMPs pose a significant risk to the natural environment and human health due to their toxicity, bioaccumulation, and non-degradable properties (Hashimi et al. 2020; Nicolopoulou-Stamati et al. 2016.). They enter the environment through various pathways, such as wastewater, irrigation, runoff, and more in “Appendix Figure A1”. Wastewater treatment plants (WWTPs) are major contributors because usually they are unable to remove or degrade these contaminants to a sufficient degree (Appleman et al. 2014). Consequently, OMPs accumulate in various media such as soils, plants, sediments, surface water, groundwater, the ocean, and rainfall, but also in animals and humans (Yong et al. 2021; Pike et al 2021; Chen et al. 2020; Sarkar 2016).

Moreover, OMPs have a negative effect on aquatic life, accumulating and affecting species ranging from phytoplankton (Davis et al. 2024) to whales (Villanger et al. 2020). These contaminants are then transferred through other trophic levels and eventually reach humans (Domingo et al. 2012). Although scientists have identified the effects of exposure to some of OMPs on both ecology and human health, the potential damage caused by the mixture these substances to natural habitats, biodiversity, and human health remains uncertain (Beghin et al. 2021; De Sousa et al. 2021; D’Almeida et al. 2020).

However, human risks associated with OMPs are alarming enough to create awareness, generate remediation measures and reduce the susceptibility of people ingesting these substances via drinking water and food (Vera et al. 2024; Rumsby 2009). A report from the National Institute for Public Health and the Environment (RIVM) in the Netherlands informed that the Dutch population is ingesting more PFAS by water and food consumption than the recommended safety limit by European health agencies (RIVM 2023). Therefore, for Dutch water authorities, the research and implementation of water treatment remediation alternatives with capabilities to remove or destroy OMPs are of relevant importance (STOWA 2019).



### 1.1.1 Per-polyfluoroalkyl substances “PFAS”

---

PFAS are a broad group of synthetic organic compounds characterized by their strong carbon-fluorine bond and chain length structure (Buck et al. 2011; Smart 1994). These man-made chemicals possess special properties including water and oil repellency, heat resistance, and chemical stability (Kissa 2001). Nevertheless, these compounds are toxic at low concentrations, difficult to measure, and their remediation from water demands further investigation to tackle their occurrence and persistence in water resources around the world (Ramírez-Canon et al. 2022; Taniyasu et al. 2022). Hence, environmental agencies in USA and Europe created regulatory measures for a list of PFAS species to be monitored in drinking water production. For instance, perfluorooctanesulfonic acid (PFOS), and perfluorooctanoic acid (PFOA) (EPA 2019).

### 1.1.2 Pharmaceuticals, corrosion inhibitors and synthetic dyes

---

— Pharmaceuticals are a class of chemical compounds designed to treat, prevent, or alleviate medical conditions in humans and animals. They play a crucial role in improving public health and quality of life in society (Lichtenberg & Virabhak 2007). Notwithstanding, the widespread use of pharmaceuticals around the world has caused these substances to become major and worrisome environmental contaminants (Li et al., 2014; Rivera-Utrilla et al. 2013; Zuccato et al. 2000). They have been detected in several locations around the world, including polar regions, water resources, soils, plants, and crops (Gonzalez-Alonso et al. 2017; Christou et al. 2017; Minh et al. 2009; Boxall et al. 2006; Ferdig et al. 2005).

— Corrosion inhibitors are substances added to equipment to mitigate or prevent material degradation. One example is Benzotriazole, which is difficult to degrade in the environment, accumulates in water resources, and affects aquatic organisms (Kimbell et al. 2023). This compound is commonly used in industrial and household applications, leading to its constant presence in domestic wastewater. (Akpan et al., 2024; Alotaibi et al 2015).

— Synthetic dyes are colorant agents fabricated from organic molecules and widely used in the textile industry and other applications (Ziarani et al., 2018). These compounds are of environmental concern due to their aesthetic impacts on water and soils, but also because of the potential hazard to ecology (Oladoye et al. 2022).



## 1.2 OMPs water remediation technologies

---

Conventional water treatment techniques are uncappable to remove PFAS and other OMPs (Ben et al. 2018). Efficiently removal or destruction of OMPs was achieved by a restricted number of technologies. These methods can be classified into two groups: separation and degradation techniques. Examples of separation technologies are reverse osmosis (RO), nanofiltration (NF) (Liu et al. 2022), ion exchange (IX) (Dixit et al. 2021), foam fractionation (FF) (Smith et al. 2023), granular activated carbon (GAC) (Belkouteb et al. 2020), and powder activated carbon (PAC) (Yu et al. 2009). The mentioned technologies separate and concentrate OMPs, but waste management actions are still required to avoid contaminants reintroduction to the environment.

Degradation technologies aim to breakdown the molecular structure of OMPs by destructive mechanisms. Examples are advanced oxidation processes (AOP) (Ganiyu et al. 2015), sonolysis (Vecitis et al. 2008), subcritical water oxidation (Hori et al. 2006), and electrochemical advance oxidation processes (EAOPs) (Krause et al. 2021) among others. The main drawback is intensive energy consumption. Studies suggested that EAOPs effectively removed targeted OMPs species with a relatively low energy consumption compared to the other degradation methods (Uwayezu et al. 2021). This experimental work aimed to integrate technologies to separate and degrade specific OMPs by treating reverse osmosis concentrate using anodic oxidation.

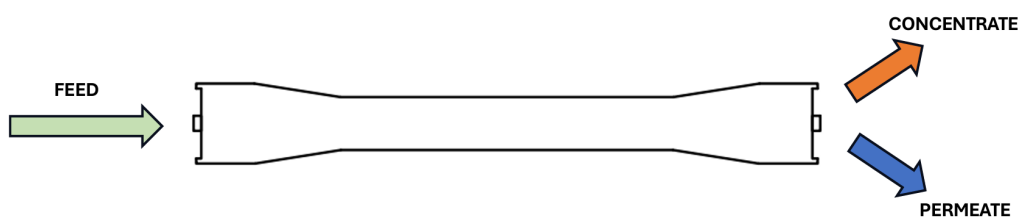
### 1.2.1

### Reverse Osmosis

---

Reverse osmosis (RO) is a well-known water treatment technology that serves to separate dissolved substances from water. RO operates pressurizing and passing water through polymeric semipermeable membranes that reject the dissolved solutes producing two streams, the permeate which is the treated water and the reverse osmosis concentrate (ROC), which is the rejected water (Zaidi & Saleem 2022). This method is commonly used to desalinate both sea and brackish water, but also as polishing treatment for wastewater and drinking water (Brião et al. 2014).

Figure 1: Membranes removal mechanism.



## 1.2.2 Electrochemical advanced oxidation processes, and anodic oxidation

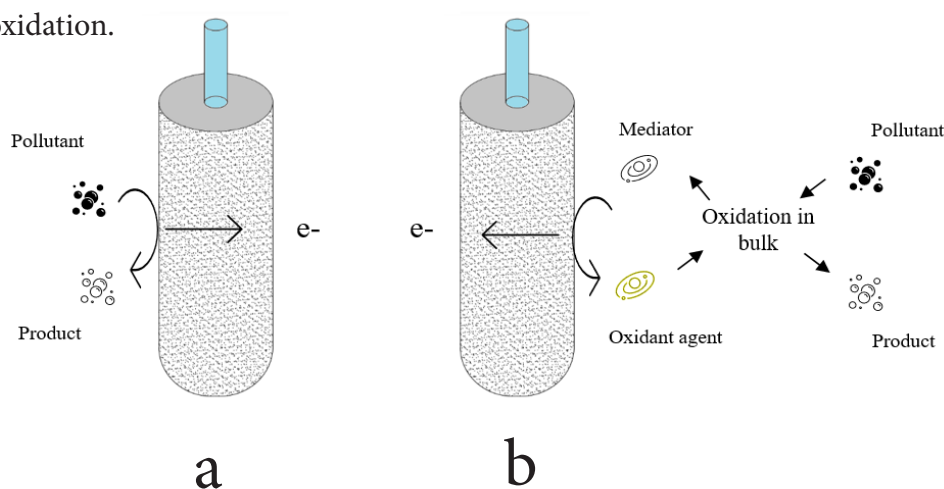
Electrochemical advanced oxidation processes (EAOPs) are a group of water treatment technologies in which pollutants are degraded by electron transfer mechanisms that produce strong oxidizers (Brillas et al. 2009). In these processes, chemical transformations are driven by the application of an external source of electric current known as current density to an electrochemical cell. Then, degradation processes occur, for instance, direct oxidation and reduction, generation of reactive oxidizing species (ROS), and indirect oxidation via intermediates (Sirés et al. 2014).

In direct oxidation, electrons are exchanged between the anode (A) and the contaminant. Besides, the oxygen evolution reactions (OER) creates hydroxyl radicals ( $\cdot\text{OH}$ ), hydrogen peroxide ( $\text{H}_2\text{O}_2$ ), hydroperoxyl radical ( $\text{HO}_2\cdot$ ), and ozone ( $\text{O}_3$ ) (Panizza & Cerisola 2009). On the other hand, with indirect oxidation, the presence of certain ions in the bulk solution triggers the production of oxidants that contribute to the degradation of contaminants or their intermediates. Examples include active chlorine species, sulfate, and phosphate radicals (Panizza & Cerisola 2009).

This research explored anodic oxidation (AO), an EAOPs technique that was shown to be effective in degrading emergent and recalcitrant contaminants (Le et al. 2019; Chaplin et al 2014). This method is a surface-controlled process which implies that oxidation mechanisms such as direct oxidation occur near the anode surface when contaminants have contact or are absorbed to the anode surface (Barrera-Diaz et al. 2014). Therefore, degradation capabilities are mainly dependent on the anode material and the mass transfer of contaminants to reach the anode surface or its proximity (Panizza & Cerisola 2009).

Figure 2: Magnéli REM anode degradation mechanisms (Chiang et al. 1995).

- (a) Direct, and
- (b) indirect oxidation.



## Mechanisms of OMPs degradation with AO treatment

---

The degradation mechanism for PFAS when applying AO is still debated in the scientific community (Radjenovic et al. 2020). An accepted theory proposed that direct electron transfer (DET) initiates the decomposition of PFOS, such a process cannot be launched by  $\cdot\text{OH}$  (Trojanowicz et al. 2018). The DET continues, triggering the breakdown of carbon-fluorine bonds until the pollutant molecules are partially or completely disassembled (Huang et al. 2020). During the process intermediate products also react with  $\cdot\text{OH}$  to produce smaller chain products via  $\text{CF}_2^-$  detachment cycle to later produce  $\text{CO}_2$  and  $\text{HF}$  (Carter & Ferrell 2008). In the case of pharmaceuticals, oxidation via  $\cdot\text{OH}$  and other radicals dominates the degradation mechanism, with some exceptions. For instance, DET influences degradation when compounds are resistant to  $\cdot\text{OH}$ , and when contaminant adsorption to the anode surface is promoted (Radjenovic et al. 2011).

Moreover, the material of the anode changes the performance of the reactions due to differences in electrochemical activity, adsorption properties, density of active sites for pollutant deposition, oxygen evolution potential, and production of  $\cdot\text{OH}$  (Radjenovic et al. 2015). There are two types of anode classification, active and non-actives, the latest exhibit high capabilities for the transformation of recalcitrant compounds (Chen et al. 2020; Comninellis et al. 1994). Examples of non-active anodes are Pt,  $\text{PbO}_2$ , Boron-doped diamond (BDD), and Magnéli phase  $\text{Ti}_4\text{O}_7$  (Marselli et al. 2003).

### Magnéli phase ( $\text{Ti}_4\text{O}_7$ )

---

The titanium oxides materials ( $\text{Ti}_n\text{O}_{2n-1}$ , with  $4 < n < 10$ ) were first developed in the 1950's by the chemist Arne Magnéli (Andersson et al. 1957). These materials are characterized by their excellent chemical stability, mechanical strength, and high electrical conductivity (Wang et al. 2020; Arif et al. 2017). The Magnéli phase anode material has been pointed out to have superior features when degrading recalcitrant contaminants than other materials. Studies have reported that the use of Magnéli phase to degrade targeted PFAS is more efficient than BDD anodes and cheaper to produce (Lin et al., 2019).

### Magnéli REM reactor

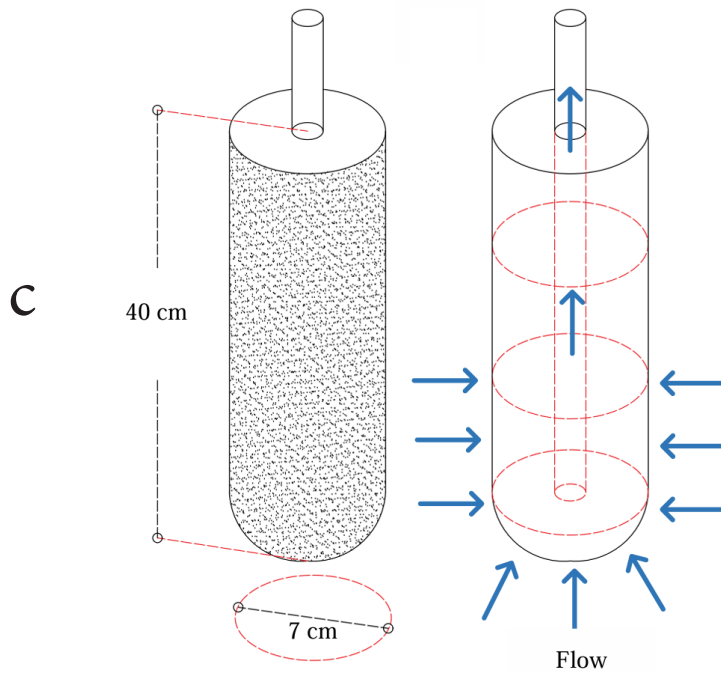
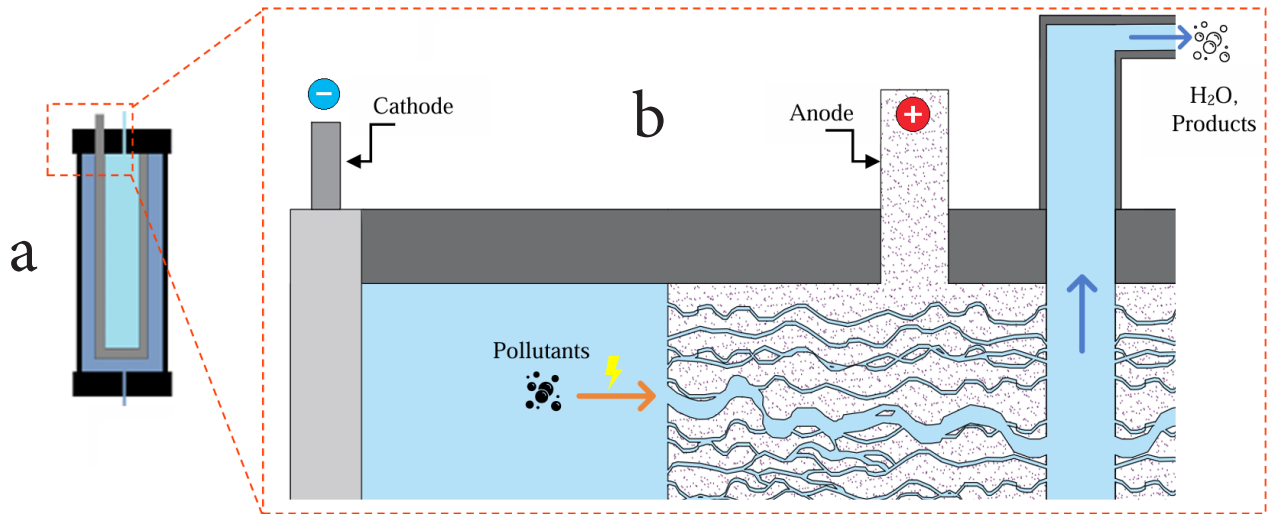
---

The reactive electrochemical membrane (REM) consist of a 3D porous medium anode shape instead of plates, that seek to increase the effective surface area in contact with solution and enhance the oxidative properties of the process. This configuration is known as reactive electrochemical membrane (REM) (Xu et al. 2016). In addition, membranes in combination with continuous flow systems significantly improve performance and reduce energy consumption due to the enhanced mass transfer of contaminants through the membranes (Ma et al. 2022). Moreover, the REM provides another decontamination mechanism apart from DET and indirect oxidation. For instance, the physical barrier of the pore size of the membranes, electro-sorption, and electro-repulsion, such properties influence the produced effluent and the degradation of pollutant performance (Almassi et al. 2019; Fan et al. 2015).



Figure 3: Magnéli REM system functionality.

(a) Magnéli REM system reactor operates in up-flow mode, (b) cross section in the top of the reactor to clearly observe the pollutant fate through the REM (c) anode characteristics, tridimensional shape allows water to enter the anode from all possible directions.





## 1.3

# Literature review

---

A literature review was conducted to identify the existent studies focused on Magnéli phase ( $\text{Ti}_4\text{O}_7$ ) REM in flow-through operation to degrade OMPs from various sources of water. The review was carried out using the databases SCOPUS and the TU Delft Library. Results were summarized and a selection of relevant studies was reviewed in more detail.

Research on Magnéli REM reactors for the treatment of ROC and the removal of OMPs is limited. To date, no studies have specifically focused on targeting PFAS or pharmaceuticals in ROC using a Magnéli flow-through reactor. However, some studies used different experimental configurations to treat artificial water matrices, and IX still bottoms.

The completed overview of the relevant literature can be found in the “Appendix Table A1 to A4”. It is important to note that the used methods vary for each research and that most were conducted on batch systems, only a few used a flow-through reactor, but only one was at a pilot scale.

Moreover, the concentrations of PFAS species in the found literature are high compared with the PFAS concentration for the ROC used in this research. In artificial water, the concentrations ranged between 4 to 207 mg/L PFOS and 3 to 1035 mg/L PFOA. Besides, in IX still bottoms wastewater the concentration ranged between 5 to 68 mg/L PFOS and 3 to 100 mg/L for PFOA.

### 1.3.1

### Knowledge gap

---

There are few but significant studies exploring the electrochemical degradation of PFAS using Magnéli phase anode that used different methodologies. PFAS degradation using a REM Magnéli phase reactor has not been evaluated using ROC or other relevant water matrices apart from still bottoms and artificial water. Studies using concentrations (100-250 ng/L) are limited. It might be relevant to compare the kinetics degradation of high and low PFAS concentration. Besides, a study of low concentrations could bring insights on the remediation alternatives for water resources.

In addition, the suitability of the technology to target multiple contaminants in combination deserves more attention. PFAS and other OMPs assessment of degradation rates and efficiency, needs further research. The existent studies only assessed PFAS along with organic carbon and chloride. Besides, so far there is no study using a similar REM configuration to treat ROC targeting the OMPs indicators suggested by the Dutch Ministry of Infrastructure and Water (I&W).

Moreover, interesting insights could be addressed on common operative limitations. For instance, energy consumption, mass transfer limitations, scaling, cleaning methods, and frequency for longer continuous treatment periods.



The study approach was designed to generate insights into the treatment of ROC using AO with the Magnéli REM reactor. The degradation of OMPs, including PFAS and pharmaceuticals, was investigated, and the performance of the reactor was evaluated through laboratory experiments. These experiments were conducted to address the primary research question as well as the secondary questions, which are presented in the following section.

## 1.4.1

Research questions

---

To what extent can persistent OMPs present in ROC be degraded using AO treatment with a Magnéli REM reactor?

---

## Sub-Research questions

- 1.- What are the degradation kinetics of Methylene blue?
  - 2.- What is the degradation efficiency of treating a mix of pharmaceuticals and corrosion inhibitors, when using artificial water matrix, and ROC?
  - 3.- What is the PFAS degradation efficiency per species?
  - 4.- What are the by-products?
  - 5.- What is the hardness influence on the treatment using the Magnéli REM reactor?
  - 6.- What is the energy consumption?
- 



# Chapter 2

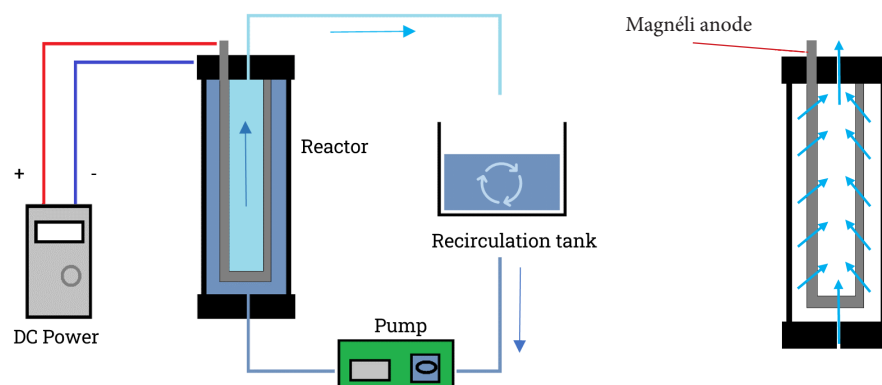
## Methodology

The methodology of this research involved laboratory experimentation, data analysis, and literature review to assess the study case of ROC treatment with AO. The laboratory work was carried out in the Water-Lab at Delft University of Technology. The experimental procedure was divided into three phases which served to answer the main and sub-research questions. Phase 1 consisted of the use of a referent pollutant to test the capabilities of the Magnéli REM reactor and degradation kinetics. Then, phase 2 explored the degradation capabilities of pharmaceuticals and corrosion inhibitors. Finally, phase 3 addressed the treatment of ROC to evaluate the PFAS degradation performance using a ROC produced in two different drinking water treatment utilities in the Netherlands.

### 2.0.1 Experimental Set-up configuration

The experimental configuration of this research is shown in Figure 4. A lab-scale Magnéli REM reactor was used, manufactured by the company Magnéli Materials LLC, (USA). The reactor was fed by a peristaltic pump (Watson Marlow 323) from the recirculating tank (3 Liters), and current was delivered by a DC power source (Tenma 72-13350) to the anode and cathode in the reactor.

Figure 4: Maneli REM reactor set up.



## 2.0.2

## Current Density

---

The current density ( $i$ ) represents for the reaction rate in terms of coulombs [C] per unit surface area [cm<sup>2</sup>], and can be calculated using Ohm's law, which relates current ( $I$ ) to voltage ( $V$ ) and resistance ( $R$ ) through the following equation (Sillanpää & Shestakova 2017).

$$i = \frac{I}{A} \quad (1)$$

Where:

$i$  is the current density [A/cm<sup>2</sup>]

$I$  is the current [A]

$A$  is the electrode surface area [cm<sup>2</sup>]

## 2.0.3

## Charge Dosage

---

Charge dosage (CD) refers to the total electric charge applied to a volume of water during the electrochemical treatment process. It is calculated by multiplying the current ( $I$ ) by the time ( $t$ ) over which the current is applied and dividing by the volume of water treated ( $V$ ). Often denoted in units of coulombs per liter [C/L], and ampere-hour per cubic meter [Ah/m<sup>3</sup>], expressed as follows.

$$CD = \frac{I * t}{V} \quad (2)$$

Where:

$I$  is the current in amperes [A; C/s]

$t$  is the time in seconds [s]

$V$  is the volume of water in liters [L]

To assess the functionality of the process, it is valuable to compute the energy consumption in function of the CD and voltage of the cell in (kWh/m<sup>3</sup>).

## 2.0.4

## Degradation efficiency

---

The following formula serves to calculate the degradation efficiency at different time intervals.

$$DE (\%) = \frac{C_0 - C_t}{C_0} * 100\% \quad (3)$$

$C_0$  is the initial concentration [mg/L]

$C_t$  is the concentration at interval time  $t$  [mg/L]



## 2.1

## Degradation of Methylene blue

---

Methylene blue (MB) is a cationic dye widely used in various industrial applications, and it is hazardous to the environment (Oladoye et al. 2022). MB is considered an OMP and was used as a reference pollutant to assess degradation in experimental phase 1. Electrochemical technologies have been successfully proven to completely mineralize MB (Panizza et al. 2007). The use of the Magnéli REM reactor was evaluated to gain insights into the reactor's performance and identify key parameters, such as the degradation kinetics of MB in an artificial water matrix (demi-water) and ROC. The clear visualization of the dye degradation process and the easy access to measurements with the UV-spectrometer provided an accessible and informative method for data collection.

### 2.1.1

### Experimental Parameters

---

In experimental phase 1, three different current densities and three different flow rates were used to assess the removal kinetics of MB, as shown in Table 1. The initial concentration of MB in the artificial water was 100 mg/L, with 0.2 M of NaCl. Additionally, ROC was spiked with the same initial concentration of MB and treated using the highest current-flow parameters.

Table 1: Series 1, MB and artificial water.

Current density [mA/cm <sup>2</sup> ]	Volume [L]	Current [A]	Flow [L/min]
3	3	2.82	0.5 - 1 - 1.75
6	3	5.64	0.5 - 1 - 1.75
9	3	8.46	0.5 - 1 - 1.75

### 2.1.2

### Sampling

---

The MB degradation was assessed by collecting 1 mL samples in cuvette vials every minute. Quenching with 0.2 mL 0.1 mmol HCl was tested. No quenching was also assessed. Then, samples were measured in the UV-spectrometer. In addition, to measure COD, 10 mL samples were obtained every 5 minutes. For the TOC, 40 mL samples were filtered with 0.2  $\mu\text{m}$  and acidified with 1.6 ml HCl were collected before and after each experiment.



## 2.2 Pharmaceuticals and corrosion inhibitor degradation

---

In the second experimental phase, the removal efficiency of a mix of OMPs was assessed. This phase applied operational parameters expected to yield better performance based on the equipment's capabilities and as demonstrated for MB degradation. Three different OMP mix concentrations were prepared from the OMP stock solutions and tested using NaCl (0.2 M) as the supporting electrolyte. First, experiment OMP-1 involved spiking a high concentration of contaminants to assess degradation by measuring COD. Subsequently, experiments OMP-2 and OMP-3 were conducted with decreased initial concentrations, as shown in Table 3. These experiments were repeated using a different supporting electrolyte ( $K_2SO_4$ ) and also with ROC. The objective of this series was to capture the degradation performance of each contaminant while applying the operational parameters described in Table 2.

### 2.2.1

### Stocks solutions

---

Stock solutions for each compound were prepared in a 250 mL glass beaker with ultrapure water, closed and stored in the fridge. Later, a solution containing a mixture of OMPs was created and spiked into 3 liters of demi water and 0.2 M NaCl, to be treated later with the Magnéli REM reactor.

### 2.2.2

### Experimental Parameters

---

For this experimental series, the operational parameters used are shown in Table 2. Additionally, the initial concentrations of the OMP mixture were prepared as shown in Table 3.

Table 2: Pharmaceuticals degradation.

Current density[mA/cm <sup>2</sup> ]	Volume [L]	Current [A]	Flow [L/min]
10	3	9.4	1.75



Table 3: OMPs spiked mixtures.

Contaminants	OMP-1	OMP-2	OMP-3
OMP	[mg/L]	[ $\mu$ g/L]	[ $\mu$ g/L]
Benzotriazole	3.12	104.97	10.49
4-5-Methyl-benzotriazole	1.91	64.42	6.44
Diclofenac	0.94	31.66	3.16
Hydrochlorothiazide	3.12	104.97	10.49
Metoprolol	3.68	123.77	12.37
Sulfamethoxazole	4.01	134.96	13.49
Metformin	3.66	123.29	12.32
Caffeine	7.99	268.80	26.88
Gabapentin	5.02	168.83	16.88
$\Sigma$	33.45	1,125.67	112.52

### 2.2.3

### Sampling

The degradation was assessed by collecting 10 mL samples in vials every 5 minutes. A dose of sodium thiosulfate was used to quench the samples. The samples were filtered with a 0.2  $\mu$ m filter, and then 2 mL LC-MS vials were prepared by adding 495  $\mu$ L of the sample and 5  $\mu$ L of an OMP internal standard, which were stored in the fridge for later measurement with the LC-MS. Additionally, the collected samples were used to measure COD, with 2 mL per sample (this was only used for OMP-1), and 1 mL per sample for chlorine. Moreover, other samples were obtained as follows: to measure TOC, 40 mL samples were filtered with 0.2  $\mu$ m and acidified with 1.6 ml HCl, collected before and after each experiment. For the IC, 10 mL samples were filtered with 0.2  $\mu$ m.



## 2.3

## ROC treatment

The ROC used in this research was produced at two different drinking water treatment utilities in the Netherlands. Both treated surface water: DWU 1 from the river Vecht and DWU 2 from the Valkenburgse Lake. The water was collected at the production site, transported to the Water Lab, and stored in a fridge at 4 °C. The ROC was pretreated with cation exchange resins to remove the calcium and magnesium content.

### 2.3.1

### Drinking water utility 1

In drinking water utility (DWU 1), water was extracted from the Overijsselsche Vecht River and treated with conventional methods based on sand filters and activated carbon; part of the flow was treated with RO. The produced ROC was then used as influent, and its water quality parameters are presented in Table 4. The electrical conductivity did not change considerably with the softening pre-treatment, remaining at approximately 2.95 mS/cm, while the pH was 8.1 after softening.

Table 4: DWU 1 - ROC water quality.

	No pre-treatment [mg/L]	SD	IX pre-treatment [mg/L]	SD
COD	64.75	±3.55	298.50	±1.5
Ca <sup>2+</sup>	349.67	± 0	1.08	±0.015
Mg <sup>2+</sup>	31.58	±0.085	0.42	±0.014
K	31.79	±0.305	5.87	±0.067
Na	173.13	±3.625	678.11	±0.39
Cl	255.08	±0.43	260.27	±3.62
NO <sub>3</sub>	18.94	±3.185	15.74	±3.185





The drinking water utility 2 (DWU 2) extracts water from the Valkenburgse Meer (Lake) and treats it as follows: First, the water is filtered through a 5 mm sieve; then, it passes through a sand filter system where coagulant addition is evaluated. Next, a 20-micrometer sieve filter precedes ultrafiltration (UF), and finally, the water is conveyed through reverse osmosis (RO). The pilot project treatment scheme is shown in Figure 5. After softening, the electrical conductivity was around 3.08 mS/cm, and the pH was 7.2.

Figure 5: DWU 2 pilot treatment scheme.

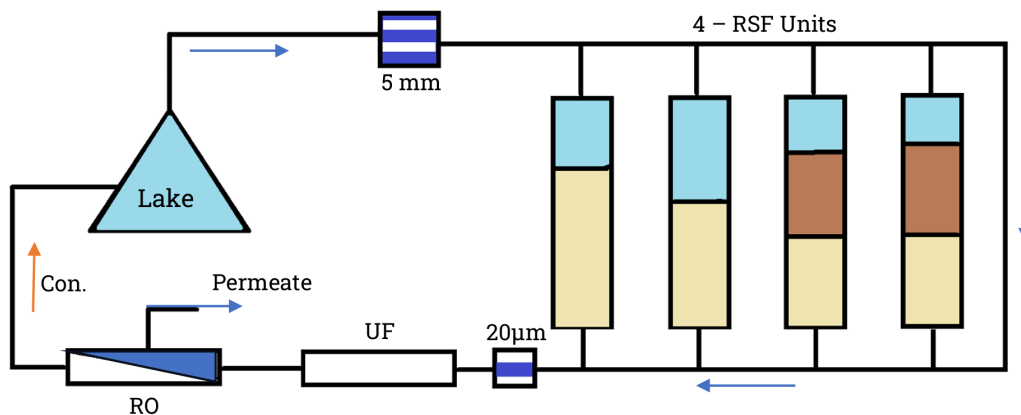


Table 5: DWU 2 - ROC water quality.

	No pre-treatment (mg/L)	SD	IX pre-treatment (mg/L)	SD
COD	56.6	±1.2	77.5	±2.6
Ca <sup>2+</sup>	264.15	± 5.7	6.22	±2.24
Mg <sup>2+</sup>	54.04	±0.99	2.49	±0.156
K	33.96	±1.22	13.35	±1.035
Na	260.51	±1.18	628.71	±8.28
Cl	517.43	±4.99	464.37	±5.205

### 2.3.3

## Experimental Parameters

In these experiments, higher CD were used for PFAS degradation. The ROC of DWU 1 and DWU 2 was tested in different experiments applying a flow rate of 1.75 L/min,  $i$  of 10 [mA/cm<sup>2</sup>], volume of 3 liters, and various CD as shown in Table 6.

Table 6: RO concentrate experiments.

DWU 1		1	2	3	4	5	6
CD	[C/L]	4,000	10,000	20,000	40,000	80,000	120,000
Time	[Hour]	0.35	0.89	1.77	3.55	7.09	10.64
DWU 2		1			4		6
CD	[C/L]	4,000			40,000		120,000
Time	[Hour]	0.35			3.55		10.64

### 2.3.4

## Sampling

The collection of samples varied between the two cases. For DWU 1, triplicate 15 mL vials were collected. In the case of DWU 2, duplicate 100 mL samples were collected and stored in the fridge for later measurements at external laboratories. Additionally, 15 mL samples were used to measure COD and chlorine. More samples were obtained as follows: to measure TOC, 40 mL samples were acidified (1.6 ml HCl) and filtered with a 0.2  $\mu$ m filter, collected before and after each experiment. For IC, a 10 mL vial was filtered with a 0.2  $\mu$ m filter.

### 2.3.5

## Blanco

Around 3 liters of ultrapure water was used to carry out a Blanco sampling. The reactor passed 1.75 L/min for a period of 3 hours, with no current. Samples in duplicates were collected afterwards.



In the first experimental phase, 300 mg MB ( $C_{16}H_{18}ClN_3S$ ), 0.2 mmol sodium chloride (NaCl; Carl Roth) were employed to prepare 3 liters of artificial water solution. Besides, hydrochloric acid 0.1 mol (HCL; Sigma-aldrich) was employed to quench the samples. Later, the OMPs used in the experimental phase 2 were 4-5 methyl-benzotriazole (MeBT; Sigma-aldrich), benzotriazole ( $C_6H_5N_3$ ; Sigma-aldrich), diclofenac ( $C_{14}H_{11}Cl_2NO_2$ ; Sigma-aldrich), hydrochlorothiazide ( $C_7H_8ClN_3O_4S_2$ ; Sigma-aldrich), metoprolol ( $C_{15}H_{25}NO_3$ ; Sigma-aldrich), sulfamethoxazole ( $C_{10}H_{11}N_3O_3S$ ; Sigma-aldrich), metformin ( $C_4H_{11}N_5$ ; Sigma-aldrich), caffeine ( $C_8H_{10}N_4O_2$ ; Sigma-aldrich). Also, sodium thiosulfate solution ( $Na_2S_2O_3 \cdot 5H_2O$ ; Sigma-aldrich) was used to quench the samples. Cation exchange resin was used to remove the hardness (DOWEX Marathon, Dow). Additionally, 0.1 mol solution of hydrochloric acid (HCL; Sigma-aldrich) was used to clean the membrane anode.

The pH was monitored using a sensor Greseninger, G1500+GE 114. The electric conductivity and temperature were checked with a sensor Greseninger GMH 34000 Series. The ions in solution were measured using an ion chromatography unit 930 Compact IC Flex Metrohm. Chlorine measurements were carried out with test kits (Sigma-aldrich) and measured in a spectroquant Nova 60. Hatch test kits were employed to test chemical oxygen demand (COD), Hardness, calcium, and manganese, and measured in spectrophotometer DR3900. Total organic carbon was measured with a TOC analyzer TOC-VCPH, Shimadzu. MB was measured with a UV-spectrometer Termo: Genesys 10s UV-Vis using a wavelength of 664nm. Pharmaceuticals were measured using the LC-MS Acquity-1 class plus, available in the WaterLab at TU Delft. PFAS were analyzed by the drinking water company laboratories and Het Water Laboratorium. These measurements were carried out using also an LC-MS.



# Chapter 3

---

## Results

---

This chapter presents the outcomes of the three experimental phases conducted and the data collected. Each phase was designed to address specific research questions and sub-questions, and the results reflect the insights gained from these studies.

### 3.1 Degradation of Methylene blue

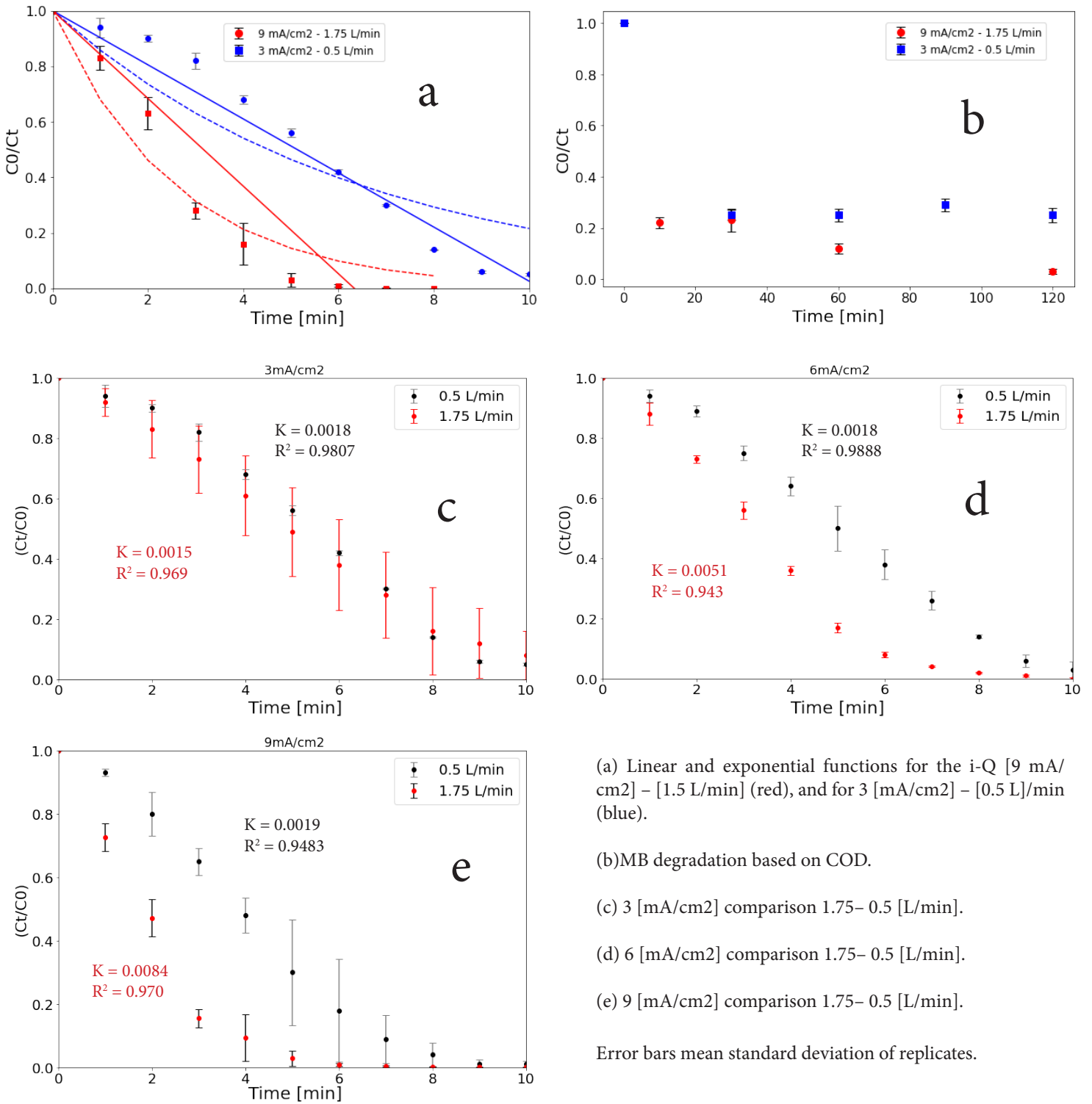
---

The colour removal rates when high current density-flow rate ( $i$ - $Q$ ) was applied compared to low  $i$ - $Q$  are presented in "Figure 6-a". Exponential and linear functions were fitted, and kinetic constants ( $K$ ) were obtained. The rate constant ( $K$ ) indicates that the degradation of MB occurred approximately twice as fast for the high  $i$ - $Q$ . Additionally, in "Figure 6-c, d, e" the degradation rates were compared for high and low flow rates, showing how the flow rate influences the degradation pattern.

In addition, the degradation was also assessed by monitoring COD, with the results shown in "Figure 6-b". The high  $i$ - $Q$  achieved 80% degradation in 15 minutes, while the low  $i$ - $Q$  took approximately 45 minutes. Moreover, the low  $i$ - $Q$  reached a degradation limit after 25 minutes, showing no further change after 2 hours of treatment, whereas the high  $i$ - $Q$  reached a degradation level of 97%. A complete overview of the degradation rates when three different current densities and three different flow rates were applied can be found in "Appendix Figure A3 to A5".



Figure 6: MB degradation rates comparison.



(a) Linear and exponential functions for the  $i$ -Q [9 mA/cm<sup>2</sup>] - [1.5 L/min] (red), and for 3 [mA/cm<sup>2</sup>] - [0.5 L/min] (blue).

(b) MB degradation based on COD.

(c) 3 [mA/cm<sup>2</sup>] comparison 1.75-0.5 [L/min].

(d) 6 [mA/cm<sup>2</sup>] comparison 1.75-0.5 [L/min].

(e) 9 [mA/cm<sup>2</sup>] comparison 1.75-0.5 [L/min].

Error bars mean standard deviation of replicates.



## 3.2 Degradation of pharmaceuticals and corrosion inhibitors

This section presents the results of the experimental phase 2, in which the degradation of a list of OMPs was tested.

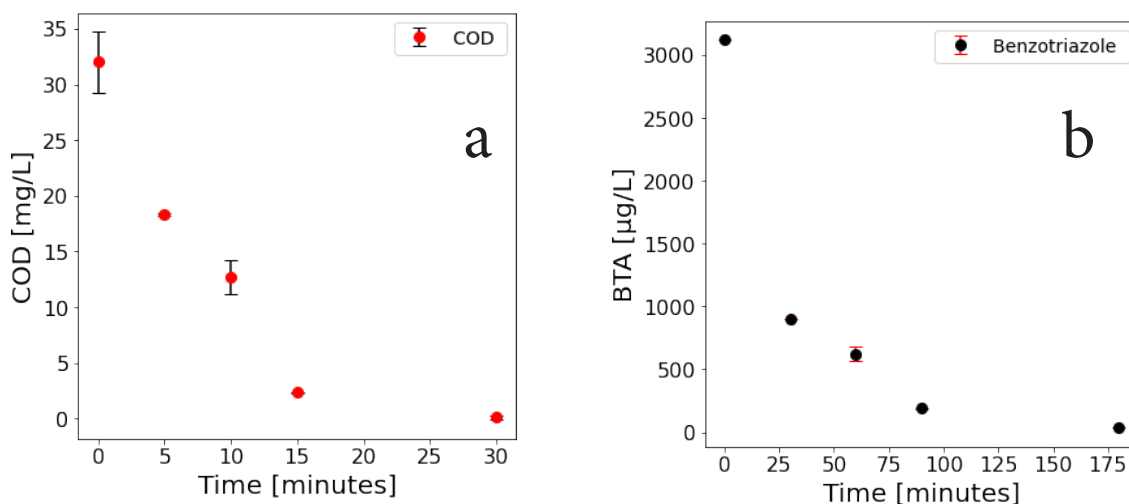
### 3.2.1 Experiment OMP-1

The OMP-1 experimental series with artificial water generated the following results. In Figure 7-a it is shown how the total COD in the solution was reduced by close to 0 [mg/L] in 30 minutes. The LC-MS measurements suggested that most of the OMPs were degraded within 1 hour. However, after 3 hours Benzotriazole was prevalent in the solution as shown in Figure 7-b, with a concentration of 38.21  $\mu\text{g/L}$ .

Despite the high degradation efficiency, it is noticeable that the degradation rate slows down after 15 minutes, entering a more gradual phase. The samples analyzed with the LC-MS were diluted by factors of 100 and 10 to fit within the detection limits of the Water Lab instruments.

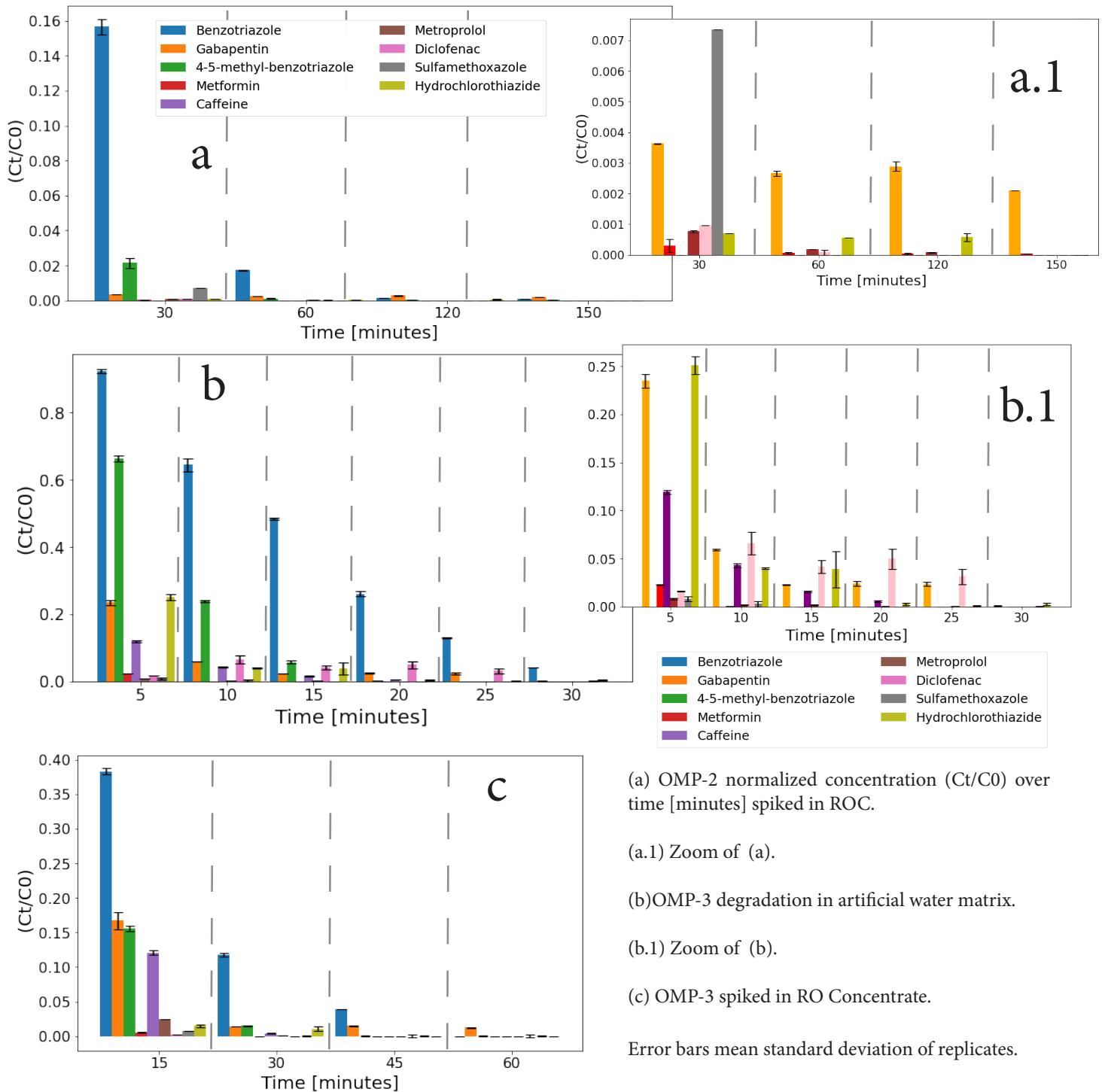
Figure 7: Experiment OMP-1

- (a) COD degradation [mg/L]
  - (b) Benzotriazole degradation [ $\mu\text{g/L}$ ].
- Error bars mean standard deviation of replicates.



For the experiments OMP-2 and OMP-3 degradation performance is shown in Figure 8. Regarding sampling using long periods (1 to 2 hours), the presence of compounds such as Benzotriazole and Gabapentin were identified after treatment in OMP-2 & 3. However, the five-minute sampling turned out to better capture the degradation trend of contaminants for experiment OMP-3 as shown in Figure 8-b.

Figure 8: OMP-2 &amp; 3 experiments.



(a) OMP-2 normalized concentration (Ct/C0) over time [minutes] spiked in ROC.

(a.1) Zoom of (a).

(b) OMP-3 degradation in artificial water matrix.

(b.1) Zoom of (b).

(c) OMP-3 spiked in RO Concentrate.

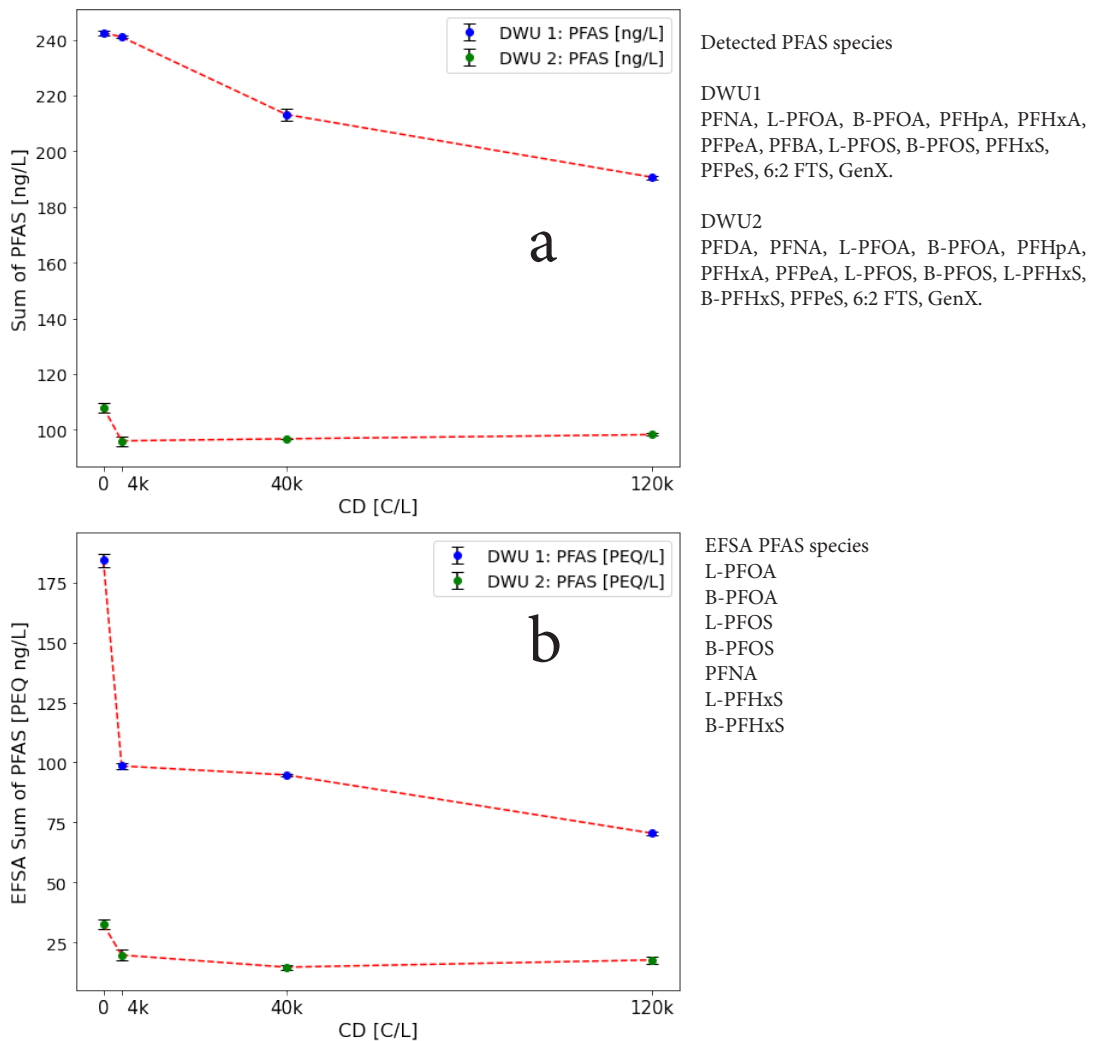
Error bars mean standard deviation of replicates.

In this section, the degradation results for the different PFAS species are presented, which were grouped into Perfluorocarboxylic acids (PFCAs) and Perfluorosulfonic acids (PFSAs). In addition, the total sum of detected PFAS species was used to estimate the overall degradation of these compounds. Figure 9-a shows the sum of the species in [ng/L]. Also, the PFAS sum in PFOA equivalent [PEQ ng/L] is shown in Figure 9-b. In both figures, a dotted red line was plotted to illustrate the connection between the measured data points and to suggest a potential degradation pathway. A degradation trend was observed for DWU 1, whereas DWU 2 exhibited a less effective outcome.

Figure 9: PFAS degradation and charge dosage.

The summaratory of PFAS concentrations in  
 (a) [ng/L], and  
 (b) [PEQ ng/L].

Error bars mean standard deviation of replicates.





The PFAS degradation performance for the detected set of PFAS species belonging to the PFCAs are shown in Figure 10, for DWU 1 (a) and DWU 2 (b). It was observed that with the application of CD, long-chain species exhibited a decreasing concentration trend, while short-chain species initially increased in concentration. When higher CDs were applied, long-chain species continued to degrade slightly, while some short-chain species maintained an increasing trend, and others showed signs of degradation.

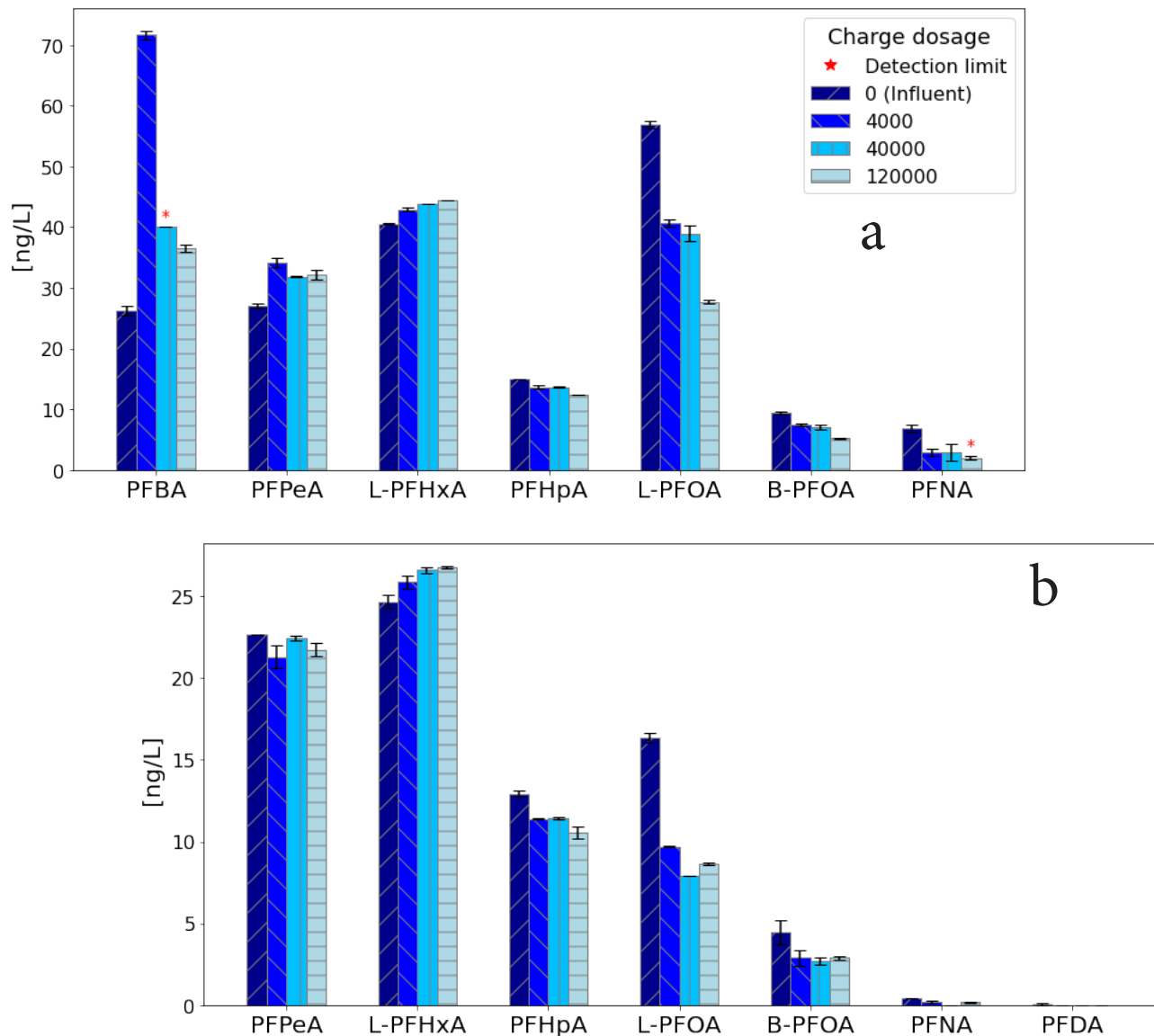
Figure 10: Perfluoro carboxylic acids degradation.

Concentration in [ng/L] of PFCAs

(a) DWU 1

(b) DWU 2

Error bars mean standard deviation of replicates.



The degradation performance of the detected PFAS species within the PFSA for DWU 1 (a) and DWU 2 (b) is presented. Similarly as with PFCAs, a degradation trend was observed for the long-chain components, along with an increase in short-chain species. However, it's important to highlight that the concentrations of these species were low, and very close to the boundaries of detection limits.

Figure 11: Perfluoro sulfonic acids group degradation.

Concentration in [ng/L]

(a) DWU 1

(b) DWU 2

Error bars mean standard deviation of replicates.

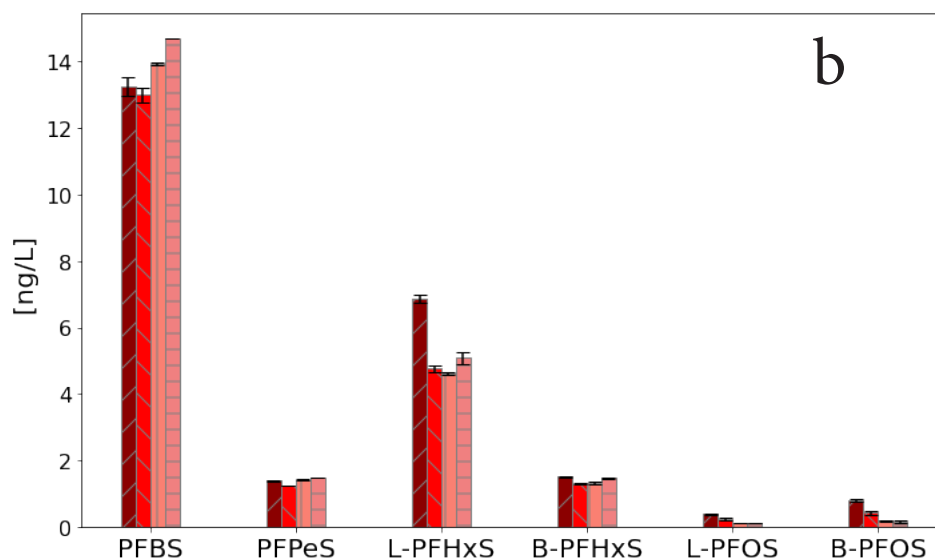
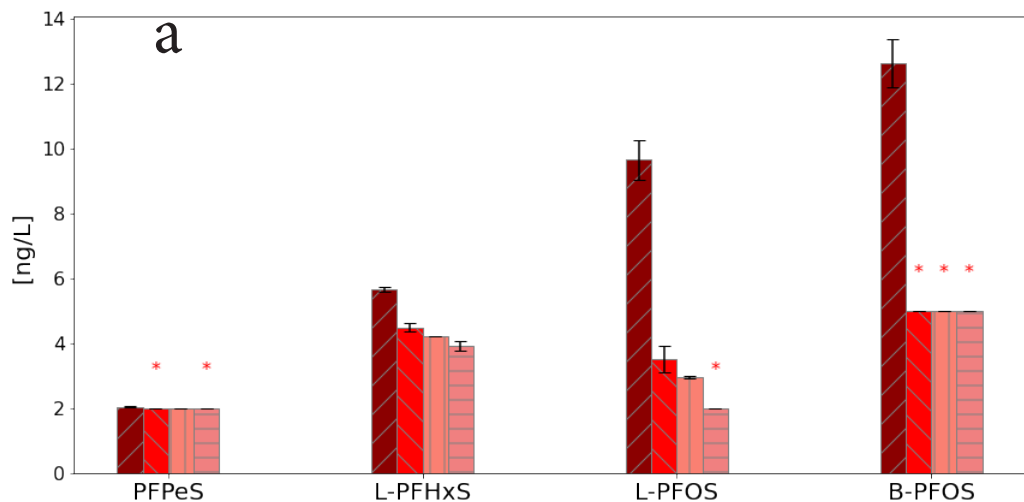
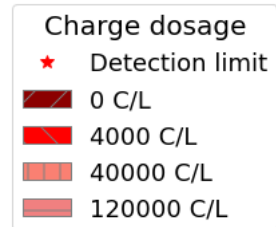


Figure 12 shows the normalized concentration ( $C_t/C_0$ ) of some of the long chain (C-8) species of PFCAs, such as PFOA in its linear and branched versions. As well as chain sizes (C6-C8) of PFASs, such as linear and branched PFOS, and perfluorohexanesulfonate (PFHxS). Also, perfluoroheptanoic acid (PFHpA), a short chain (C7) species of PFCAs, is presented.

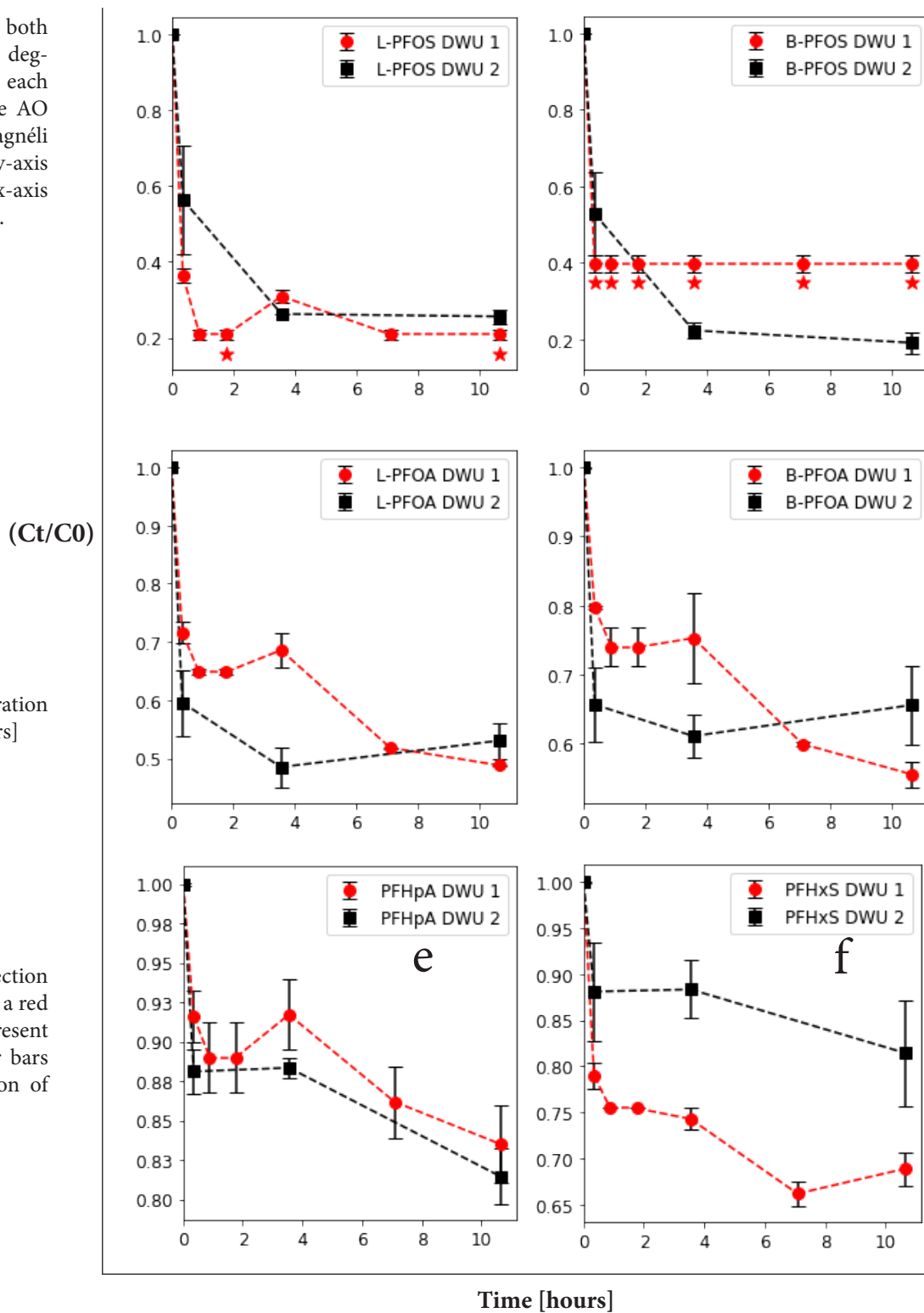
Figure 12: Medium and long chain PFAS degradation.

Each plot compares both DWUs to observe the degradation trend of each component during the AO treatment with the Magnéli REM reactor. In the y-axis the ( $C_t/C_0$ ) and the x-axis are the time in [hours].

Normalized concentration ( $C_t/C_0$ ) over time [hours]

- (a) L-PFOS
- (b) B-PFOS
- (c) L-PFOA
- (d) B-PFOA
- (e) PFHpA
- (f) PFHxS.

Data points below detection limit are remarked with a red star. Dotted lines represent linear regression. Error bars mean standard deviation of replicates.



# Chapter 4

---

## Discussion

---

The Magnéli REM reactor was used to degrade recalcitrant contaminants under the previously mentioned operational parameters, and its performance is further discussed in this section. The relevance of OMP remediation from surface water using the Magnéli REM is addressed, along with the limitations of this study.

### 4.1

### MB degradation

---

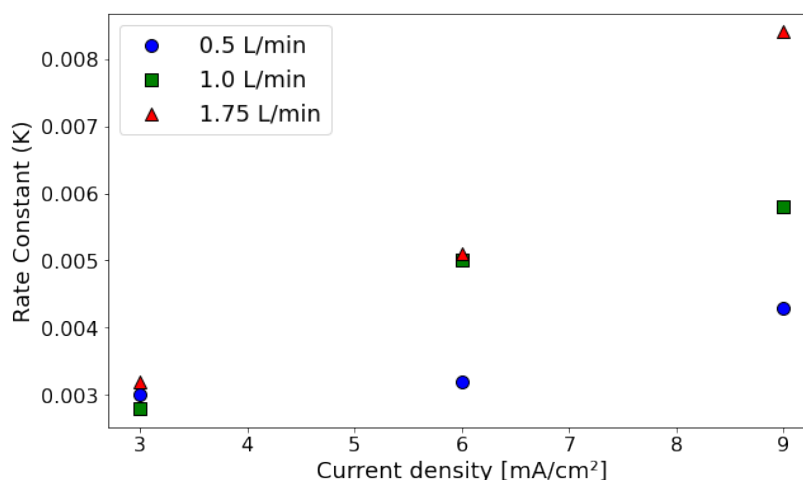
The results indicated that the degradation kinetics of the Magnéli REM reactor when treating MB in artificial water followed either a first-order or a zero-order reaction, depending on the applied  $i$ - $Q$ . These results confirmed the influence of current density and flow rate on degradation performance and kinetics.

A comparison of the calculated rate constants ( $K$ ) and the applied  $i$ - $Q$  is presented in Figure 13. In this figure, it is observed that the kinetics are dependent on applied  $i$ - $Q$ . For low flow rates in combination with low, medium and high current densities, the observed degradation kinetics followed a zero-order reaction (linear trend). But, for high flow rate in combination with high and medium current densities the degradation kinetics followed a first order equation (exponential trend). The application of a higher flow rate triggered an enhancement of the mass transfer of pollutants to the vicinity of the anode (Chaplin et al. 2014).

In addition, the performance could be assessed to determine optimal parameter settings. As demonstrated in another study that treated similar initial concentration of MB applying a  $i$  of  $10 \text{ mA/cm}^2$  showed better results in terms of degradation rates, and energy consumption (Xiong et al. 2022). Furthermore, it is expected that a broader spectrum of applied  $i$ - $Q$  would result in a plot where  $K$  reaches a plateau; beyond this point, increasing either  $i$  or  $Q$  will no longer speed up the degradation rate (Huang et al. 2016).



Figure 13: MB kinetic rates.



Moreover, another parameter that influenced the degradation rate of MB is the initial concentration and type of the supporting electrolyte. The water composition has an impact on the kinetics because indirect oxidation is promoted or muted depending on the structure of the ions in solution. In this experiment, NaCl facilitated the production of chlorinated reactive species, accelerating the color removal during treatment (Panizza et al. 2007). Experiments using a different supporting electrolyte ( $K_2SO_4$ ) showed a slower degradation rate.

Nevertheless, it should be noted that the degradation rates when treating an artificial water matrix will differ from those observed when treating relevant environmental water matrices. As shown when the ROC was spiked with MB, color removal occurred more slowly, as illustrated in “Appendix Figure A16”. This could be a result of interactions between other components in the water matrix and the produced oxidizing agents.

Finally, it is important to point out that when dyes are treated from water, color removal does not necessarily indicate the absence of dye content. This is because MB can undergo oxidation and/or reduction processes that result in a colorless form (Campbell 1963). Therefore, measuring multiple parameters in combination, such as COD or TOC, could provide a better picture of the actual degradation of MB in water.



## 4.2 Pharmaceuticals and corrosion inhibitors degradation

---

The objective of the experimental phase 2 was to determine the degradation performance for a mixed solution (artificial water and ROC) spiked with pharmaceuticals and corrosion inhibitors and subjected to treatment with the Magnéli REM reactor.

### 4.2.1 Preparation of Stock Solutions

---

The preparation of stock solutions was a critical initial step in this experimental series, with each solution prepared solely for its respective compound. These stock solutions were then diluted and measured to confirm that the target concentration was achieved. The material of the containers is important, since some studies suggest a sorption potential for OMPs (Odehnalová et al. 2023). In this study, glass beakers were used. In addition, the use of ultrapure water ensured the non-influence of other compounds present in demi-water such as humic acids (Matsubara et al. 2003). The stock solutions were stored in a refrigerator at 4 °C and wrapped in aluminum foil. These practices help to maintain the integrity and consistency of the experiments, as the concentration of each OMP remains controlled and predictable.

### 4.2.2 OMPs degradation

---

Literature suggests that during AO the degradation mechanisms direct and indirect oxidation could work synergistically to transform contaminants into intermediates, water (H<sub>2</sub>O), dioxide of carbon (CO<sub>2</sub>), and their inorganic forms (Oller et al. 2011). The results showed that the Magnéli REM reactor has capabilities to degrade the list of OMPs from spiked artificial water and ROC. Due to the limitations to measure samples using the LC-MS, the experiment OMP-1 was performed, in which high contaminants concentration was spiked and degradation was assessed using COD. The results showed that 34 mg/L of a OMPs mix were 99.68 % degraded after a CD of 5,640 C/L.

In addition, when OMPs were spiked into ROC, a delayed degradation compared to artificial water was expected. However, the results showed no significant difference in the degradation pattern. This could be due to the matrix content and enriched salt types in the ROC, which may enhance the wetness of the anode and produce radical species from various compounds, as pointed out by Saha et al. (2022). Furthermore, the degradation efficiency of the pharmaceuticals and corrosion inhibitors mix, in artificial water and spiked ROC overpassed 80% after a treatment of 5,640 C/L. Corrosion inhibitors benzotriazole and 4-5 methyl-benzotriazole were the more stable compounds. For pharmaceuticals, gabapentin showed to be the more persistent compound.

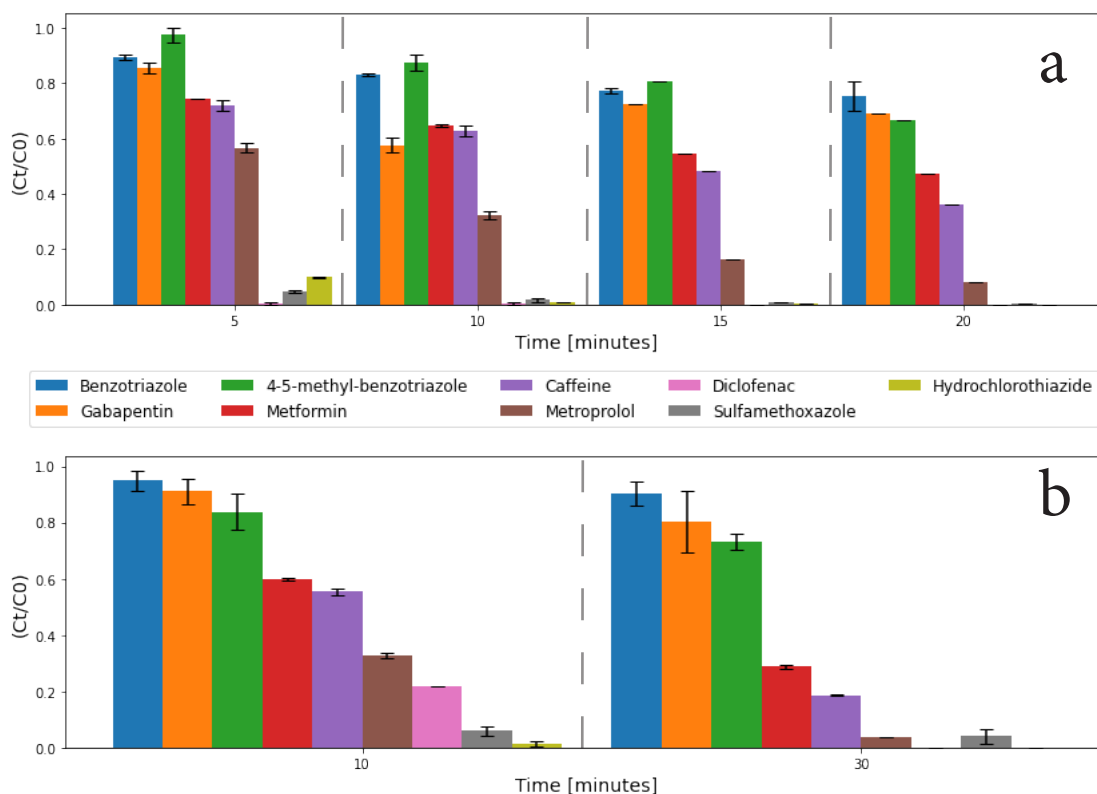


The OMP-2 & OMP-3 experiments were carried out using two different supporting electrolytes NaCl and K<sub>2</sub>SO<sub>4</sub>. The results suggested that the degradation of some compounds is strongly influenced by the presence of chloride. Remarking that chlorine reactive species accelerate the degradation of some compounds. Figure 14 shows the degradation when K<sub>2</sub>SO<sub>4</sub> was used, in which was possible to capture a degradation rate slower than when using NaCl.

As mentioned before, studies suggested that radicals formed from the electrolyte composition impact the degradation of OMPs. Such influence of sulfate and chlorine radicals might have different effects on each compound (Lan et al. 2017). The previous can be confirmed with the results of this research, for instance metformin, caffeine and metoprolol were rapidly degraded in the presence of chloride, while they prevailed in solution when K<sub>2</sub>SO<sub>4</sub> was used. That effect was less noticeable in more stable compounds such as benzotriazole, and 4, 5 methyl-benzotriazole.

Figure 14: Role of supporting electrolyte.

- (a) Degradation in artificial water matrix with K<sub>2</sub>SO<sub>4</sub> as electrolyte OMP-2.  
 (b) OMP-3. Error bars mean standard deviation of replicates.



Among all the tested OMPs, benzotriazole (BTA) was the compound that was the most persistent during the treatment. That behaviour was consistent for different initial concentrations and supporting electrolyte. That is due to the stability properties and structure of BTA (Gelman et al. 2014). No studies were found that tested BTA degradation from ROC water using a Magnéli REM reactor.

However, some work has been done using different anode materials and set-up configurations targeting BTA degradation (Tamilmani et al. 2004). In which, the reported efficiency was very optimistic. As shown in Table 7, in this study 84 & 88 % degradation was achieved after a dosage of 5,649 C/L for OMP-2 and OMP-3 respectively. Besides, the degradation kinetics followed a zero-order reaction, as shown in “Appendix Figure A14”.

In this research, the Magnéli REM showed sufficient capabilities to degrade BTZ from artificial water matrix and from ROC. The effluent BTA concentration in ROC after 28,200 C/L treatment was 114 ng/L ( $\pm 5.9$ ) for the OMP-2. Similarly, the BTA in the effluent for OMP-3 with a dosage 8460 C/L resulted in 814 ng/L ( $\pm 5$ ), a higher CD resulted in the no detection of BTA, which suggests that BTA was fully degraded or reached the lower detection limit of the measurement device.

Additionally, the presence of chloride modestly contributed to accelerate the degradation rate. BTA intermediates were not assessed in this research, and degradation pathways using AO need further investigation. Nevertheless, research has proposed a degradation pathway for BTA and indicated that the intermediates are less toxic than the parent compound (Wang et al., 2022). BTA is a highly toxic compound, so further oxidation of the intermediates is preferred, but that is matter of further research.

Table 7: BTA degradation comparison.

RO Concentrate spiked and treated for 30 minutes.

	C0 ( $\mu\text{g/L}$ )	SD ( $\pm$ )	Log-removal	Ct/C0
OMP-2	104.14	3.17	0.8056	0.1551
OMP-3	20.98	0.04	0.9308	0.1172



As indicated earlier in this report, pharmaceuticals, corrosion inhibitors among other OMPs have become a global threat to ecology. WWTPs are one of the primary sources of these substances entering to water resources (Watkinson et al. 2009). As suggested in the literature and observed in this research, some pharmaceuticals are easily degradable, while others are more resistant to degradation. However, their continuous discharge into surface waters allows them to persist at trace concentrations (Daughton et al. 2004).

Remediating pharmaceuticals in the environment is a difficult task not only due to their recalcitrant properties (Zwiener et al., 2007), but also because its production cannot be easily limited, unlike other OMPs mitigation approaches, due to their medical importance (Moermond & de Rooy 2022). As a result, water authorities are confronted with the urgent challenge of mitigating these compounds to reduce OMPs emissions and safeguard the quality of surface water, but also drinking water production.

Furthermore, the wide variety of OMPs makes it difficult to monitor these substances in the environment. The creation of guidelines to group classes of contaminants based on their toxicity and recalcitrant properties could serve as an approach to deal with this pollution. For instance, the I&W in the Netherlands have set a list of compounds to monitor in WWTPs and discharges to surface water. Such indicators comprise a list of compounds with different characteristics that can be monitored to assess overall OMPs degradation or removal (STOWA et al., 2019). The I&W indicators list includes benzotriazole, 4-5 methyl-benzotriazole, diclofenac, metoprolol, hydrochlorothiazide, and sulfamethoxazole, which were studied in this research.



## 4.3

## RO Concentrate treatment (PFAS)

---

### 4.3.1

### Influent characteristics

---

The sums of the detected PFAS species concentration were 187.87 ng/L for DWU 1 and 108.03 ng/L for DWU 2. In literature, limited studies exist that treated relevant water matrices at low concentration (ng- $\mu$ g/L) and low EC (>3 mS/cm) using Magnéli REM reactor, or other type of anode material. The recovery applied in the RO treatment have influenced the PFAS species contained in the water matrix, higher recoveries are expected to remove long chain, shorter chain species are less rejected (Wang J. et al., 2018). Besides, the water sources source likely have different PFAS contamination origins, and thereby differ in PFAS species content.

### 4.3.2

### Softening pretreatment

---

For the ROC from DWU 1, cation exchange pre-treatment removed 99% of the calcium and magnesium from the water, but also increased 300% the COD. The softening was carried out with a filtration column that contained more IX resin that the needed, which might cause the cross contamination, augmenting the COD exponentially. In the case of DWU 2 the softening was done in batch with low dose of resin, such method did not alter significantly the COD. It can be concluded that during the pretreatment in one hand the overdosage of resin ensured the total removal of hardness but increased the COD, and in the other hand the small dosage did not totally remove the calcium and magnesium.

### 4.3.3

### PFAS degradation

---

The results showed that AO treatment caused the reduction of long chain species (PFOA, PFNA, PFOS PFHpA, PFHxS), and the simultaneous increase of small chain species (PFBA, PFPeA, PFHxA, PFBS). Giving the indication that the production of small chain species exceeds the degradation rate, getting accumulated and increasing their concentration. Note that the concentrations of each PFAS species were very close to the detection limits. That condition made difficult to have a complete degradation overview for certain compounds, for simplicity the concentrations that reached the threshold were assumed to be the value of the detection limit. The complete list of measured PFAS species that were below detection limits is presented in “Appendix Table A6”.

In this study, degradation efficiencies were below observed performances in other studies (Lin et al., 2019). An overview of the PFAS degradation efficiency for the detected PFAS species from the PFCAs and PFSAs are shown in Figure 15, in which it is possible to observe that the applied CD and resulted degradation efficiency. In the case of L-PFOA after a dosage of 120,000 C/L for DWU 1 and DWU 2 respectively, the degradation approximates 51 and 47 %, for PFHxA -8.6 and -9.5 %, for L-PFOS 79 and 74 %, for PFHxS 31 and 25 %.



Moreover, all experiments were carried out separately, but as an analysis exercise the results were grouped to create a data set of applied CD, degradation and time. Thus, an estimation of the degradation rates were calculated. In literature the measure of fluorine ions was used to account for the degradation of PFAS. Unfortunately, in this research the IC measurements for fluorine were below detection (1 mg/l). Making difficult to complete a mass balance analysis.

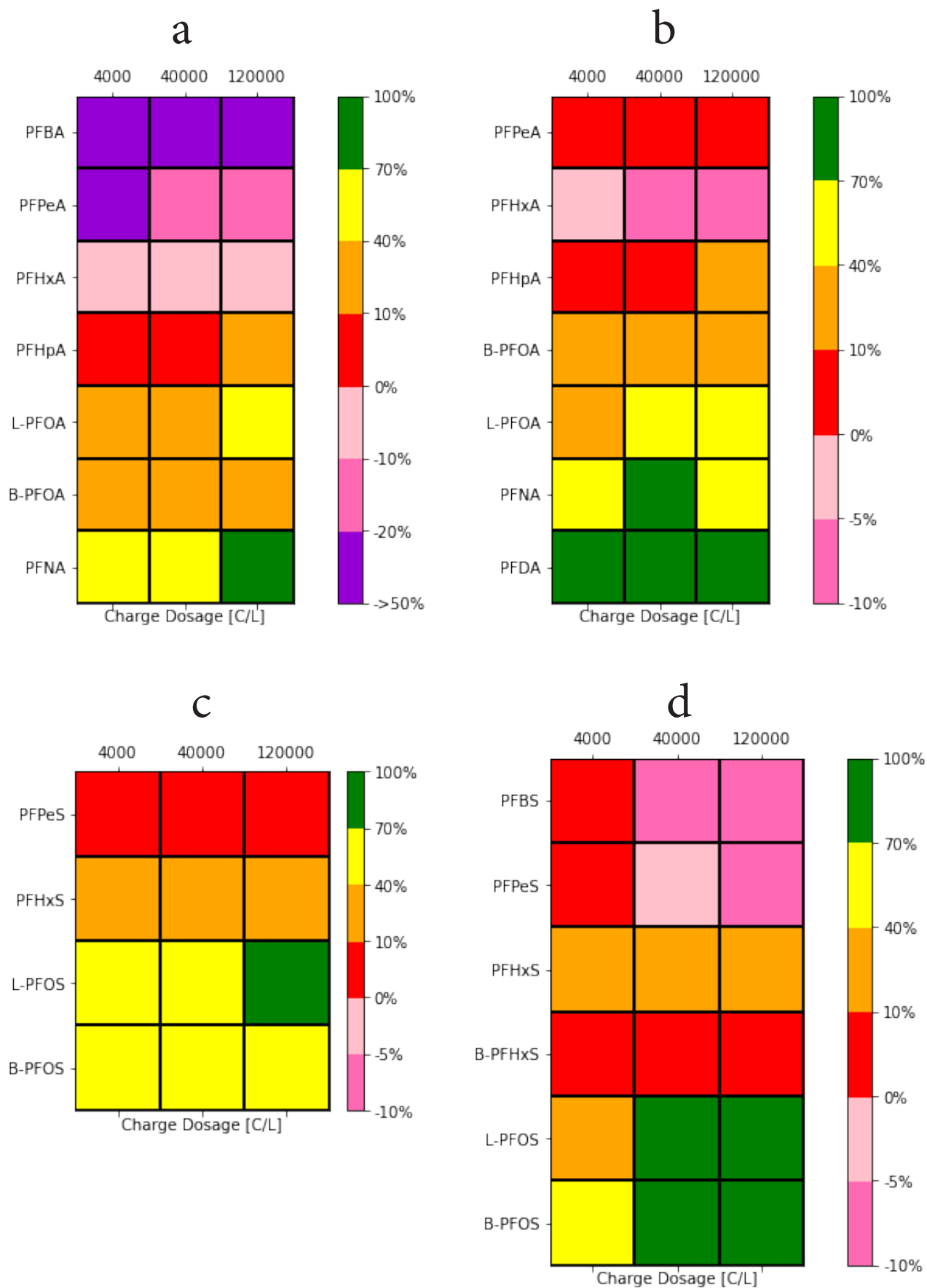
The degradation rates of PFOA and PFBA, when applying same current density as in this research were pointed out to follow a pseudo- first order kinetics (Ma et al., 2024). Other research suggested that PFOS kinetics also follows pseudo- first order kinetics but remarking that r-square were below other analysis indicating a complex process. PFHxA, PFHpA, PFBA, PFPA, and TFA were pointed out as byproducts of PFBA and PFOA degradation. Also, indicated products from PFOS degradation were PFBS, PFPeS, PFHxS, PFHpS. The PFOS kinetics were pointed out as slower than PFOA, due to differences in terminal functions groups potentials for oxidizing (PFOA: 2 V; PFOS: 2.2 V) (Luo et al., 2023).

However, in this research a higher degradation of PFOS was observed compared to PFOA. That can be attributed to the difference in initial concentrations, 9.64 and 0.387 ng/L (PFOS), and 56.82 and 16 ng/L (PFOA) for DWU 1 and DWU 2 respectively. In the above reference PFOA and PFOS degradation were evaluated using approximately the same initial concentration (25 and 20.7 mg/L). Besides, PFOA was identified to be a degradation product of PFOS in previous works. This process was explained with the assumption that PFOS degradation entails the sequential breakdown of the carbon chain (Shi et al., 2019). Notwithstanding, other studies reported no detection of PFCAs when treating PFOS (Fenti et al., 2022).

Furthermore, regarding short chain PFAS degradation, there is limited literature employing Magnéli REM reactors. Density functional theory (DTF) was used to simulate PFBS degradation with a Magnéli anode, but experimental research was not found so far. Then, from existing literature focused on testing BDD, is noted that short chain PFAS, like Gen-X are degraded with AO (Olvera-Vargas et al., 2022). Approaches such as modelling served to propose degradation of PFAS pathways and mechanisms. For instance, DTF to determine free energies of compounds activation, and asses the dependance of chain length to get activated in the anode surface (Pica et al., 2019).



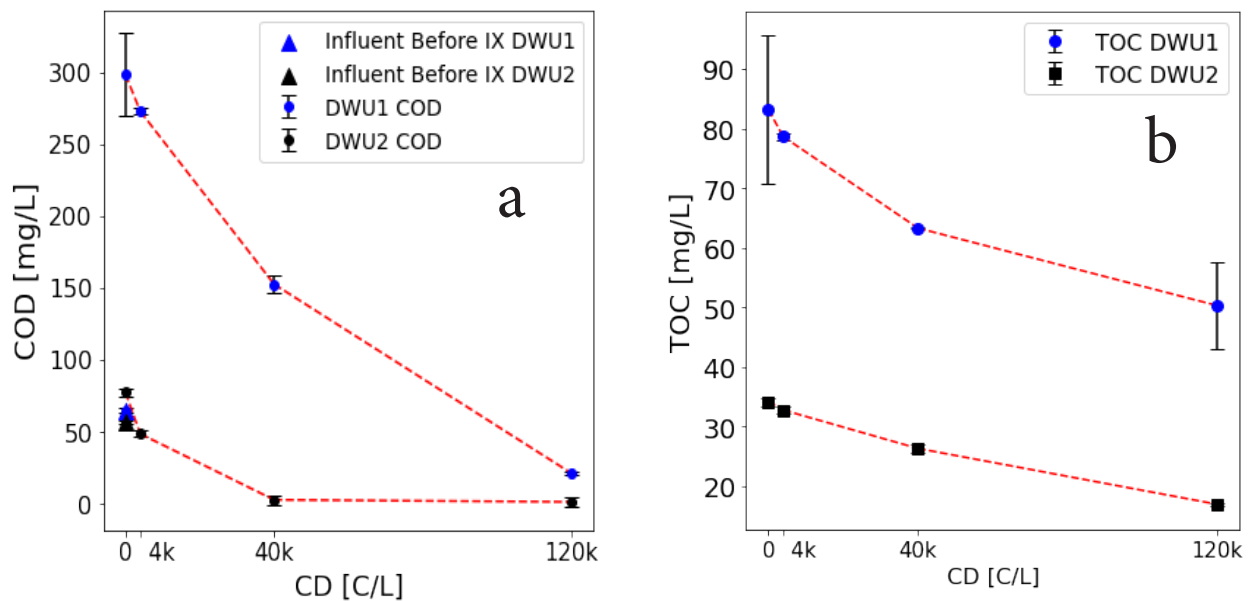
Figure 15: Degradation efficiency. DWU 1 (left) and DWU 2 (right). Perfluoro carboxylic (a & b). Perfluoro sulfonic acids (c & d). Degradation efficiency in (%) and Charge dosage in [C/L].



COD and TOC serve as reliable indicators of water quality and the efficiency of contaminant degradation. Such assessment offers broad applicability, rapid analysis, and indication of treatment efficiency. In literature the assessment of these parameters was used to complement the PFAS degradation performance (Uwayezu et al., 2021). Both measurements were carried out in this research and results are shown in Figure 16. The COD showed a degradation efficiency of 92 and 96 %, for DWU 1 and DWU 2. But, it is important to remark that the COD was altered for the DWU 1 in the pretreatment step. It is assumed that degradation of COD could occur much faster without such contamination. The TOC degradation showed a slower degradation rate 39 and 50 %. For TOC, influent and effluent samples were taken only, which resulted in limited analysis. For future research, it is recommended to make more extensive use of this parameter.

Figure 16: COD and TOC degradation.

- (a) Chemical oxygen demand in [mg/L] and CD in [C/L].  
 (b) Total organic carbon in [mg/L] and CD in [C/L].  
 Error bars mean standard deviation of replicates.



An important indicator for determining the safety of treated effluent for environmental discharge or reuse is the presence of generated toxic products. Necessary measures must be taken to assess the potential formation of these products, such as short-chain PFAS, Trihalo-methanes (THMs), bromate, and other contaminants.

### Shorter chain PFAS

The ROC treatment with the Magnéli REM produced an interesting trend in concentration of short chain PFAS. According to literature, that phenomenon is due to the degradation of longer chains species, which are broken to smaller structures as suggested by (Shi et al., 2019).

In the case of PFCAs group laboratory analyses showed that when charge dosage of 4,000 C/L was applied Perfluorobutanoic acid (PFBA), Perfluoropentanoic acid (PFPeA) and Perfluorohexanoic acid (PFHxA) increased in concentration 175 %, 26 % 5.8 % and respectively for DWU 1. And, for DWU 2, a slightly different trend was observed, PFBA was not detected, PFPeA was reduced with such CD, to later give signs of modest increase when higher CD was applied. It is possible that the peak of the increasing trend was not captured by the measurement which could had occur between 40,000 to 120,000 C/L. Finally, PFHxA also had an augmentation trend from 4.8 to 8.6 %.

In addition, regarding the PFSA group, for DWU 1, perfluorobutane sulfonate (PFBS) was not detected. Perfluoropentanesulfonic acid (PFPeS) was below detection. PFHxS had a reduction tendency. On the other hand, for DWU 2, PFBS was first marginally reduced to later increase 11% when the higher dosage was applied.

Moreover, a CD of 120,000 C/L was not sufficient to completely degrade medium chain species, meaning that short chain will be further produced until the complete degradation of parent compounds. Also, as pointed out by Puttamreddy & Nippatlapalli (2024) short chain species are expected to have more recalcitrant properties than parent compounds, which imply that higher CD is required for its further degradation.

The predominance of ultra short PFAS has become a tendency on water resources impacting directly drinking water production (Zheng et al., 2023). For instance, in this research, an abundant ultra-short chain species is the trifluoroacetic acid (TFA), which was measured only for DWU 1, but can be used as indicator to evaluate the degradation of this ultra-short chain type, and its precursors.

Hence, when applying PFAS remediation is recommended to increase the CD and the flow rate to achieve better degradation rates and/or apply removal techniques after treatment such as IX, in order to safely discharge the effluent in surface water.

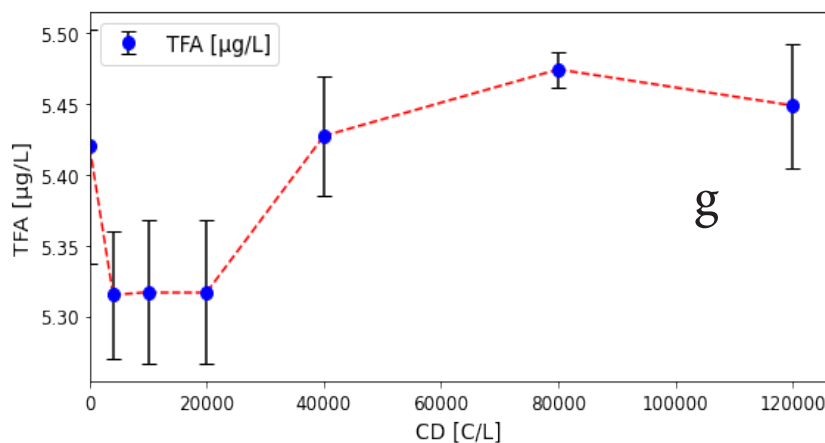
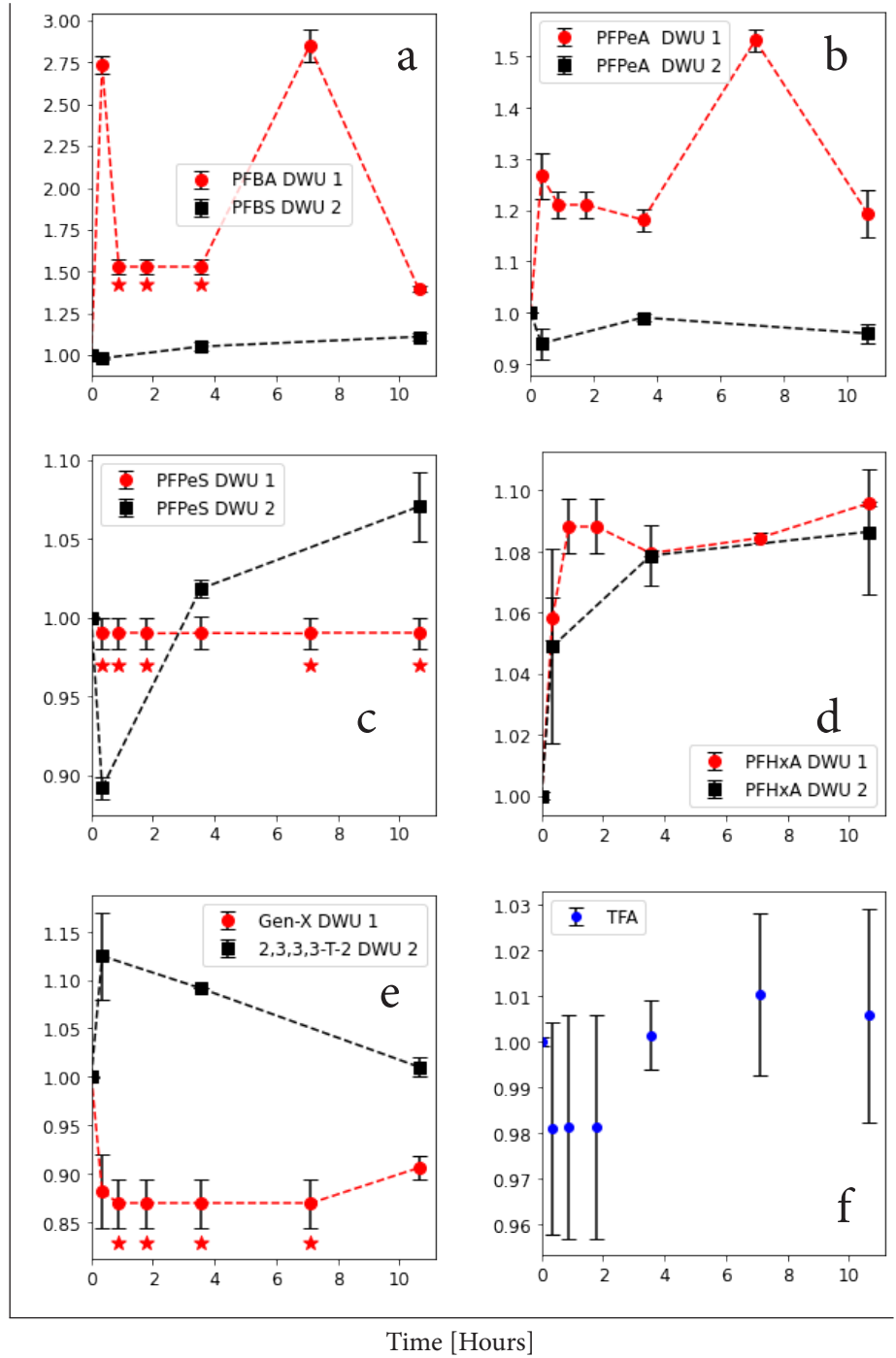


Figure 17: Short chain PFAS.

Normalized concentration ( $C_t/C_0$ ) over time [hours] of short chain species PFCAs, and PFSAs. Data points below detection limit are remarked with a red star. Linear connection between the data points is illustrated with the dotted lines.

(a) PFBA (DWU 2 not detected) and PFBS (DWU2 not detected). (b) PFPeA, (c) PFPeS, (d) PFHxA, (e) Gen-X, (f) TFA ( $C_t/C_0$ ), (g) TFA in [ $\mu\text{g/L}$ ]. Error bars mean standard deviation of replicates.

$C_t/C_0$



## Chlorination by-products

---

The IC measurements proved that the chlorine transformation capabilities of the Magnéli REM are very high. Both RO concentrates contained chloride concentration ranging from (250-450 mg/L), after a charge dosage of 120,000 C/L, dropped to below 50 mg/L. The measurements of free chlorine suggest that chloride was further transformed to other chlorinated reactive species that can be formed such as chlorate ( $\text{ClO}_3^-$ ), perchlorate ( $\text{ClO}_4^-$ ), and chlorine gas ( $\text{Cl}_2$ ). This assessment is essential to determine the toxicity of the effluent and its possible discharge to surface water. In order to avoid further formation of other possible by-products that can be created from chlorination and the presence of other substances for instance humic acids. Such byproducts are THMs, and haloacetic acids (Zhai et al., 2022). Note that the experiments were carried out in a fume hood, reducing the risk of  $\text{Cl}_2$  exposure. However, for further research the usage of  $\text{Cl}_2$  sensor is encouraged or the improvement of the reactor and recirculating tank to measure and capture the produced gas.

## Bromate

---

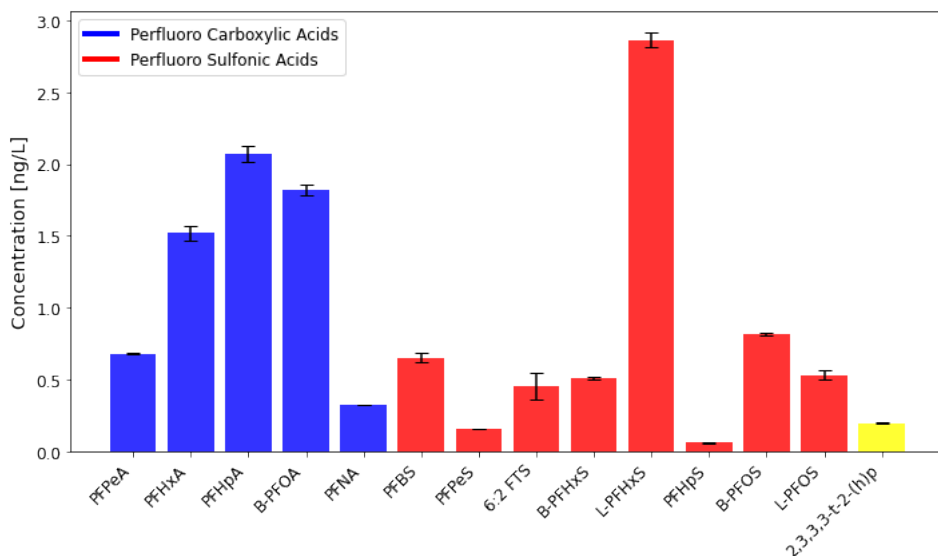
Using the IC measurements, it was found out that the bromide in the influent was approximately 1.6 mg/L, which can be transformed to bromate during AO treatment. Bromate is generated through the oxidation of naturally occurring bromide, a process that can be triggered by the presence of ozone, which is formed by the OER (Von Gunten, & Oliveras, 1998). The formation of this byproduct is one of the main drawbacks and concerns of AOPs and aEOPs (Richardson et al., 2007). Bromate is considered highly toxic and its concentration limit for water production in the Netherlands is 1  $\mu\text{g/L}$ .





The measurement of blanks is very important to assess the PFAS degradation and clarify the fate of the contaminants. By measuring enough blanks, it is possible to evaluate remotion and/or addition of PFAS, since laboratory equipment was pointed out to cause cross contamination (Björnsdotter et al. 2020). For that reason, the use of PTFE was avoided during the experiments. Important to acknowledge that PFAS analysis were expensive. In Figure 18 is shown how a little portion of PFAS species remain in the reactor after treatment. Also, it is interesting to point out that in the blank PFHpS was detected but not in the experiment measurements, which might indicate that some species could have higher affinity to sorbed in the anode pores. Nevertheless, in this research only one blank was tested for the DWU 2 series. No blanks were measured for DWU 1.

Figure 18: Blanco.



PFAS species concentration in blank sample DWU 2. The blank experiment was carried out after the experiment DWU - 4,000 C/L. In which, 3 liters of ultra-pure water were flowed through the REM, for 3 hours. Error bars mean standard deviation of replicates.

### 4.3.7

#### Non detected parent compounds

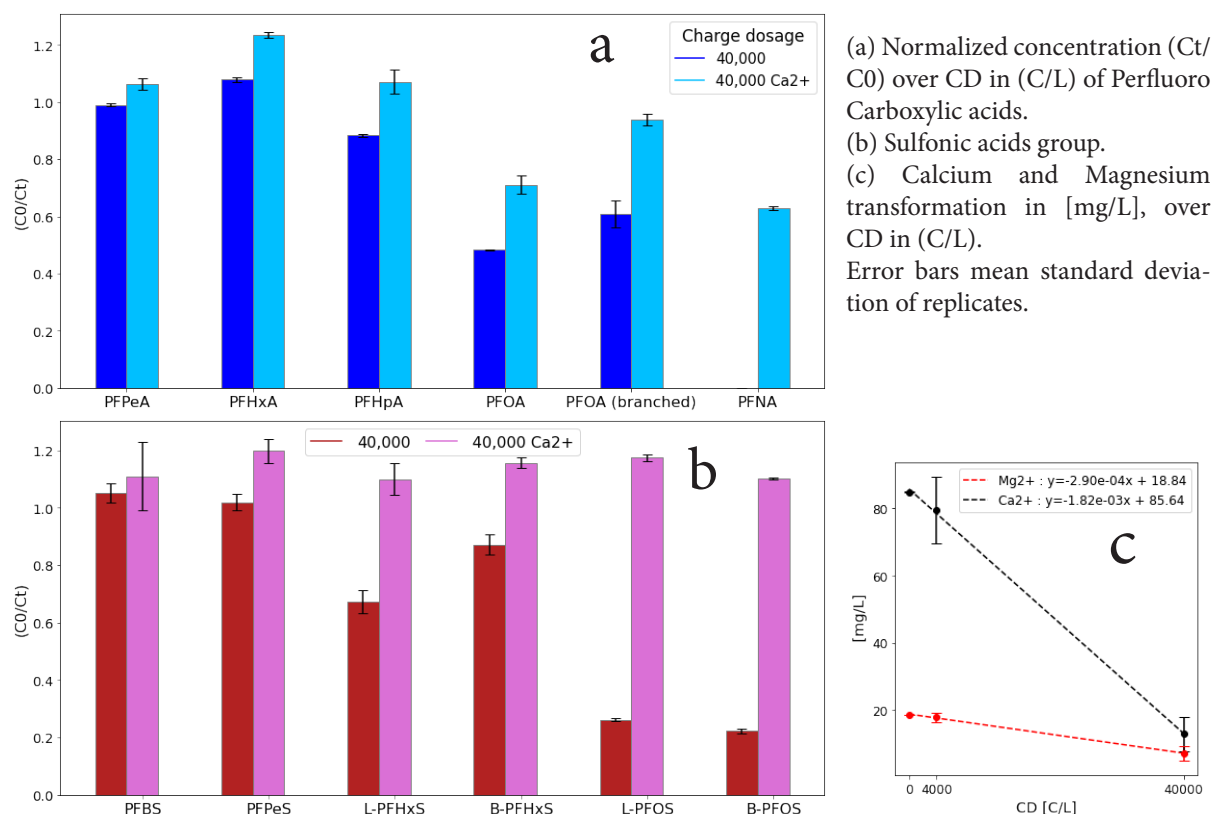
The results showed a trending increase of certain compounds. But the presence of potential parent compounds was not detected. For instance, 6:2 fluorotelomer sulfonamide alkyl betaine (6:2 FTSAB) could be the predecessor compound of 6:2 fluorotelomer sulfonate (6:2 FTS) which increased its concentration after treatment (Trouborst 2016). Besides, degradation efficiencies are altered due to the breakdown of parenting compounds, making it a challenge to assess performance. That confirms the suggestions of literature on the presence of non-detected PFAS that degrade to sum on the PFAS regular indicators (Joerss et al., 2020). In addition, the low degradation of PFOA may be due to the existence of precursors, apart from PFOS, that contribute to the slow degradation of this component.

Experimentation using ROC with a concentration of 82 mg/L  $\text{Ca}^{2+}$  and 17 mg/L  $\text{Mg}^{2+}$  tested the influence that hardness has on the performance of the Magnéli REM. Which is shown in Figure 19 for the concentration of (a) Carboxylic acids and (b) Sulfonic acids groups respectively, when applying a CD of 40,000 C/L.

The results suggest that the hardness content delays the degradation process. According to (Lewis et al., 2023) divalent cations can bind with PFAS to form complexes, such process could decrease the degradation efficiency. Additionally, the presence of calcium and manganese also could trigger scaling on the anode surface, decreasing the effective area. During the operation of the reactor abundant scaling was observed when treating the ROC without pre-treatment. In contrast the pretreated water did not produce scaling and self-cleaning of the system was the dominant maintenance of the reactor. The hardness effect increases while applying higher CD.

Moreover, the scale in flotation might contribute to reducing the mass transfer of the contaminants to reach the anode proximity. Using the IC was possible to capture the precipitation of calcium and magnesium. Showing a decreasing trend with the increase of CD. Therefore, low hardness water is preferred to not reduce the reactor functionality, and not to employ frequent maintenance with chemicals such as acids to remove the produced scaling.

Figure 19: Influence of hardness.

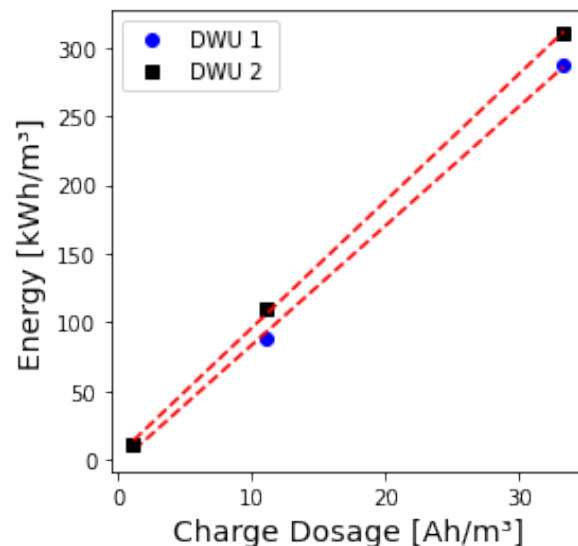


## Energy consumption

## 4.4.1

In this study average energy consumption was approximately 299 kWh/m<sup>3</sup>. That amount is without accounting pumping, mixing and monitoring sensors equipment. The small amount of treated water and the long treatment period resulted in a very high energy consumption compared to other treatment technologies applied in full scale. In literature a current density of 10 mA/cm<sup>2</sup> was suggested to be sufficient to degrade PFOA and PFOS from IX still bottoms in batch and using 2D anode system, with optimistic efficiencies (Lin et al., 2018). But the applied treatment was longer (24 hours).

Figure 20: Energy consumption Magnéli REM.



## Coupling Magnéli REM &amp; Reverse Osmosis

## 4.4.2

The energy consumption of coupling RO and Magnéli REM was assessed using existent literature on these technologies and the data of this research. RO can be coupled to eAOP to treat the RO waste stream and facilitate its discharge back to the environment or for further production of drinking water. Studies that focused on research alternatives to treat ROC and eliminate the contained OMPs are highly relevant for drinking water companies (Yaqub et al., 2022). According to literature, the energy consumption of a UF-RO unit is approximately 0.7 to 1.8 kWh/m<sup>3</sup> (Sim & Mauter, 2021; Tow et al., 2021). Besides, the energy consumption of a Magnéli REM unit will be directly dependent on the applied CD. To give a perspective, AO was pointed out to consume 116 kWh/m<sup>3</sup> in other study (Mostefaoui et al., 2024). Future research is encouraged to assess the coupling of RO and AO for full-scale applications.

Novel components in AO like the 3D Magnéli REM anode aim to upgrade the overall performance of the technology and evolve for its upscaling in the water treatment industry. The employment of several anode materials, shapes, and operative configurations is proof of the robustness and the application of EAOPs.

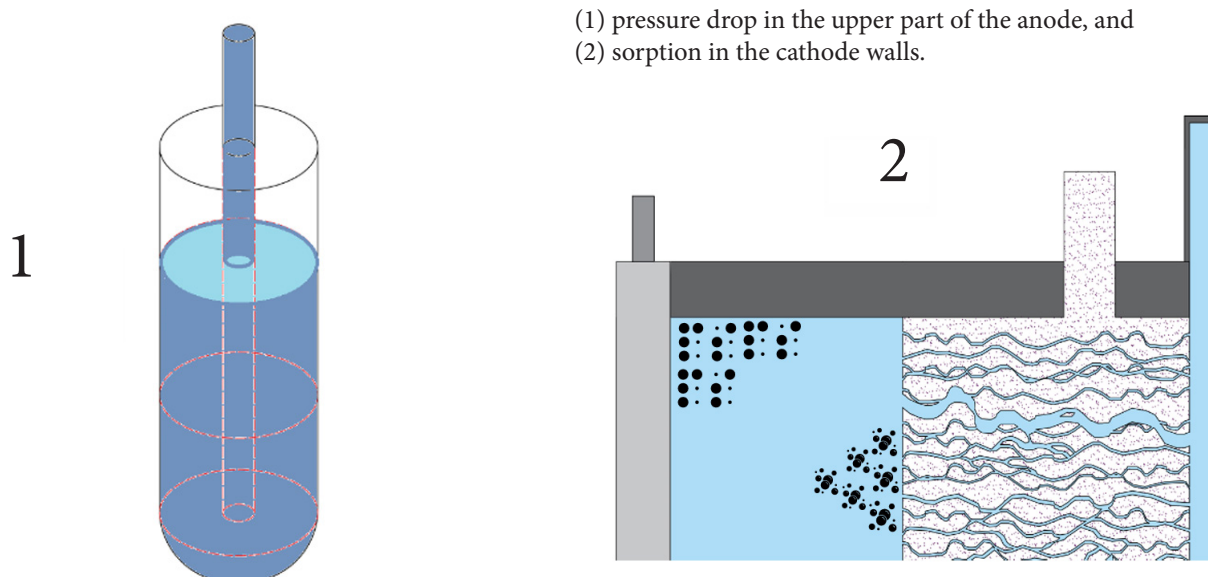
The Magnéli REM reactor is an enclosed system and difficult to access, so it is complicated to evaluate its operation visually. In this section, mechanisms that can minimize the efficiency of the equipment are proposed. Additionally, further research is encouraged to assess these mechanisms.

To begin with, the flow rate was set at 1.75 L/min. However, the REM instruction manual suggests that the reactor can operate at up to 3 L/min. It is expected that the reactor will perform better at the highest possible flow rate. Lower flow rates could not only reduce diffusion and mass transfer but also cause the anode to be incompletely submerged or lead to air being trapped at the top of the reactor, as proposed in Figure 21-1.

In addition, pore blockages can potentially occur at the anode surface due to suspended solids or scaling formation. Precipitates accumulate but also interact with target pollutants, causing a cake layer to formation and reduction of effective reactive spaces in the anode (Mo et al. 2025). Besides, target compounds could get attached to the cathode surface and get entrapped forming dead zones in the reactor edges as shown in Figure 21-2.

Moreover, as discussed earlier the materials used can have an impact on the fate of OMPs, in this research, a crystal baker was used as a recirculating tank (RT). The functionality of the recirculating tank could also have an influence on OMPs degradation. Therefore, researches focused on improving the functionality of the flowthrough REM operational elements are valuable.

Figure 21: Reactor potential efficiency inhibitors.



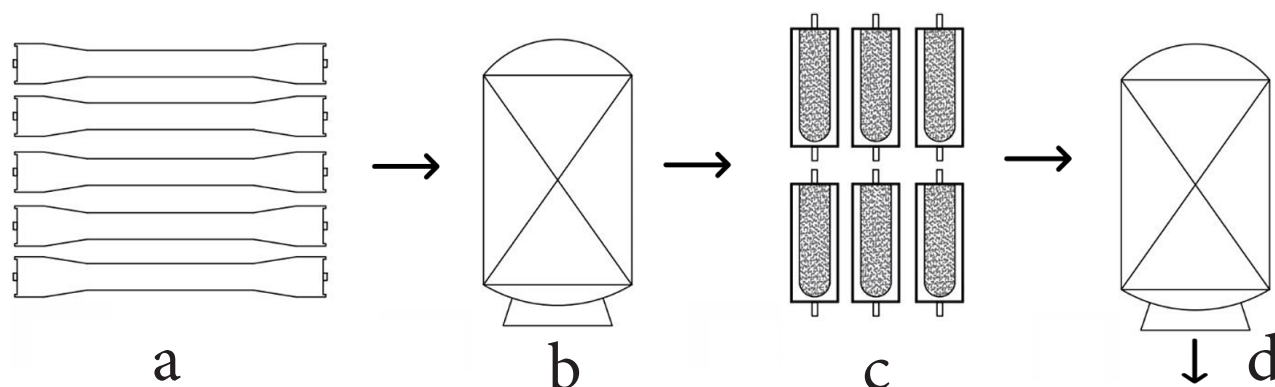
The coupling of RO with AO requires careful consideration to ensure that the ROC is treated safely before being discharged into water resources. The application of higher CDs might further destroy PFAS species. But, as previously mentioned, the production of byproducts is one main drawback of the eAOPs. Short and ultra short-chain PFAS need to be monitored and further investigation is encouraged.

The implementation of IX units before and after the Magnéli REM unit allow to treat the ROC with less risk of scaling during the process, with calcium and manganese removal in the cation exchange. Additionally, after treatment, anion exchange could capture the produced byproducts (short chains, bromate, chlorates, and perchlorates) to prevent their discharge into the environment. The waste produced during the ion exchange process can also be treated in the REM unit. Implementing such a treatment scheme will significantly reduce the chances of disposing of OMPs and byproducts in the effluent that flows into surface water.

Moreover, considering that the effectiveness of PFAS degradation was not very promising compared to other studies, it would be worthwhile to explore combining an additional process to concentrate PFAS in ROC solution and enhance its destruction efficiency. A foam fractionation unit could be a potential approach, and this could be tested in future research.

Figure 22: Treatment scheme.

(a) RO, (b) cation exchange, (c) Magnéli REM reactor unit, (d) anion exchange.



# Chapter 5

---

## 5.1 Conclusion

---

This study aimed to analyze the Magnéli REM reactor's ability to degrade a variety of OMPs at different concentrations but especially at low concentrations comparable to what can be found in the environment. It provided insight into how OMPs with different properties contained in ROC respond to AO treatment.

The first experimental phase helped to understand the functionality of the reactor and assessed the removal kinetics of MB. The observed kinetics corresponded to either a zero-order or first-order reaction, depending on the applied  $i$ -Q. Zero-order kinetics were observed at low flow rates combined with low, medium, and high  $i$ . First-order kinetics were obtained when a high flow rate was applied in combination with high and medium  $i$ . The degradation rate was highly influenced by the applied  $i$ , flow rate, initial concentration, and supporting electrolyte.

The second experimental phase evaluated the performance of degrading a mixture of OMPs (Pharmaceuticals and corrosion inhibitors). Overall degradation efficiency was good when treating ROC and artificial water matrix containing NaCl. Pharmaceuticals and corrosion inhibitors spiked in artificial water matrix and ROC were degraded above 80% after applying a charge dosage of 5.64 kC/L. Benzotriazole, 4-5-methyl-benzotriazole, and gabapentin were the compounds that showed more resistance to degradation. Additionally, degradation rates were influenced by the supporting electrolyte.

In the third and final experimental phase, the degradation of PFAS was explored. Results suggest that applying a CD of 120 kC/L resulted in average PFOA and PFOS degradation rates of 49.5% and 76.90%, respectively, for DWU 1 and DWU 2. The PFAS degradation efficiency was low compared with other studies. Besides, the degradation of short-chain species was not very effective with the applied treatment. Also, the average energy consumption was approximately 299 kWh/m<sup>3</sup>. The estimated value is significantly higher than what is typically consumed in large-scale applications.

Furthermore, water hardness inhibits the degradation capacity of this technology by reducing the effective area due to scaling, which increases maintenance requirements. The application of softening pre-treatment is essential to facilitate the functionality of the system.

To conclude, the Magnéli REM reactor has been shown to be capable of degrading a variety of OMPs and remediating ROC produced in drinking water facilities in the Netherlands. The application of higher current densities (CDs) could enhance the degradation of PFAS species. Further research is recommended to assess ultrashort-chain PFAS, such as TFA, which was abundant in ROC-DWU 1 and minimally degraded. Additionally, studies should focus on halogenated compounds, bromate, chlorates, and perchlorates, as the removal of these compounds after treatment is essential to ensure safe effluent discharge into the environment.



Further research on the degradation of recalcitrant compounds like PFAS is highly recommended. Given the high cost and specialized equipment required for such analyses, this type of research is often limited in certain parts of the world. However, it is crucial for various stakeholders to invest in and expand studies on PFAS in water resources, particularly regarding drinking water.

To more accurately determine the kinetics in degradation experiments, increasing the sampling frequency is advised, along with collecting blank samples before and after equipment operation. Additionally, exploring new measurement methods that would enable more frequent sampling at a lower cost is important.

In addition, since the analyses in this research were conducted in different laboratories, the detection limits vary among them. It is crucial to identify these limits and implement treatment strategies that facilitate a more objective assessment of compound degradation.

As noted earlier in the report, the degradation of certain PFAS species was not very promising. Therefore, it is recommended to explore the combination of another type of treatment to increase PFAS concentrations in the ROC and further examine its AO degradation effectiveness. It is important to note that pretreatment to reduce water hardness is essential to prevent scaling in the system. Also, evaluating the impact of cation exchange pretreatment is recommended to determine how it influences PFAS content.

Moreover, it is strongly recommended to continue AO studies that focus on the byproducts of various PFAS species, particularly ultra-short chain compounds. Further research is crucial for gaining insights into the degradation rates of these substances.

Finally, in order to enhance the understanding of PFAS degradation processes, it is highly recommended to incorporate alternative research tools such as computational modeling. These tools can provide valuable insights into the complex chemical reactions and mechanisms at play, allowing researchers to predict the behavior of PFAS under various conditions. By simulating different scenarios, computational models can help identify the most effective treatment strategies, optimize experimental design, and reduce the need for costly and time-consuming laboratory analyses.





# References

## References

Akpan E., Singh A., Lgaz H., Quadri T., Shukla S., Mangla B., Dwivedi A., Dagdag O., Sheetal, Inyang E., Ebenso E., (2024)., Coordination compounds as corrosion inhibitors of metals: A review, *Coordination Chemistry Reviews*, Volume 499, 215503, ISSN 0010-8545., <https://doi.org/10.1016/j.ccr.2023.215503>.

Almassi, S., Li, Z., Xu, W., Pu, C., Zeng, T., & Chaplin, B. P. (2019). Simultaneous Adsorption and Electrochemical Reduction of N-Nitrosodimethylamine Using Carbon-TiO<sub>2</sub> Composite Reactive Electrochemical Membranes. *Environmental Science & Technology*, 53(2), 928–937. <https://doi.org/10.1021/acs.est.8b05933>.

Alotaibi, M.D., Patterson, B.M., McKinley, A.J., Reeder, A., & Furness, A. (2015). Benzotriazole and 5-methylbenzotriazole in recycled water, surface water and dishwashing detergents from Perth, Western Australia: analytical method development and application. *Environmental science. Processes & impacts*, 17 2, 448-57.

Andersson, S., Coll'én, B., Kuylenstierna, U., Magneli, A., (1957). Pure Analysis Studies on the Titanium-Oxygen System. *Acta Chem. Scand.* 11, 1641–1652.

Arif, A.F., Balgis, R., Ogi, T., Iskandar, F., Kinoshita, A., Nakamura, K., Okuyama, K., (2017). Highly conductive nano-sized Magneli phases titanium oxide (TiO<sub>x</sub>). *Sci. Rep.* 7, 1–9. <https://doi.org/10.1038/s41598-017-03509-y>.

Appleman, T. D., Higgins, C. P., Quiñones, O., Vanderford, B. J., Kolstad, C., Zeigler-Holady, J. C., & Dickenson, E. R. (2014). Treatment of poly- and perfluoroalkyl substances in U.S. full-scale water treatment systems. *Water research*, 51, 246–255. <https://doi.org/10.1016/j.watres.2013.10.067>.

Beghin, M., Schmitz, M., Betoulle, S., Palluel, O., Baekelandt, S., Mandiki, S. N. M., Gillet, E., Nott, K., Porcher, J.-M., Robert, C., Ronkart, S., & Kestemont, P. (2021). Integrated multi-biomarker responses of juvenile rainbow trout (*Oncorhynchus mykiss*) to an environmentally relevant pharmaceutical mixture. *Ecotoxicology and Environmental Safety*, 221, 112454. <https://doi.org/10.1016/j.ecoenv.2021.112454>.

Ben, W., Zhu, B., Yuan, X., Zhang, Y., Yang, M., & Qiang, Z. (2018). Occurrence, removal and risk of organic micropollutants in wastewater treatment plants across China: Comparison of wastewater treatment processes. *Water research*, 130, 38–46. <https://doi.org/10.1016/j.watres.2017.11.057>.





- Belkouteb, N., Franke, V., McCleaf, P., Köhler, S., & Ahrens, L. (2020). Removal of per- and polyfluoroalkyl substances (PFASs) in a full-scale drinking water treatment plant: Long-term performance of granular activated carbon (GAC) and influence of flow-rate. *Water research*, 182, 115913. <https://doi.org/10.1016/j.watres.2020.115913>.
- Bhadouria, R., Tripathi, S., Singh, P., Singh, R., & Singh, H. P. (2024). Organic micropollutants in aquatic and terrestrial environments. Springer. <https://doi.org/10.1007/978-3-031-48977-8>.
- Björnsdotter, M. K., Yeung, L. W. Y., Kärrman, A., & Ericson Jogsten, I. (2020). Challenges in the analytical determination of ultra-short-chain perfluoroalkyl acids and implications for environmental and human health. *Analytical and Bioanalytical Chemistry*, 412(20), 4785–4796. <https://doi.org/10.1007/s00216-020-02692-8>.
- Brião V., Magoga, Hemkemeier J., Brião M., Girardelli E, Sbeghen L., Favaretto L., Danúbia. (2014). Reverse osmosis for desalination of water from the Guarani Aquifer System to produce drinking water in southern Brazil. *Desalination*. 344. 402–411. 10.1016/j.desal.2014.04.008.
- Brillas, E., Sirés, I., & Oturan, M. A. (2009). Electro-Fenton process and related electrochemical technologies based on Fenton's reaction chemistry. *Chemical reviews*, 109(12), 6570–6631. <https://doi.org/10.1021/cr900136g>.
- Boxall, A. B.; Johnson, P.; Smith, E. J.; Sinclair, C. J.; Stutt, E.; Levy, L. S. (2006). Uptake of Veterinary Medicines from Soils into Plants. *J. Agric. Food Chem.*, 54, 2288–2297.
- Buck, R. C., Franklin, J., Berger, U., Conder, J. M., Cousins, I. T., de Voogt, P., Jensen, A. A., Kannan, K., Mabury, S. A., & van Leeuwen, S. P. (2011). Perfluoroalkyl and polyfluoroalkyl substances in the environment: terminology, classification, and origins. *Integrated environmental assessment and management*, 7(4), 513–541. <https://doi.org/10.1002/ieam.258>.
- Campbell, J. A. (1963). Kinetics—Early and often. *Journal of Chemical Education*, 40(11), 578. <https://doi.org/10.1021/ed040p578>.
- Carter, K. E., & Farrell, J. (2008). Oxidative Destruction of Perfluorooctane Sulfonate Using Boron-Doped Diamond Film Electrodes. *Environmental Science & Technology*, 42(16), 6111.
- Chaplin B.P. (2014). Critical review of electrochemical advanced oxidation processes for water treatment applications. *Environmental Sciences: Processes and Impacts*, 16(6), 1182–1203. <https://doi.org/10.1039/c3em00679d>.
- Chen, G., Feng, Q., & Wang, J. (2020). Mini-review of microplastics in the atmosphere and their risks to humans. *Science of the Total Environment*, 703. <https://doi.org/10.1016/j.scitotenv.2019.135504>.



Chiang, L.-C., Chang, J.-E., & Wen, T.-C. (1995). Indirect oxidation effect in electrochemical oxidation treatment of landfill leachate. *Water Research*, 29(2), 671–678. [https://doi.org/10.1016/0043-1354\(94\)00146-X](https://doi.org/10.1016/0043-1354(94)00146-X).

Chow, S. J., Ojeda, N., Jacangelo, J. G., & Schwab, K. J. (2021). Detection of ultrashort-chain and other per- and polyfluoroalkyl substances (PFAS) in U.S. bottled water. *Water Research*, 201. <https://doi.org/10.1016/j.watres.2021.117292>.

Christou, A.; Karaolia, P.; Hapeshi, E.; Michael, C.; FattaKassinos, D. (2017). Long-Term Wastewater Irrigation of Vegetables in Real Agricultural Systems: Concentration of Pharmaceuticals in Soil, Uptake and Bioaccumulation in Tomato Fruits and Human Health Risk Assessment. *Water Res.* 2017, 109, 24–34.

Comninellis, C. (1994). Electrocatalysis in the electrochemical conversion/combustion of organic pollutants for waste-water treatment. *Electrochimica Acta*, 39(11), 1857–1862. [https://doi.org/10.1016/0013-4686\(94\)85175-1](https://doi.org/10.1016/0013-4686(94)85175-1).

Cordner, A., Brown, P., Cousins, I. T., Scheringer, M., Martinon, L., Dagorn, G., Aubert, R., Hosea, L., Salvidge, R., Felke, C., Tausche, N., Drepper, D., Liva, G., Tudela, A., Delgado, A., Salvatore, D., Pilz, S., & Horel, S. (2024). PFAS Contamination in Europe: Generating Knowledge and Mapping Known and Likely Contamination with “Expert-Reviewed” Journalism. *Environmental Science & Technology*, 58(15), 6616–6627. <https://doi.org/10.1021/acs.est.3c09746>.

D’Almeida, M., Sire, O., Lardjane, S., & Duval, H. (2020). Development of a new approach using mathematical modeling to predict cocktail effects of micropollutants of diverse origins. *Environmental Research*, 188, 109897. <https://doi.org/10.1016/j.envres.2020.109897>.

Daughton, C. G., (2004). Non-Regulated Water Contaminants: Emerging Research. *Environ. Impact Assess. Rev.* 2004, 24, 711–732.

Davis, S. N., Klumker, S. M., Mitchell, A. A., Coppage, M. A., Labonté, J. M., & Quigg, A. (2024). Life in the PFAS lane: The impact of perfluoroalkyl substances on photosynthesis, cellular exudates, nutrient cycling, and composition of a marine microbial community. *The Science of the Total Environment*, 927, 171977. <https://doi.org/10.1016/j.scitotenv.2024.171977>.

De Sousa, M. L., dos Santos, D. Y. A. C., Chow, F., & Pompêo, M. L. M. (2021). Caffeine as a contaminant of periphyton: ecological changes and impacts on primary producers. *Ecotoxicology*, 30(4), 599–609. <https://doi.org/10.1007/s10646-021-02381-x>.

Dixit, F., Dutta, R., Barbeau, B., Berube, P., & Mohseni, M. (2021). PFAS removal by ion exchange resins: A review. *Chemosphere*, 272, 129777. <https://doi.org/10.1016/j.chemosphere.2021.129777>.



Domingo, J. L., Jogsten, I. E., Eriksson, U., Martorell, I., Perelló, G., Nadal, M., & Bavel, B. v. (2012). Human dietary exposure to perfluoroalkyl substances in Catalonia, Spain. Temporal trend. *Food Chemistry*, 135(3), 1575–1582. <https://doi.org/10.1016/j.foodchem.2012.06.054>.

East, A., Anderson, R. H., & Salice, C. J. (2021). Per- and Polyfluoroalkyl Substances (PFAS) in Surface Water Near US Air Force Bases: Prioritizing Individual Chemicals and Mixtures for Toxicity Testing and Risk Assessment. *Environmental Toxicology and Chemistry*, 40(3), 859–870. <https://doi.org/10.1002/etc.4893>.

EPA (U.S. Environmental Protection Agency). (2019). Validated test method 8327: Per- and polyfluoroalkyl substances (PFAS) using external standard calibration and multiple reaction monitoring (MRM) liquid chromatography/tandem mass spectrometry (LC/MS/MS). February.

Fan, X., Zhao, H., Liu, Y., Quan, X., Yu, H., & Chen, S. (2015). Enhanced permeability, selectivity, and antifouling ability of CNTs/Al<sub>2</sub>O<sub>3</sub> membrane under electrochemical assistance. *Environmental Science & Technology*, 49(4), 2293–2300. <https://doi.org/10.1021/es5039479>.

Fenti, A., Jin, Y., Rhoades, A. J. H., Dooley, G. P., Iovino, P., Salvestrini, S., Musmarra, D., Mahendra, S., Peaslee, G. F., & Blotvogel, J. (2022). Performance testing of mesh anodes for in situ electrochemical oxidation of PFAS. *Chemical Engineering Journal Advances*, 9. <https://doi.org/10.1016/j.ceja.2021.100205>.

Ferdig, M.; Kaleta, A.; Buchberger, W., (2005). Improved Liquid Chromatographic Determination of Nine Currently Used (Fluoro) Quinolones with Fluorescence and Mass Spectrometric Detection for Environmental Samples. *J. Sep. Sci.* 2005, 28, 1448–1456.

Ganiyu, S. O., van Hullebusch, E. D., Cretin, M., Esposito, G., & Oturan, M. A. (2015). Coupling of membrane filtration and advanced oxidation processes for removal of pharmaceutical residues: A critical review. *Separation and Purification Technology: Part 3*, 156, 891–914. <https://doi.org/10.1016/j.seppur.2015.09.059>.

Gonzalez-Alonso, S.; Merino, L. M.; Esteban, S.; de Alda, M. L.; Barcelo, D.; Duran, J. J.; Lopez-Martínez, J.; Acena, J.; Perez, S.; Mastroianni, N. (2017). Occurrence of Pharmaceutical, Recreational and Psychotropic Drug Residues in Surface Water on the Northern Antarctic Peninsula Region. *Environ. Pollut.*, 229, 241–254.

Hartmann, J. (2022). Being prepared for the drinking water contaminants of tomorrow: An interdisciplinary approach for the proactive risk governance of emerging chemical and microbial drinking water contaminants. [Dissertation (TU Delft), Delft University of Technology]. <https://doi.org/10.4233/uuid:666aa030-557f-4a68-bf6e-8a464a3f0b9c>.

Hashimi MH, Hashimi R, Ryan Q (2020) Toxic effects of pesticides on humans, plants, animals, pollinators and beneficial organisms. *APRJ* 5:37–47. <http://www.sdiarticle4.com/reviewhistory/59338>.



Hoffman, K., Webster, T.F., Bartell, S.M., Weiskopf, M.G., Fletcher, T., Vieira, V.M., (2011). Private drinking water wells as a source of exposure to perfluorooctanoic acid (PFOA) in communities surrounding a fluoropolymer production facility. *Environ. Health Perspect.* 119 (1), 92e97.

Hori, H., Nagaoka, Y., Yamamoto, A., Sano, T., Yamashita, N., Taniyasu, S., Kutsuna, S., Osaka, I., & Arakawa, R. (2006). Efficient decomposition of environmentally persistent perfluorooctanesulfonate and related fluorochemicals using zerovalent iron in subcritical water. *Environmental science & technology*, 40(3), 1049–1054. <https://doi.org/10.1021/es0517419>.

Huang, G., Yao, J., Pan, W., & Wang, J. (2016). Industrial-scale application of the plunger flow electro-oxidation reactor in wastewater depth treatment. *Environmental Science and Pollution Research*, 23(18), 18288–18295. <https://doi.org/10.1007/s11356-016-7033-2>.

Huang, D., Wang, K., Niu, J., Chu, C., Weon, S., Zhu, Q., Lu, J., Stavitski, E., & Kim, J.-H. (2020). Amorphous Pd-Loaded Ti<sub>4</sub>O<sub>7</sub> Electrode for Direct Anodic Destruction of Perfluorooctanoic Acid. *Environmental Science & Technology*, 54(17), 10954. <https://doi.org/10.1021/acs.est.0c03800>.

Joerss, H., Schramm, T.-R., Sun, L., Guo, C., Tang, J., & Ebinghaus, R. (2020). Per- and polyfluoroalkyl substances in Chinese and German river water - Point source- and country-specific fingerprints including unknown precursors. *Environmental Pollution*, 267. <https://doi.org/10.1016/j.envpol.2020.115567>.

Kimbell L., LaMartina E., Kohls S., Wang Y., Newton R., McNamara P., Bradford P., (2023); Impact of corrosion inhibitors on antibiotic resistance, metal resistance, and microbial communities in drinking water, *mSphere*, Volume 8, Issue 5., ISSN 2379-5042., <https://doi.org/10.1128/msphere.00307-23>.

Kissa E. (2001). *Fluorinated surfactants and repellents* (2nd edition revised and expanded) (Surfactant science series 97). New York (NY): Marcel Dekker. 640 p.

Krause, M., Magnuson, M., Crone, B., (2021). Potential PFAS destruction technology: electrochemical oxidation, U.S. EPA Office of Research and Development Research Brief. [https://www.epa.gov/sites/default/files/2021-01/documents/pitt\\_research\\_brief\\_electrochemical\\_oxidation\\_final\\_jan\\_25\\_2021\\_508.pdf](https://www.epa.gov/sites/default/files/2021-01/documents/pitt_research_brief_electrochemical_oxidation_final_jan_25_2021_508.pdf).

Lan, Y., Coetsier, C., Causserand, C., & Groenen Serrano, K. (2017). On the role of salts for the treatment of wastewaters containing pharmaceuticals by electrochemical oxidation using a boron doped diamond anode. *Electrochimica Acta*, 231, 309–318. <https://doi.org/10.1016/j.electacta.2017.01.160>.

Le T., Haflich H., Shah A., and Chaplin B., (2019)., Energy-Efficient Electrochemical Oxidation of Perfluoroalkyl Substances Using a Ti<sub>4</sub>O<sub>7</sub> Reactive Electrochemical Membrane Anode., *Environmental Science & Technology Letters* 2019 6 (8), 504-510., DOI: 10.1021/acs.estlett.9b00397.



Lewis, A. J., Yun, X., Lewis, M. G., McKenzie, E. R., Spooner, D. E., Kurz, M. J., Suri, R., & Sales, C. M. (2023). Impacts of divalent cations (Mg<sup>2+</sup> and Ca<sup>2+</sup>) on PFAS bioaccumulation in freshwater macroinvertebrates representing different foraging modes. *Environmental Pollution*, 331. <https://doi.org/10.1016/j.envpol.2023.121938>.

Li, W. C. (2014). Occurrence, Sources, and Fate of Pharmaceuticals in Aquatic Environment and Soil. *Environ. Pollut.* 2014, 187, 193–201.

Liang S., Mora R., Huang Q., Casson R., Wang Y., Woodard S., Anderson H., (2022)., Field demonstration of coupling ion-exchange resin with electrochemical oxidation for enhanced treatment of per- and polyfluoroalkyl substances (PFAS) in groundwater., *Chemical Engineering Journal Advances*, Volume 9, 100216, ISSN 2666-8211, <https://doi.org/10.1016/j.cej.2021.100216>.

Lichtenberg F. & Virabhak S., (2007). Pharmaceutical-Embodied Technical Progress, Longevity, and Quality of Life: Drugs as “Equipment for Your Health”. *Managerial and Decision Economics*. 28. 371-392. [10.1002/mde.1347](https://doi.org/10.1002/mde.1347).

Lin, A.Y., Panchangam, S.C., Chang, C.Y., Hong, P.K., Hsueh, H.F., (2012). Removal of perfluorooctanoic acid and perfluorooctane sulfonate via ozonation under alkaline condition. *J. Hazard. Mater.* 243, 272–277. <https://doi.org/10.1016/j.jhazmat.2012.05.047>.

Lin, H., Niu, J., Liang, S., Wang, C., Wang, Y., Jin, F., Luo, Q., & Huang, Q. (2019). Development of macroporous Magnéli phase Ti<sub>4</sub>O<sub>7</sub> ceramic materials: As an efficient anode for mineralization of poly- and perfluoroalkyl substances. *Chemical Engineering Journal*, 354, 1058–1067. <https://doi.org/10.1016/j.cej.2018.07.210>.

Ling A. L. (2024). Estimated scale of costs to remove PFAS from the environment at current emission rates. *The Science of the total environment*, 918, 170647. <https://doi.org/10.1016/j.scitotenv.2024.170647>.

Liu C., Zhao X., Faria A., Deliz Quiñones K., Zhang C., He Q., Ma J., Shen Y., Zhi Y.; (2022); Evaluating the efficiency of nanofiltration and reverse osmosis membrane processes for the removal of per- and polyfluoroalkyl substances from water: A critical review; *Separation and Purification Technology*, Volume 302, 122161, ISSN 1383-5866; <https://doi.org/10.1016/j.seppur.2022.122161>.

Liu, F., Hua, L., & Zhang, W. (2020). Influences of microwave irradiation on performances of membrane filtration and catalytic degradation of perfluorooctanoic acid (PFOA). *Environment international*, 143, 105969. <https://doi.org/10.1016/j.envint.2020.105969>.

Luo, Y., Khoshyan, A., Al Amin, M., Nolan, A., Robinson, F., Fenstermacher, J., Niu, J., Megharaj, M., Naidu, R., & Fang, C. (2023). Ultrasound-enhanced Magnéli phase Ti<sub>4</sub>O<sub>7</sub> anodic oxidation of per- and polyfluoroalkyl substances (PFAS) towards remediation of aqueous film forming foams (AFFF). *Science of the Total Environment*, 862. <https://doi.org/10.1016/j.scitotenv.2022.160836>.



Ma, Q., Gao, J., Cheng, K., Young, J., Zhao, M.-Q., Ronen, A., & Zhang, W. (2024). Electrooxidation of Perfluorocarboxylic Acids by an Interfacially Engineered Magnéli Phase Titanium Oxide (Ti<sub>4</sub>O<sub>7</sub>) Electrode with MXene. *ACS ES&T Engineering*, 4(5), 1102–1112. <https://doi.org/10.1021/acsestengg.3c00571>.

Ma J., Trelu C., Oturan N., Raffy S., Oturan M., (2022)., Porous Magnéli phase obtained from 3D printing for efficient anodic oxidation process. *Chemical Engineering Journal*, 2023, 456, pp.141047. [ff10.1016/j.cej.2022.141047](https://doi.org/10.1016/j.cej.2022.141047). [ffhal-04125396](https://doi.org/10.1016/j.cej.2022.141047).

Marselli, B. ; Garcia-Gomez, J. ; Michaud, P. A. ; Rodrigo, M. A. ; Comninellis, Ch ; (2003). Electrogeneration of Hydroxyl Radicals on Boron-Doped Diamond Electrodes; *Journal of the Electrochemical Society*,. 150, 3 ,D79-D83.

Matsubara, J., Takahashi, J., Ikeda, K., Shimizu, Y., & Matsui, S. (2003). The effects of humic substances on the intake of micro-organic pollutants into the aquatic biota. *Water Science and Technology : A Journal of the International Association on Water Pollution Research*, 47(7-8), 117–124.

Minh, T. B.; Leung, H. W.; Loi, I. H.; Chan, W. H.; So, M. K.; Mao, J. Q.; Choi, D.; Lam, J. C.; Zheng, G.; Martin, M.; Lee, J. H.; Lam, P. K. S.;(2009)., Richardson, B. J. Antibiotics in the Hong Kong Metropolitan Area: Ubiquitous Distribution and Fate in Victoria Harbour. *Mar. Pollut. Bull.* 2009, 58, 1052–1062.

Mo, Y., Li, Y., Wang, L., Wang, Y., Guo, H., & S. Mahmoud, M. (2025). Opposite influences of alginate and humic acid fouling on the degradation of sulfamethoxazole by electroactive membranes: Phenomena and mechanisms. *Separation and Purification Technology*, 355, 129799. <https://doi.org/10.1016/j.seppur.2024.129799>.

Moermond CTA, de Rooy M. (2022)., The Dutch chain approach on pharmaceuticals in water: Stakeholders acting together to reduce the environmental impact of pharmaceuticals. *Br J Clin Pharmacol.* Dec;88(12):5074-5082. doi: 10.1111/bcp.15509. Epub 2022 Sep 14. PMID: 36000992; PMCID: PMC9826305.

Mostefaoui, N., Oturan, N., Bouafia, S. C., Hien, S. A., Gibert-Vilas, M., Lesage, G., Pechaud, Y., Tassin, B., Oturan, M., & Trelu, C. (2024). Integration of electrochemical processes in a treatment system for landfill leachates based on a membrane bioreactor. *Science of the Total Environment*, 912. <https://doi.org/10.1016/j.scitotenv.2023.168841>.

Nicolopoulou-Stamati P, Maipas S, Kotampasi C, Stamatis P, Hens L (2016) Chemical pesticides and human health: the urgent need for a new concept in agriculture. *Front Public Health* 4:148. <https://doi.org/10.3389/fpubh.2016.00148>.

Odehnalová, K., Přibilová, P., Zezulka, Š., & Maršálek, B. (2023). The Material Matters: Sorption/Desorption Study of Selected Estrogens on Common Tubing or Sampling Materials Used in Water Sampling, Handling, Analysis or Treatment Technologies. *Applied Sciences*, 13(5), 3328. <https://doi.org/10.3390/app13053328>.



Nicolopoulou-Stamati P, Maipas S, Kotampasi C, Stamatis P, Hens L (2016) Chemical pesticides and human health: the urgent need for a new concept in agriculture. *Front Public Health* 4:148. <https://doi.org/10.3389/fpubh.2016.00148>.

Odehnalová, K., Přibilová, P., Zezulka, Š., & Maršálek, B. (2023). The Material Matters: Sorption/Desorption Study of Selected Estrogens on Common Tubing or Sampling Materials Used in Water Sampling, Handling, Analysis or Treatment Technologies. *Applied Sciences*, 13(5), 3328. <https://doi.org/10.3390/app13053328>.

OECD (Organisation for Economic Co-operation and Development). (2015). Working towards a global emission inventory of PFASs: Focus on PFCAs – Status quo and the way forward. Paris: Environmental, Health and Safety, Environmental Directorate, OECD/UNEP Global PFC Group.

Oladoye P, Ajiboye t., Omotola E., Oyewola O., (2022)., Methylene blue dye: Toxicity and potential elimination technology from wastewater, *Results in Engineering*, Volume 16, 100678, ISSN 2590-1230., <https://doi.org/10.1016/j.rineng.2022.100678>.

Oller, I., Malato, S., & Sánchez-Pérez, J. A. (2011). Combination of Advanced Oxidation Processes and biological treatments for wastewater decontamination--a review. *The Science of the total environment*, 409(20), 4141–4166. <https://doi.org/10.1016/j.scitotenv.2010.08.061>.

Olvera-Vargas, H., Wang, Z., Xu, J., & Lefebvre, O. (2022). Synergistic degradation of GenX (hexafluoropropylene oxide dimer acid) by pairing graphene-coated Ni-foam and boron doped diamond electrodes. *Chemical Engineering Journal*, 430. <https://doi.org/10.1016/j.cej.2021.132686>.

Panizza, M., Barbucci, A., Ricotti, R., & Cerisola, G. (2007). Electrochemical degradation of methylene blue. *Separation and Purification Technology*, 54(3), 382–387. <https://doi.org/10.1016/j.seppur.2006.10.010>.

Panizza, M., & Cerisola, G. (2009). Direct and mediated anodic oxidation of organic pollutants. *Chemical reviews*, 109(12), 6541–6569. <https://doi.org/10.1021/cr9001319>.

Pica, N. E., Funkhouser, J., Yin, Y., Zhang, Z., Ceres, D. M., Tong, T., & Blotevogel, J. (2019). Electrochemical Oxidation of Hexafluoropropylene Oxide Dimer Acid (GenX): Mechanistic Insights and Efficient Treatment Train with Nanofiltration. *Environmental Science & Technology*, 53(21), 12602–12609. <https://doi.org/10.1021/acs.est.9b03171>.

Pike, K.A., Edmiston, P.L., Morrison, J.J., Faust, J.A., (2021). Correlation analysis of perfluoroalkyl substances in regional U.S. precipitation events. *Water Res.* 190, 116685 <https://doi.org/10.1016/j.watres.2020.116685>.



Puttamreddy, S., & Nippatlapalli, N. (2024). Advanced insights into sustainable electrooxidation technique and futuristic strategies: Multifaceted approach for PFAS degradation. *Journal of Environmental Chemical Engineering*, 12(5). <https://doi.org/10.1016/j.jece.2024.113307>.

Radjenovic, J., Bagastyo, A., Rozendal, R. A., Mu, Y., Keller, J., & Rabaey, K. (2011). Electrochemical oxidation of trace organic contaminants in reverse osmosis concentrate using RuO<sub>2</sub>/IrO<sub>2</sub>-coated titanium anodes. *Water Research*, 45(4), 1579–1586. <https://doi.org/10.1016/j.watres.2010.11.035>.

Radjenovic, J., & Sedlak, D. L. (2015). Challenges and Opportunities for Electrochemical Processes as Next-Generation Technologies for the Treatment of Contaminated Water. *Environmental Science & Technology*, 49(19), 11292.

Radjenovic, J., Duinslaeger, N., Avval, S. S., & Chaplin, B. P. (2020). Facing the Challenge of Poly- and Perfluoroalkyl Substances in Water: Is Electrochemical Oxidation the Answer? *Environmental Science & Technology*, 54(23), 14815. <https://doi.org/10.1021/acs.est.0c06212>.

Ramírez-Canon A., Becerra-Quiroz A., & Herrera-Jacquelin F., (2022). Perfluoroalkyl and polyfluoroalkyl substances (PFAS): First survey in water samples from the Bogotá River, Colombia. *Environmental Advances*, 8, 100223–. <https://doi.org/10.1016/j.envadv.2022.100223>.

Richardson, S. D., Plewa, M. J., Wagner, E. D., Schoeny, R., & DeMarini, D. M. (2007). Occurrence, genotoxicity, and carcinogenicity of regulated and emerging disinfection by-products in drinking water: A review and roadmap for research. *Mutation Research-Reviews in Mutation Research*, 636(1-3), 178–242. <https://doi.org/10.1016/j.mrrev.2007.09.001>.

Rivera-Utrilla, J.; Sanchez-Polo, M.; Ferro-García, M. A.; PradosJoya, G.; Ocampo-Perez, R. (2013)., Pharmaceuticals as Emerging Contaminants and Their Removal from Water. A Review. *Chemosphere* 2013, 93, 1268–1287.

RIVM., (2023)., Risk assessment of exposure to PFAS through food and drinking water in the Netherlands., <https://www.rivm.nl/publicaties/risk-assessment-of-exposure-to-pfas-through-food-and-drinking-water-in-netherlands>.

Rumsby, P. C., McLaughlin, C. L., & Hall, T. (2009). Perfluorooctane sulphonate and perfluorooctanoic acid in drinking and environmental waters. *Philosophical transactions. Series A, Mathematical, physical, and engineering sciences*, 367(1904), 4119–4136. <https://doi.org/10.1098/rsta.2009.0109>.

Saha, P., Wang, J., Zhou, Y., Carlucci, L., Jeremiase, A. W., Rijnaarts, H. H. M., & Bruning, H. (2022). Effect of electrolyte composition on electrochemical oxidation: Active sulfate formation, benzotriazole degradation, and chlorinated by-products distribution. *Environmental Research*, 211. <https://doi.org/10.1016/j.envres.2022.113057>.





Sarkar, S. K. (2016). Marine organic micropollutants : a case study of the sundarban mangrove wetland. Springer. <https://search.ebscohost.com/login.aspx?direct=true&scope=site&db=nlebk&db=nlabk&AN=1260937>.

Shi H., Wang Y., Li C., Pierce R., Gao S., and Huang Q., (2019)., Degradation of Perfluorooctanesulfonate by Reactive Electrochemical Membrane Composed of Magnéli Phase Titanium Suboxide., *Environmental Science & Technology* 2019 53 (24), 14528-14537., DOI: 10.1021/acs.est.9b04148.

Sillanpää, M. E. T., & Shestakova, M. (2017). *Electrochemical water treatment methods : fundamentals, methods and full scale applications*. Butterworth-Heinemann, an imprint of Elsevier. <https://search.ebscohost.com/login.aspx?direct=true&scope=site&db=nlebk&db=nlabk&AN=1465592>.

Sim, A., & Mauter, M. S. (2021). Cost and energy intensity of U.S. potable water reuse systems. *Environmental Science: Water Research & Technology*, 7(4), 748–761. <https://doi.org/10.1039/d1ew00017a>.

Sirés, I., Brillas, E., Oturan, M.A. et al. (2014). Electrochemical advanced oxidation processes: today and tomorrow. A review. *Environ Sci Pollut Res* 21, 8336–8367. <https://doi.org/10.1007/s11356-014-2783-1>.

Smart, B.E. (1994). Characteristics of C-F Systems. In: Banks, R.E., Smart, B.E., Tatlow, J.C. (eds) *Organofluorine Chemistry. Topics in Applied Chemistry*. Springer, Boston, MA. [https://doi.org/10.1007/978-1-4899-1202-2\\_3](https://doi.org/10.1007/978-1-4899-1202-2_3).

Smith, S. J., Lewis, J., Wiberg, K., Wall, E., & Ahrens, L. (2023). Foam fractionation for removal of per- and polyfluoroalkyl substances: Towards closing the mass balance. *The Science of the total environment*, 871, 162050. <https://doi.org/10.1016/j.scitotenv.2023.162050>.

STOWA (Ministry of Infrastructure and Water Management)., (2019), Preliminary guidelines for sampling and chemical analysis of pharmaceutical residues in wastewater for the purpose of support regulation ‘treatment pharmaceutical residues’, Innovation program ‘micropollutants in WWTP-wastewater’, (STOWA / Ministry I and W)., Report 3 (in Dutch).

Sturm M., Myers E., Schober D., Thege C., Korzin A., & Schuhen K., (2022). Adaptable Process Design as a Key for Sustainability Upgrades in Wastewater Treatment: Comparative Study on the Removal of Micropollutants by Advanced Oxidation and Granular Activated Carbon Processing at a German Municipal Wastewater Treatment Plant. *Sustainability*. 14. 11605. [10.3390/su141811605](https://doi.org/10.3390/su141811605).

Tamilmani, S., Huang, W. H., Raghavan, S., & Farrell, J. (2004). Electrochemical treatment of simulated copper CMP wastewater using boron doped diamond thin film electrodes-a feasibility study. *IEEE Transactions on Semiconductor Manufacturing*, 17(3). <https://doi.org/10.1109/TSM.2004.831528>.



Tow, E. W., Hartman, A. L., Jaworowski, A., Zucker, I., Kum, S., AzadiAghdam, M., Blatchley, E. R., Achilli, A., Gu, H., Urper, G. M., & Warsinger, D. M. (2021). Modeling the energy consumption of potable water reuse schemes. *Water Research X*, 13. <https://doi.org/10.1016/j.wroa.2021.100126>.

Trojanowicz, M., Bojanowska-Czajka, A., Bartosiewicz, I., & Kulisa, K. (2018). Advanced Oxidation/Reduction Processes treatment for aqueous perfluorooctanoate (PFOA) and perfluorooctanesulfonate (PFOS) - A review of recent advances. *Chemical Engineering Journal*, 336, 170–199. <https://doi.org/10.1016/j.cej.2017.10.153>.

Trouborst LJ (2016), Aqueous photolysis of 6:2 fluorotelomer sulfonamide alkylbetaine. University of Toronto, Accessed February 2019 at <https://tspace.library.utoronto.ca>.

Uwayezu, J. N., Carabante, I., Lejon, T., van Hees, P., Karlsson, P., Hollman, P., & Kumpiene, J. (2021). Electrochemical degradation of per- and poly-fluoroalkyl substances using boron-doped diamond electrodes. *Journal of environmental management*, 290, 112573. <https://doi.org/10.1016/j.jenvman.2021.112573>.

Vecitis, C. D., Park, H., Cheng, J., Mader, B. T., & Hoffmann, M. R. (2008). Kinetics and mechanism of the sonolytic conversion of the aqueous perfluorinated surfactants, perfluorooctanoate (PFOA), and perfluorooctane sulfonate (PFOS) into inorganic products. *The journal of physical chemistry. A*, 112(18), 4261–4270. <https://doi.org/10.1021/jp801081y>.

Vera, P., Canellas, E., Dreolin, N., Goshawk, J., & Nerín, C. (2024). The analysis of the migration of per and poly fluoroalkyl substances (PFAS) from food contact materials using ultrahigh performance liquid chromatography coupled to ion-mobility quadrupole time-of-flight mass spectrometry (UPLC- IMS-QTOF). *Talanta*, 266(Pt 1), 124999. <https://doi.org/10.1016/j.talanta.2023.124999>.

Villanger, G. D., Kovacs, K. M., Lydersen, C., Haug, L. S., Sabaredzovic, A., Jensen, B. M., & Routti, H. (2020). Perfluoroalkyl substances (PFASs) in white whales (*Delphinapterus leucas*) from Svalbard - A comparison of concentrations in plasma sampled 15 years apart. *Environmental Pollution: Part A*, 263. <https://doi.org/10.1016/j.envpol.2020.114497>.

Von Gunten, U., & Oliveras, Y. (1998). Advanced Oxidation of Bromide-Containing Waters: Bromate Formation Mechanisms. *Environmental Science & Technology*, 32(1), 63–70. <https://doi.org/10.1021/es970477j>.

Wang, J., Wang, L., Xu, C., Zhi, R., Miao, R., Liang, T., Yue, X., Lv, Y., & Liu, T. (2018). Perfluorooctane sulfonate and perfluorobutane sulfonate removal from water by nanofiltration membrane: The roles of solute concentration, ionic strength, and macromolecular organic foulants. *Chemical Engineering Journal*, 332, 787–797. <https://doi.org/10.1016/j.cej.2017.09.061>.

Wang G., Liu Y., Ye J., Lin Z., Yang X., (2020)., Electrochemical oxidation of methyl orange by a Magnéli phase Ti<sub>4</sub>O<sub>7</sub> anode, *Chemosphere*, Volume 241, 125084, ISSN 0045-6535, <https://doi.org/10.1016/j.chemosphere.2019.125084>.



Wang G., Liu Y., Duan Y., Ye J., Lin Z., (2023)., Effects of porosity on the electrochemical oxidation performance of Ti<sub>4</sub>O<sub>7</sub> electrode materials, *Ceramics International*, Volume 49, Issue 10, Pages 15357-15364, ISSN 0272-8842, <https://doi.org/10.1016/j.ceramint.2023.01.120>.

Wang L., Lu J., Li L., Wang Y., Huang Q. (2020)., Effects of chloride on electrochemical degradation of perfluorooctanesulfonate by Magnéli phase Ti<sub>4</sub>O<sub>7</sub> and boron doped diamond anodes., *Water Research*,. Volume 170,. 115254,. ISSN 0043-1354,. <https://doi.org/10.1016/j.watres.2019.115254>.

Wang L., Nickelsen M., Chiang S., Woodard S., Wang Y., Liang S., Mora R., Fontanez R., Anderson H., Huang Q., (2021)., Treatment of perfluoroalkyl acids in concentrated wastes from regeneration of spent ion exchange resin by electrochemical oxidation using Magnéli phase Ti<sub>4</sub>O<sub>7</sub> anode., *Chemical Engineering Journal Advances*., Volume 5., 100078, ISSN 2666-8211., <https://doi.org/10.1016/j.cej.2020.100078>.

Wang, S., Pei, S., Zhang, J., Huang, J., & You, S. (2022). Flow-through electrochemical removal of benzotriazole by electroactive ceramic membrane. *Water Research*, 218. <https://doi.org/10.1016/j.watres.2022.118454>.

Wang Y., Li L., Huang Q., (2022)., Electrooxidation of per- and polyfluoroalkyl substances in chloride-containing water on surface-fluorinated Ti<sub>4</sub>O<sub>7</sub> anodes: Mitigation and elimination of chlorate and perchlorate formation., *Chemosphere*, Volume 307, Part 2, 135877, ISSN 0045-6535, <https://doi.org/10.1016/j.chemosphere.2022.135877>.

Wang, Z., Cousins, I. T., Scheringer, M., Buck, R. C., & Hungerbühler, K. (2014). Global emission inventories for C<sub>4</sub>-C<sub>14</sub> perfluoroalkyl carboxylic acid (PFCA) homologues from 1951 to 2030, Part I: production and emissions from quantifiable sources. *Environment International*, 70, 62–75. <https://doi.org/10.1016/j.envint.2014.04.013>.

Watkinson A.J., Murby E.J., Kolpin D.W., Costanzo S.D., (2009); The occurrence of antibiotics in an urban watershed: From wastewater to drinking water, *Science of The Total Environment*, Volume 407, Issue 8, Pages 2711-2723, ISSN 0048-9697., <https://doi.org/10.1016/j.scitotenv.2008.11.059>.

Xiong, F., Ye, J., Liu, Y. et al. (2022). High-Performance Electrochemical Degradation of Methylene Blue by a Ti<sub>4</sub>O<sub>7</sub> Anode Prepared via Industrial Tailing Titanium Powder. *J. Electron. Mater.* 51, 3560–3568. <https://doi.org/10.1007/s11664-022-09596-6>.

Xu, B., Sohn, H.Y., Mohassab, Y., Lan, Y., (2016). Structures, preparation and applications of titanium suboxides. *RSC Adv.* 6, 79706–79722. <https://doi.org/10.1039/c6ra14507h>.

Yaqub M., Nguyen M. N., Lee W., (2022)., Treating reverse osmosis concentrate to address scaling and fouling problems in zero-liquid discharge systems: A scientometric review of global trends, *Science of The Total Environment*, Volume 844,157081, ISSN 0048-9697., <https://doi.org/10.1016/j.scitotenv.2022.157081>.



Yong, Z. Y., Kim, K. Y., & Oh, J. E. (2021). The occurrence and distributions of per- and poly-fluoroalkyl substances (PFAS) in groundwater after a PFAS leakage incident in 2018. *Environmental pollution (Barking, Essex : 1987)*, 268(Pt B), 115395. <https://doi.org/10.1016/j.envpol.2020.115395>.

Yu, Q., Zhang, R., Deng, S., Huang, J., & Yu, G. (2009). Sorption of perfluorooctane sulfonate and perfluorooctanoate on activated carbons and resin: Kinetic and isotherm study. *Water research*, 43(4), 1150–1158. <https://doi.org/10.1016/j.watres.2008.12.001>.

Zaidi S., Saleem H., (2022)., Chapter 1 - Introduction to Reverse Osmosis, Editor(s): Syed Javaid Zaidi, Haleema Saleem, Reverse Osmosis Systems, Elsevier, Pages 1-32, ISBN 9780128239650, <https://doi.org/10.1016/B978-0-12-823965-0.00010-9>.

Zhai, H., Cheng, S., Zhang, L., Luo, W., & Zhou, Y. (2022). Formation characteristics of disinfection byproducts from four different algal organic matter during chlorination and chloramination. *Chemosphere*, 308. <https://doi.org/10.1016/j.chemosphere.2022.136171>.

Zheng, G., Eick, S. M., & Salamova, A. (2023). Elevated Levels of Ultrashort- and Short-Chain Perfluoroalkyl Acids in US Homes and People. *Environmental Science & Technology*, 57(42), 15782–15793. <https://doi.org/10.1021/acs.est.2c06715>.

Ziarani G., Moradi R., Lashgari N., Kruger H., (2018)., Chapter 1 - Introduction and Importance of Synthetic Organic Dyes., Editor(s): Ghodsi Mohammadi Ziarani, Razieh Moradi, Negar Lashgari, Hendrik G. Kruger, Metal-Free Synthetic Organic Dyes, Elsevier, Pages 1-7, ISBN 9780128156476., <https://doi.org/10.1016/B978-0-12-815647-6.00001-7>.

Zuccato, E.; Calamari, D.; Natangelo, M.; Fanelli, R. (2000)., Presence of Therapeutic Drugs in the Environment. *Lancet*, 355, 1789– 1790.

Zwiener, Christian. (2007). Occurrence and Analysis of Pharmaceuticals and Their Transformation Products in Drinking Water Treatment. *Analytical and bioanalytical chemistry*. 387. 1159-62. [10.1007/s00216-006-0818-2](https://doi.org/10.1007/s00216-006-0818-2).





# Appendix

## Appendix

Figure A-1: OMPs pathways to water resources.

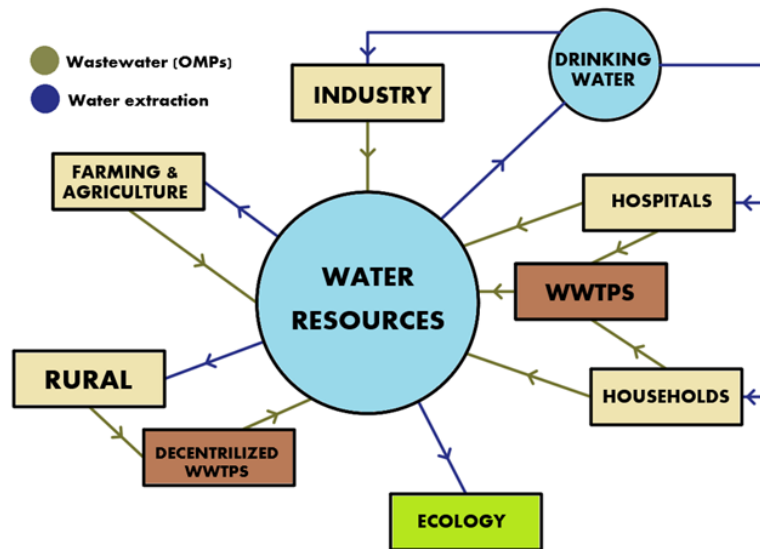


Figure A-2: PFAS family classification (OECD, 2015).

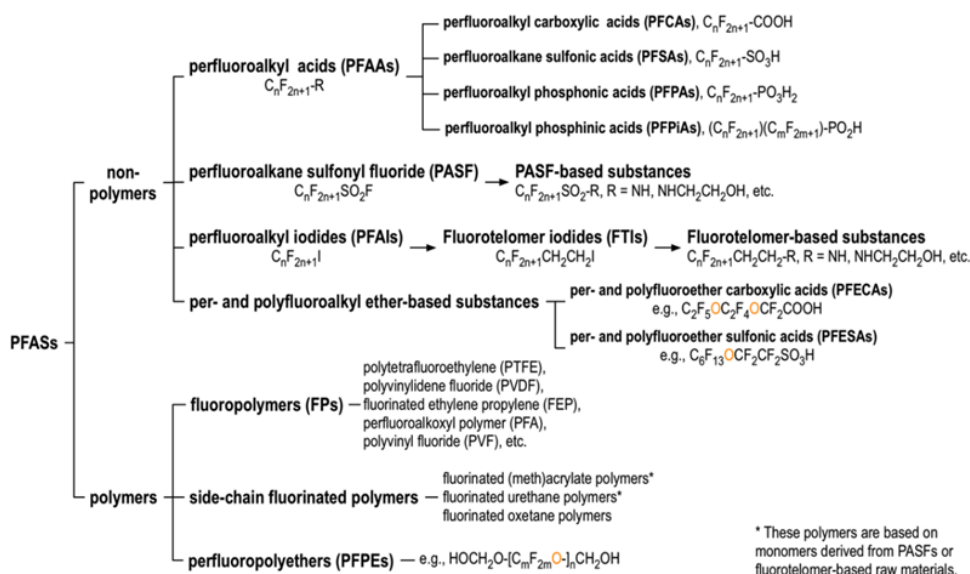


Table A1: Literature review

Key words	# Documents
Anode oxidation AND Magneli	44
Reactive electrochemical membrane AND Magneli	14
Reactive electrochemical membrane AND Pharmaceuticals	26
Ti4O7 AND PFAS	9
Anode AND oxidation AND pharmaceuticals AND Ti4O7	5
Reactive electrochemical membrane AND PFAS	4
Reactive electrochemical membrane AND PFAS AND Ti4O7	3
Reverse Osmosis Concentrate AND Anode oxidation AND pharmaceuticals	4
Reverse Osmosis Concentrate AND PFAS	12
Reactive electrochemical membrane AND reverse osmosis concentrate	6
Flow-through AND Magneli	7

Table A2: Charge Dosage Literature review.

Research	Current Density (mA/cm <sup>2</sup> )	Time (h)	Volume (L)	Area (cm <sup>2</sup> )	Intensity (A)	Charge Density (Ah/L)
Liang et al., 2018	10	17	0.2	100	1	85
	10	16	0.2	100	1	80
Lin et al., 2018	10	24	0.2	100	1	120
Liang et al., 2022		80	19			126
Wang et al., 2021	10	40	0.1	100	1	400
Lin et al., 2018	5	3	0.2	100	0.50	7.50
Le et al., 2019		0.18		0.5	0.00	126
Wang et al., 2020	10	4	0.2	78	0.78	15.60
	5	0.33	0.2	78	0.39	0.64
Shi et al., 2019	4	1.67	4	156.83	0.63	0.26
	4	0.17	0.4	156.83	0.63	0.26
Wang et al., 2022	40	1	0.05	15.2	0.61	12.16
	5	7	0.05	15.2	0.08	10.64
	5	7	0.05	15.2	0.08	10.64
Luo et al., 2023	10	3	0.12	75	0.75	18.75



Table A3: Still botom water containing PFAS.

Water	Anode	Cathode	Medium	Volume (Lts)	Current (mA/cm2)	Time (h)	PFOA (mg/l)	PFOS (mg/l)	Rem PFOA	Rem PFOS	Cl (mg/l)	TOC (mg/L)
Still bottom	Ti4O7 5x10 cm	304 SS 2x	E cell	0.2	10	17	100.5	68.6	77.2	96.5	6850	15800
Still bottom	Ti4O7 5x10 cm	304 SS 2x	E cell	0.2	10	16	15.6	25.5	100	100	853	9880
Liang et al., 2018												
Still bottom	Ti4O7	304 SS	Batch	0.2	10	24	96.01	32.03	91	97	6445	43774
Lin et al., 2018												
Still bottom	Ti4O7 24 units	304 SS	Reactor 3.8 L/min	19	30V, 10 Amp 126 Ah/L	80	3.05	4.42	80	85	7460	31500
Liang et al., 2022												
Still bottom E cell 10x5x2.5 cm	Ti4O7 2x	304 SS 2.5 cm gap	Batch	0.1	10	40	7.56	8.08	94.8	98.9	62716	13280
undivided Wang et al., 2021	10x5 cm	2.5 cm gap		700 rpm stirred	10	200	11.92	12.02	98.7	96.5	3579	201529
							MeOH/NaCl					
							MeOH/NaCl					

Table A4: Spiked PFAS to artificial water.

Water	Anode	Cathode	Medium	Volume (Lts)	Current (mA/cm2)	Time (h)	PFOA (mg/l)	PFOS (mg/l)	Rem PFOA	Rem PFOS	Cl (mg/l)	TOC (mg/L)
Still bottom	Ti4O7 5x10 cm	304 SS 2x	E cell	0.2	10	17	100.5	68.6	77.2	96.5	6850	15800
Still bottom	Ti4O7 5x10 cm	304 SS 2x	E cell	0.2	10	16	15.6	25.5	100	100	853	9880
Liang et al., 2018												
Still bottom	Ti4O7	304 SS	Batch	0.2	10	24	96.01	32.03	91	97	6445	43774
Lin et al., 2018												
Still bottom	Ti4O7 24 units	304 SS	Reactor 3.8 L/min	19	30V, 10 Amp 126 Ah/L	80	3.05	4.42	80	85	7460	31500
Liang et al., 2022												
Still bottom E cell 10x5x2.5 cm	Ti4O7 2x	304 SS 2.5 cm gap	Batch	0.1	10	40	7.56	8.08	94.8	98.9	62716	13280
undivided Wang et al., 2021	10x5 cm	2.5 cm gap		700 rpm stirred	10	200	11.92	12.02	98.7	96.5	3579	201529
							MeOH/NaCl					
							MeOH/NaCl					



Figure A3: MB Degradation.

MB Degradation (a) 3mA/cm<sup>2</sup> – 0.5 L/min, (b) 3mA/cm<sup>2</sup> – 1 L/min, and (c) 3mA/cm<sup>2</sup> – 1.75 L/min.

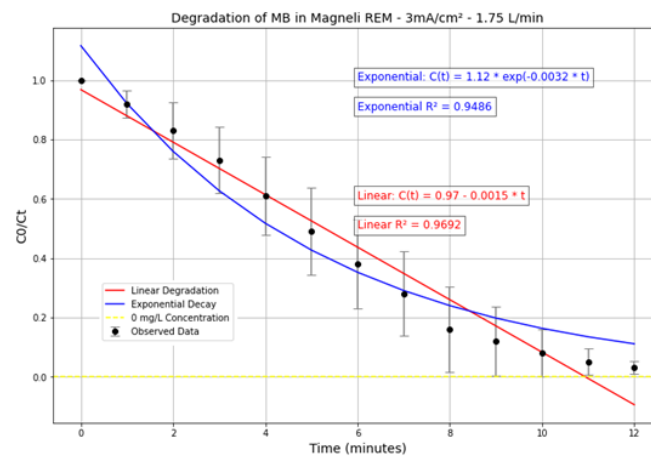
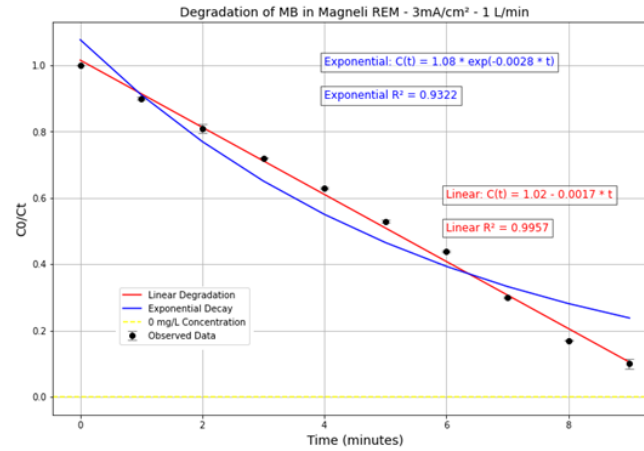
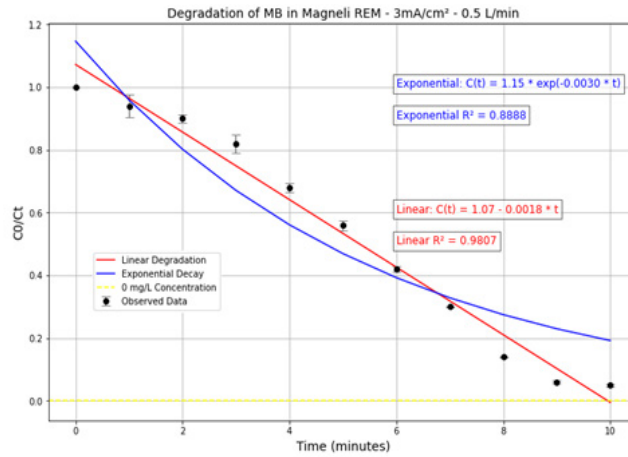




Figure A4: MB Degradation 2

(a) 6 mA/cm<sup>2</sup> – 0.5 L/min, (b) 6 mA/cm<sup>2</sup> – 1 L/min, (c) 3mA/cm<sup>2</sup> – 1.75 L/min.

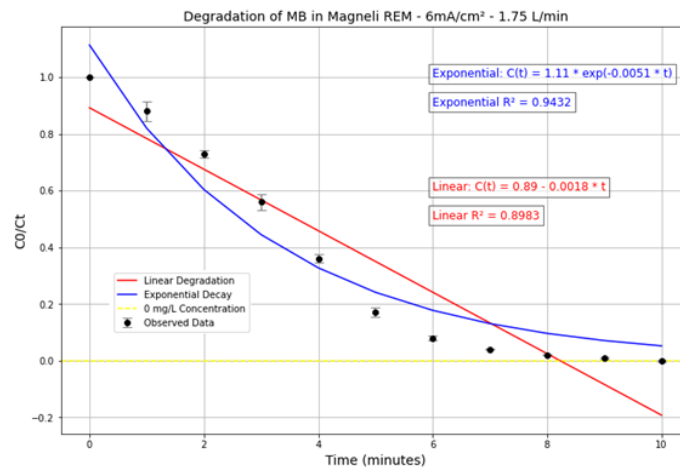
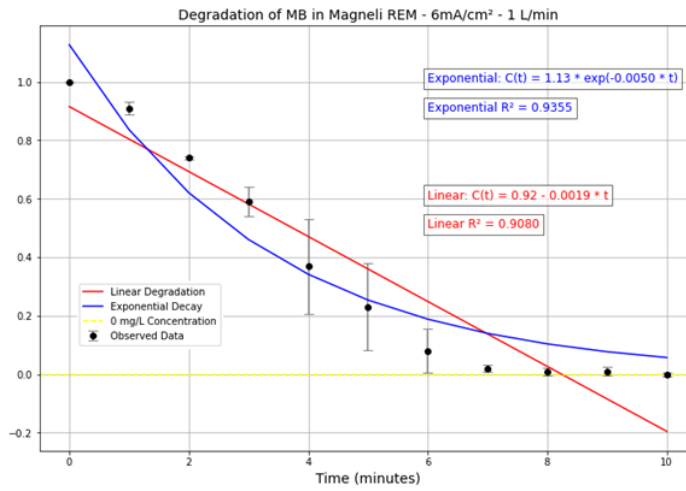
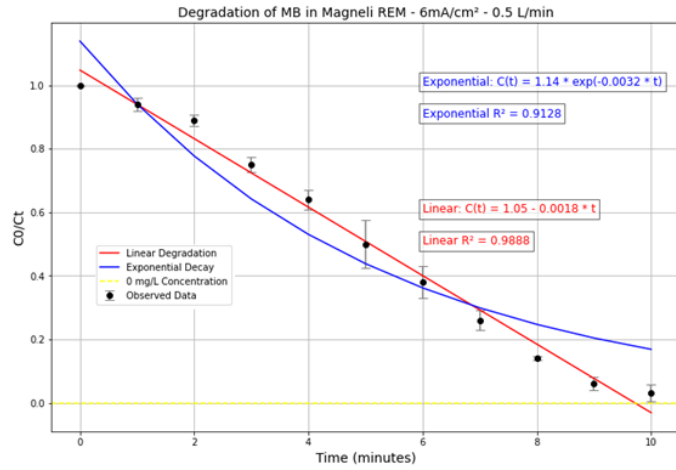


Figure A5: MB degradation 3

MB Degradation (a) 9 mA/cm<sup>2</sup> – 0.5 L/min, (b) 9 mA/cm<sup>2</sup> – 1 L/min, (c) 9mA/cm<sup>2</sup> – 1.75 L/min.

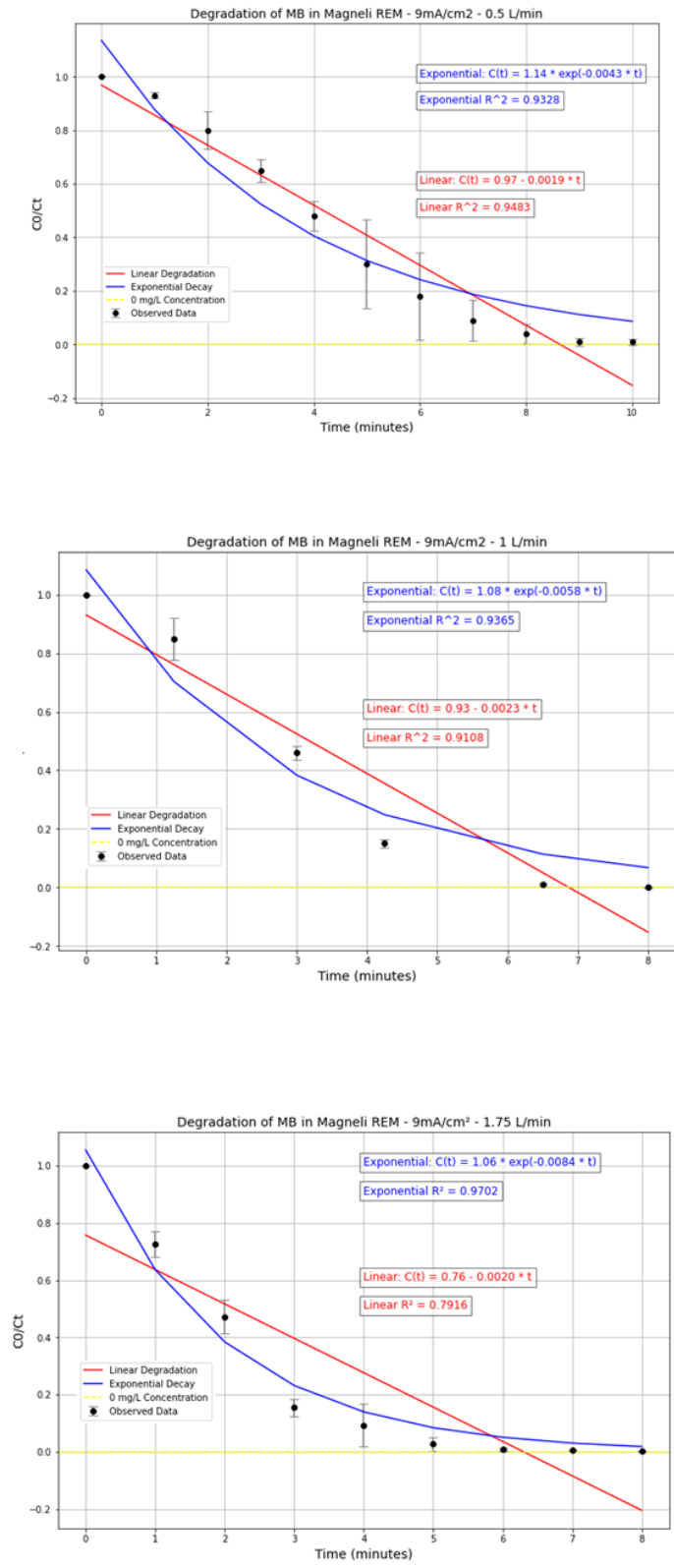


Figure A6: PFAS Degradation DWU 1.

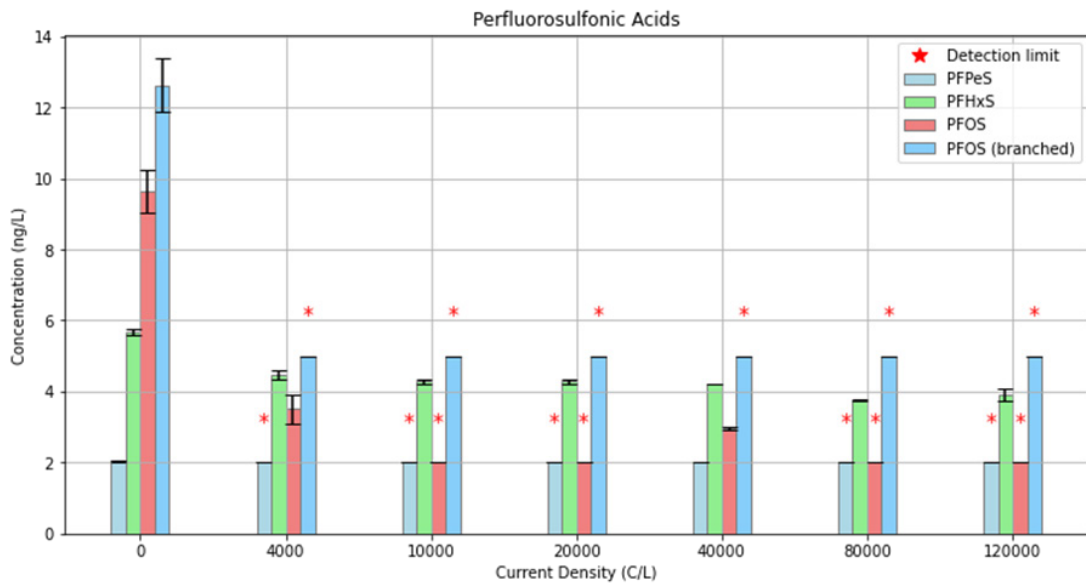
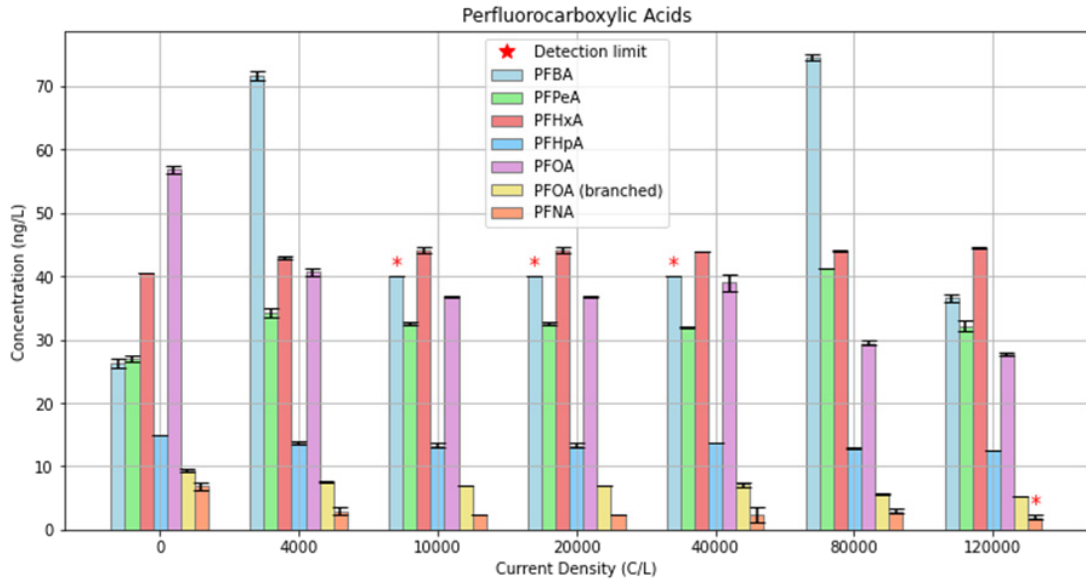


Figure A7: PFOA and PFOS, PFHxA , PFPeA, PFHxS and PFHpA normalized degradation.

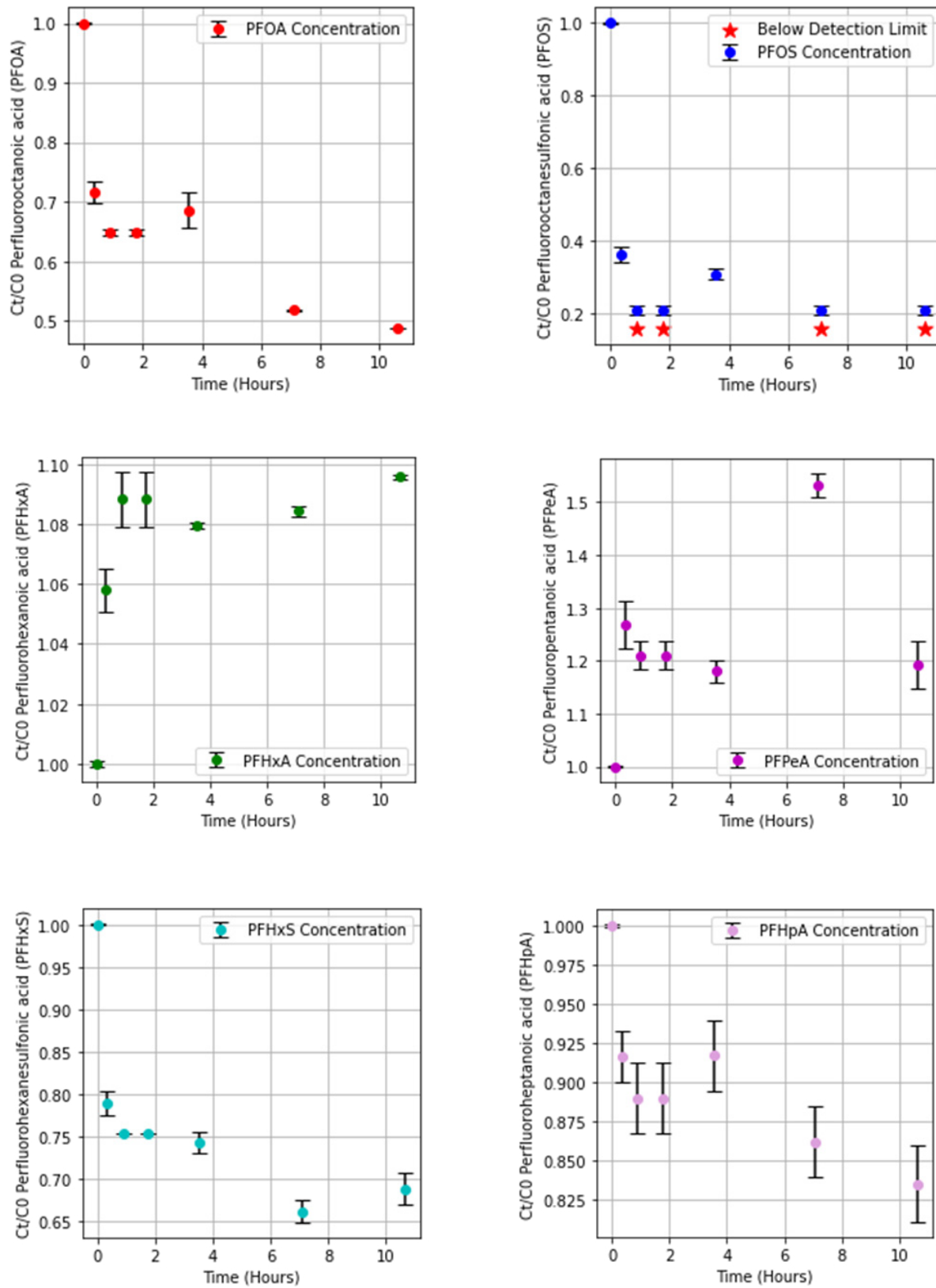


Figure A8: PFBA, PFNA, 6:2 FTS, HFPO-DA (GEN-X) and PFPeS and FBSA normalized degradation.

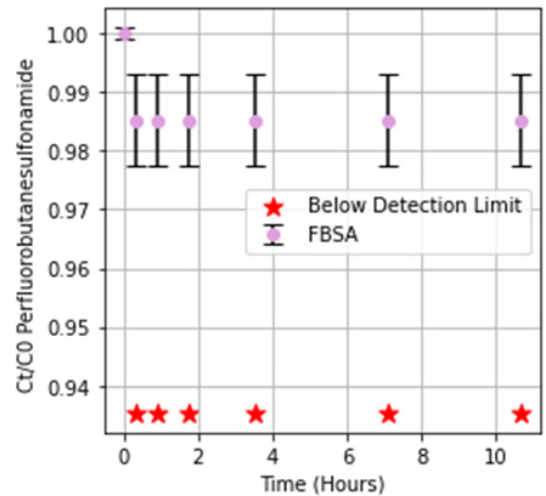
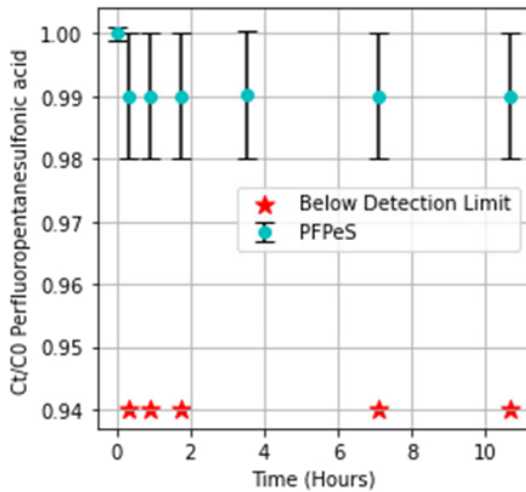
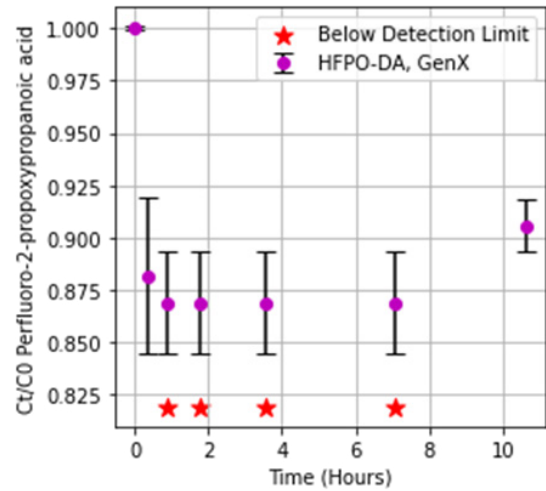
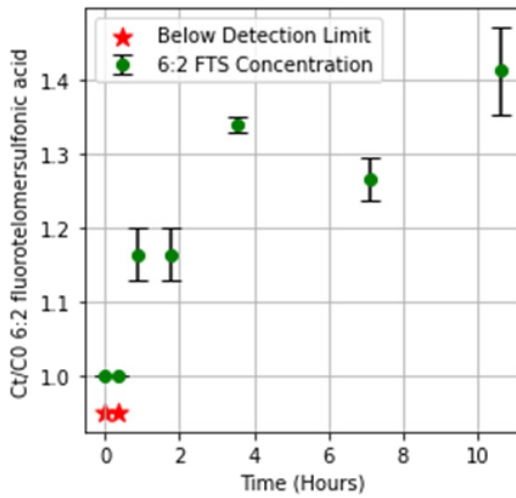
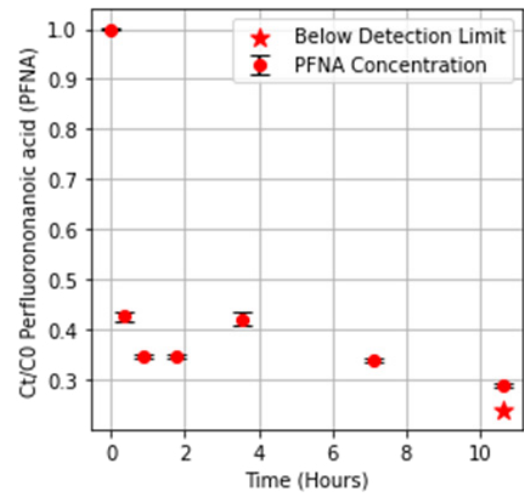
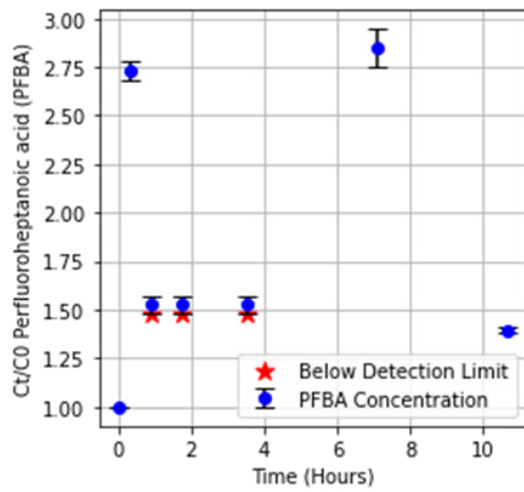
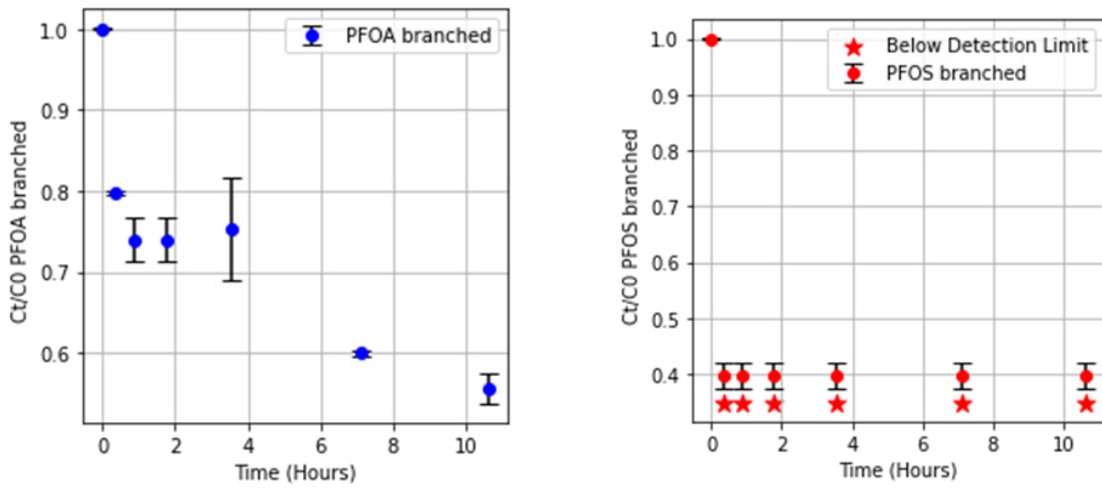


Figure A9: PFOA branched and PFOS branched normalized degradation.



DWU 2

Figure A10: PFOA , PFOS , PFHxA and PFPeA normalized degradation.

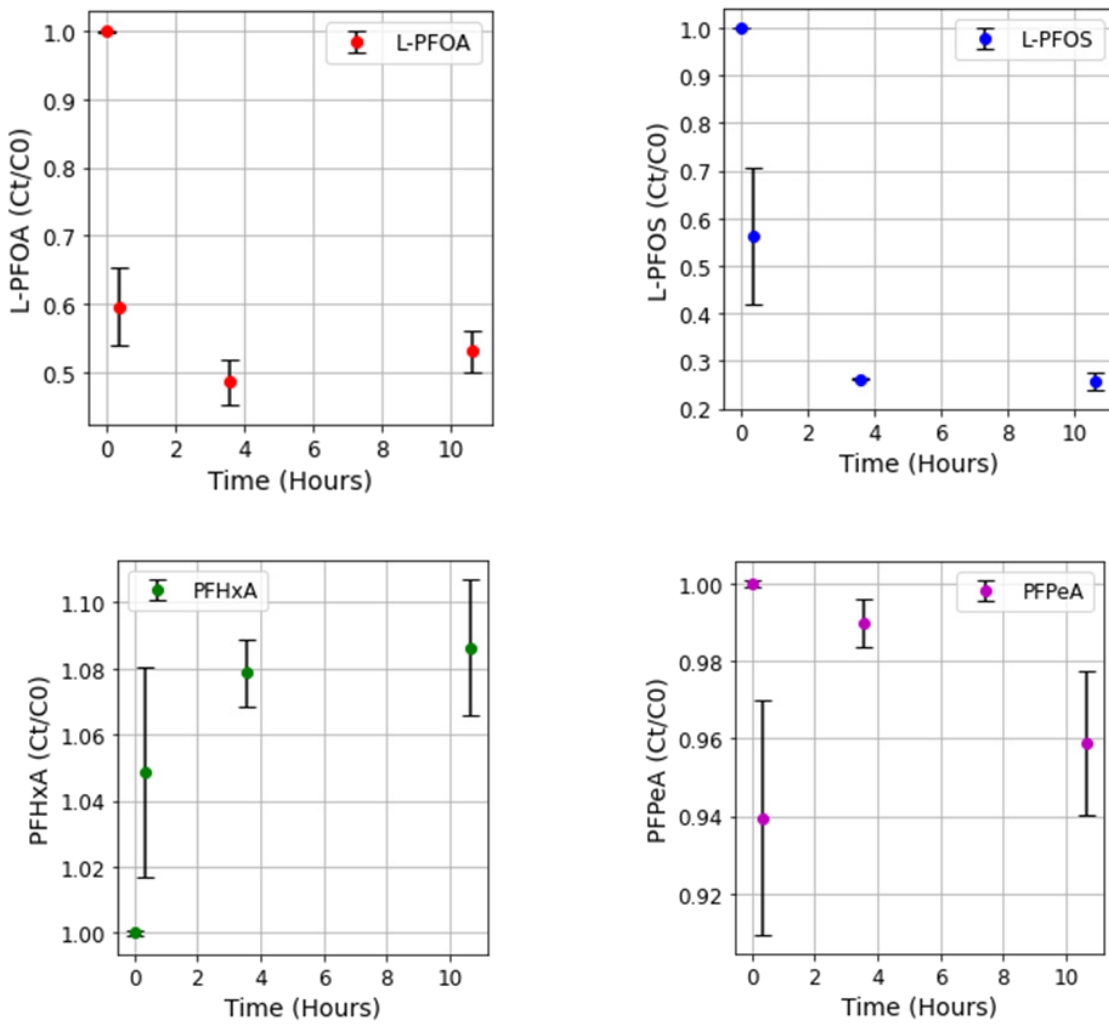


Figure A11: PFHxS and PFHpA, B-PFOA, B-PFOS, 6:2 FTS, PFNA, PFPeS, HFPO and PFBS normalized degradation.

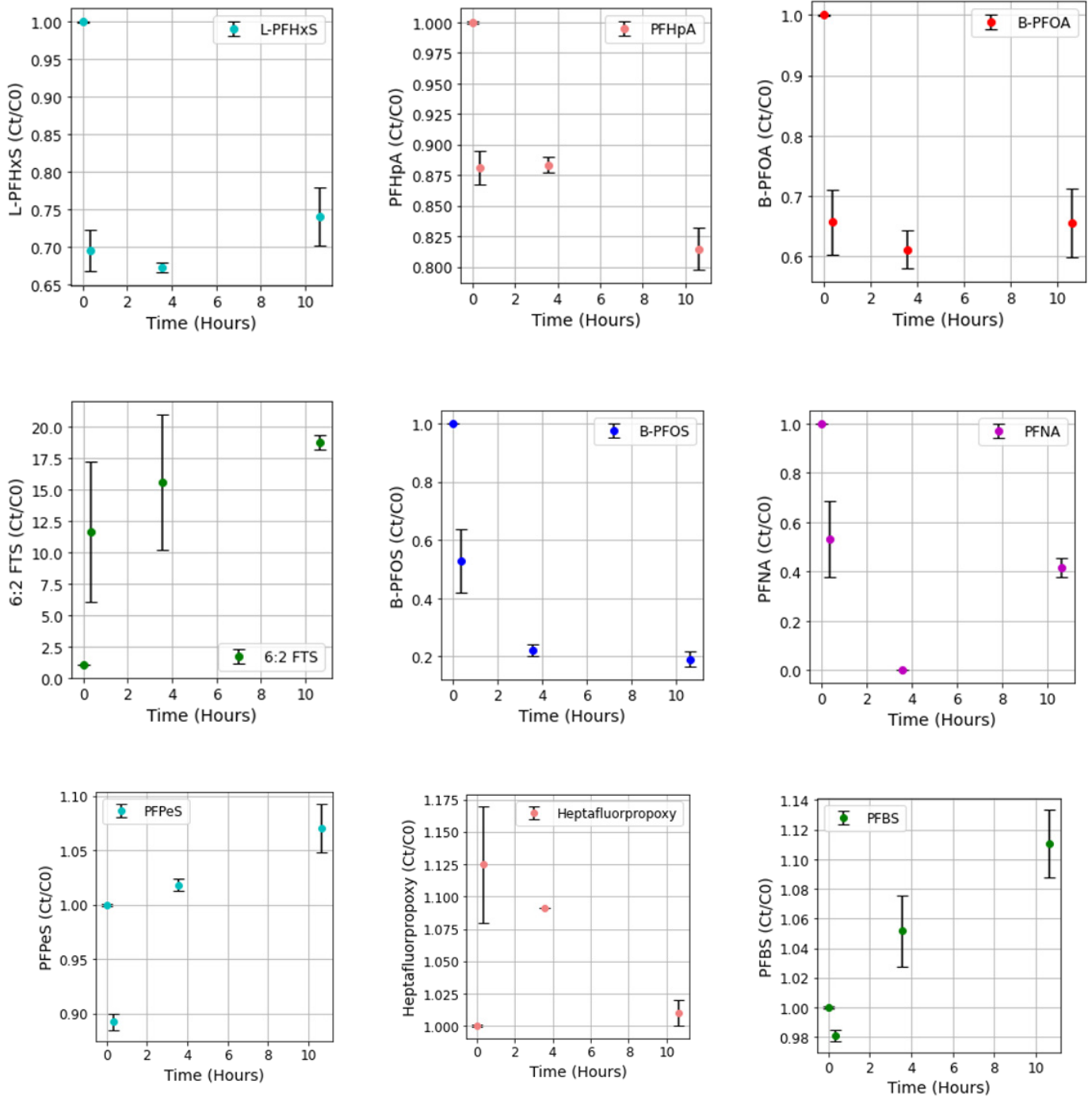


Table A5: Measured PFAS under detection limits.

PFAS Species	Detection limit (ng/L)
Trifluoromethanesulphonic acid	100
Perfluoroundecanoic acid (PFUnDA)	5
Perfluorododecanoic acid (PFDoDA)	5
Perfluorodecanoic acid (PFDA)	3
Perfluorotetradecanoic acid (PFTeDA)	5
Perfluorotridecanoic acid (PFTrDA)	2
Perfluorooctanesulfonamide (PFOSA)	2
Perfluorobutanesulfonic acid (PFBS)	20
Perfluoroheptanesulfonic acid (PFHpS)	2
Perfluorodecanesulfonic acid (PFDS)	2
Perfluorononanesulfonic acid (PFNS)	2
4:2 fluorotelomersulfonic acid (4:2 FTS)	5
8:2 fluorotelomersulfonic acid (8:2 FTS)	5
N-methyl perfluorooctanesulfonamidoacetic acid (N-MeFOSAA)	5
N-ethyl perfluorooctanesulfonamidoacetic acid (N-EtFOSAA)	10
4,8-Dioxa-3H-perfluorononanoic acid (DONA)	2
Perfluorohexadecanoic acid (PFHxDA)	10
Perfluorooctadecanoic acid (PFODA)	10
Perfluoroundecanesulfonic acid (PFUnDS)	5
Perfluorododecanesulfonic acid (PFDoDS)	10
Perfluorotridecanesulfonic acid (PFTrDS)	2
9-Chlorohexadecafluoro-3-oxanonane-1-sulfonic acid (9Cl-PF3ONS)	10
11-chloroeicosafluoro-3-oxaundecane-1-sulfonic acid (11Cl-PF3OUds)	10
8:2 Fluorotelomer unsaturated carboxylic acid (8:2FTUCA)	5
8:2 Fluorotelomer phosphate diester (8:2 diPAP)	10
Perfluorobutanesulfonamide (FBSA)	3
Perfluorohexanesulfonamide (FHxSA)	2
N-methyl perfluorooctanesulfonamide (N-MeFOSA)	2
N-ethyl perfluorooctanesulfonamide (N-EtFOSA)	1
Perfluorohexanesulfonic acid (PFHxS) branched	2
N-ethyl perfluorooctanesulfonamidoacetic acid (N-EtFOSAA) branched	10
N-methyl perfluorooctanesulfonamidoacetic acid (N-MeFOSAA) branched	10





Table A6: Measured PFAS Blanco DWU 2.

Carboxylic		Concentration	SD
perfluorpentaanzuur (PFPeA)	ng/l	0.6795	0.0035
perfluorhexaanzuur (PFHxA)	ng/l	1.518	0.047
perfluorheptaanzuur (PFHpA)	ng/l	2.0695	0.0535
B-perfluoroctaanzuur (B-PFOA),	ng/l	1.8185	0.0385
perfluornonaanzuur (PFNA)	ng/l	0.324	0.001

Sulfonic		Concentration	SD
perfluorbutaansulfonzuur (PFBS)	ng/l	0.649	0.032
perfluorpentaansulfonzuur (PFPeS)	ng/l	0.1585	0.0015
L-perfluorhexaansulfonzuur (L-PFHxS)	ng/l	2.865	0.051
B-perfluorhexaansulfonzuur (B-PFHxS)	ng/l	0.51	0.006
perfluorheptaansulfonzuur (PFHpS)	ng/l	0.058	0.002
L-perfluoroctaansulfonzuur (L-PFOS)	ng/l	0.5285	0.0315
B-perfluoroctaansulfonzuur (B-PFOS)	ng/l	0.8185	0.0095

Figure A12: Chloride & Total organic carbon C1.

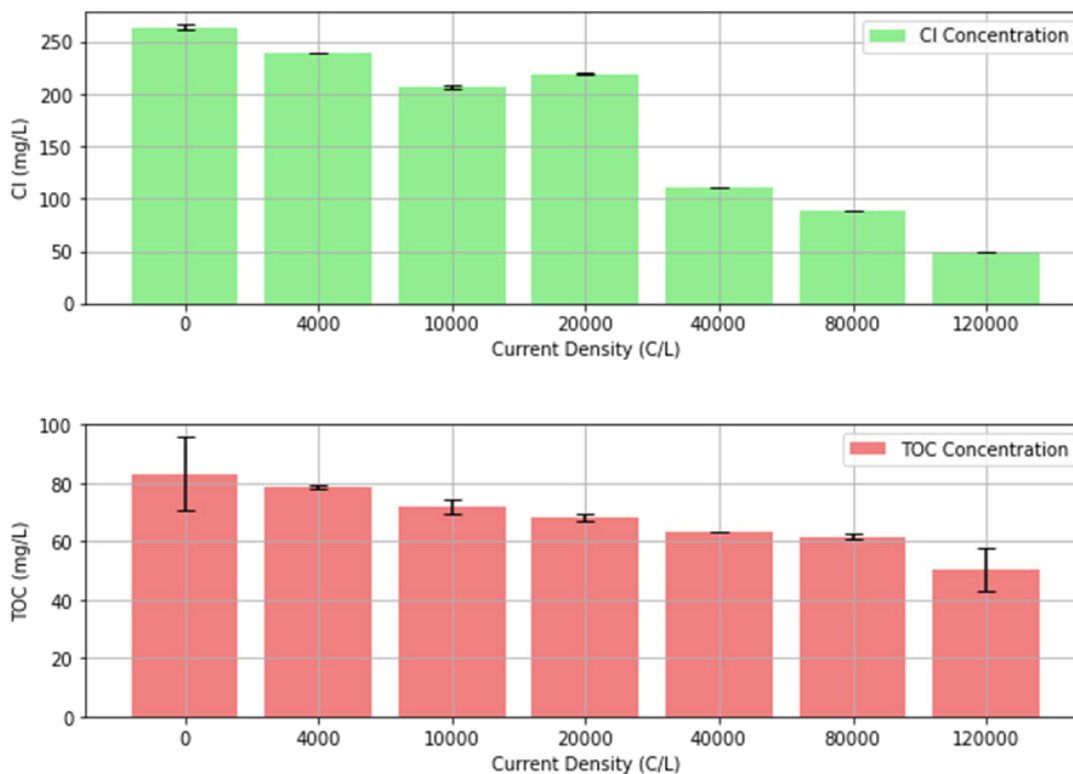


Figure A13: Chloride & active chlorine DWU1 & DWU2.

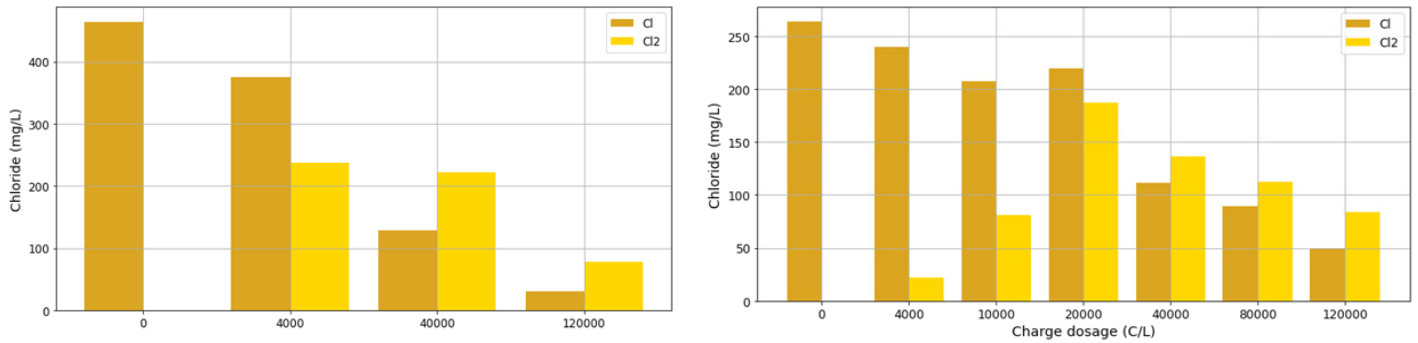


Figure A14: Degradation kinetics of corrosion inhibitors OMP-3.

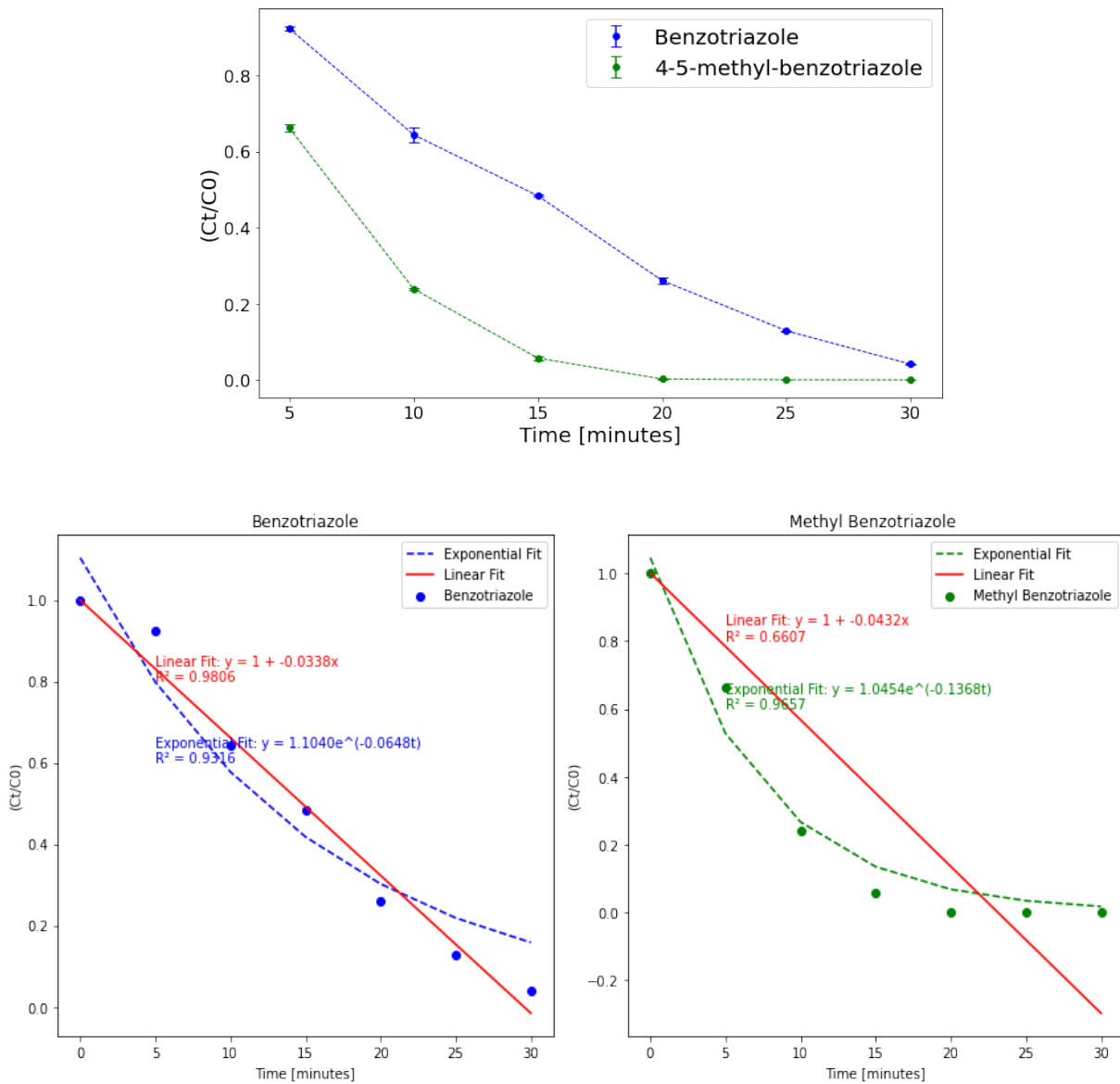


Figure A15: Degradation of pharmaceuticals OMP-3.

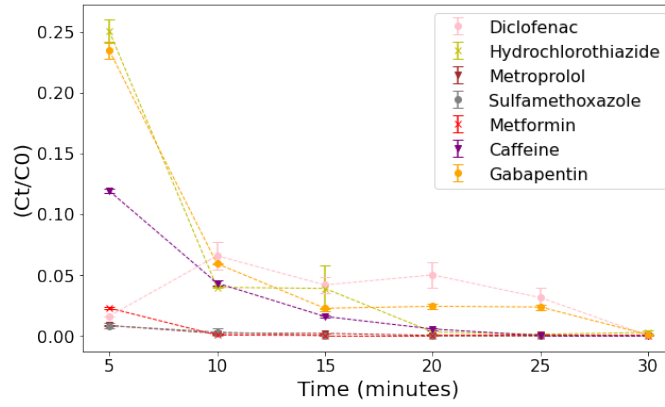


Figure A16: MB degradation in ROC

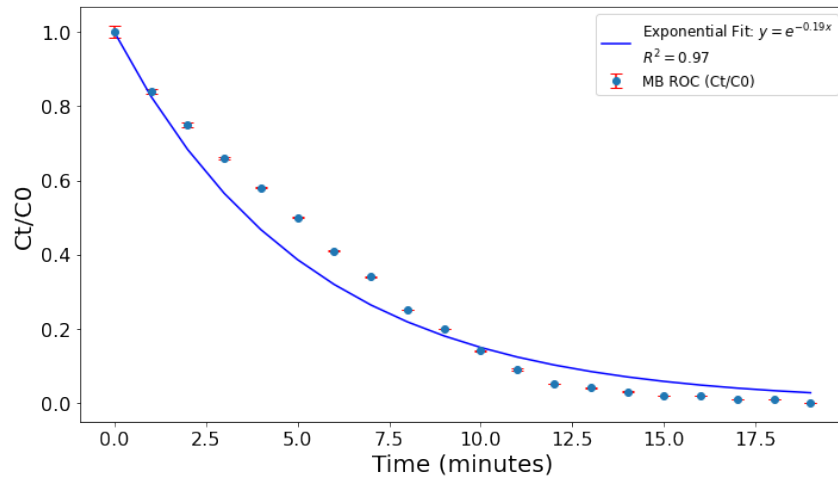


Figure A17: Magneli REM reactor experimental set-up.

